

A service of the U.S. National Library of Medicine
and the National Institutes of Health

MyNCBI
[Sign in] [Register]

All Databases
Journals Books

PubMed

Nucleotide

Protein

Genome

Structure

OMIM

PMC

Search PubMed

for 66[volume] AND 1991[pdat] AND renfranz[author]

Go

Clear

[Advanced Search \(beta\)](#) [Save Search](#)

Limits

Preview/Index

History

Clipboard

Details

Display

AbstractPlus

Show 20

Sort By

Send to

All: 1

Review: 0

☐ 1: Cell. 1991 Aug 23;66(4):713-29.

Cell Press Links

Region-specific differentiation of the hippocampal stem cell line HIB5 upon implantation into the developing mammalian brain.

Renfranz PJ, Cunningham MG, McKay RD.

Department of Brain and Cognitive Sciences, Massachusetts Institute of Technology, Cambridge 02139.

Proliferating precursors to the distinct cell types constituting the mammalian brain can be identified by the presence of the nestin intermediate filament. We report the establishment of a nestin-positive cell line, HIB5, from embryonic precursor cells to the rat hippocampus. Since it was immortalized using the temperature-sensitive allele tsA58 of SV40 large T antigen, these cells grow continuously at 33 degrees C, but not at 39 degrees C, the body temperature of rodents. To test their developmental capacity, HIB5 cells were implanted into both the neonatal hippocampus and cerebellum. The cells integrated into the host tissue and acquired morphologies characteristic of the neurons and glial cells found at the implant site. HIB5 cells might thus be useful in characterizing the signals regulating cell type determination in the mammalian brain.

PMID: 1878969 [PubMed - indexed for MEDLINE]

Display

AbstractPlus

Show 20

Sort By

Send to

Related Articles

Survival, integration, and differentiation of neural stem cell lines after transplantation to the adult rat striatum. [1997]

Neural precursor differentiation following transplantation into neocortex is dependent on intrinsic developmental state and receptor coregulation. [1999]

Neural stem and progenitor cells in nestin-GFP transgenic mice. [Neurosci. 2004]

Neuroprotective and behavioral efficacy of nerve growth factor-transfected hippocampal progenitor cell transplants after experimental traumatic brain injury. [2005]

Altered differentiation of CNS neural progenitor cells after transplantation into the injured adult rat neocortex. [1997]

» See all Related Articles...

[Write to the Help Desk](#)

[NCBI](#) | [NLM](#) | [NIH](#)

[Department of Health & Human Services](#)

[Privacy Statement](#) | [Freedom of Information Act](#) | [Disclaimer](#)

Multipotent Neural Cell Lines Can Engraft and Participate in Development of Mouse Cerebellum

Evan Y. Snyder,*†‡ David L. Deltcher,*
Christopher Walsh,*† Susan Arnold-Aldea,*§
Erika A. Hartwig,† and Constance L. Cepko*

*Department of Genetics

†Department of Neurology

‡Department of Pediatrics

§Department of Obstetrics-Gynecology

Harvard Medical School

Boston, Massachusetts 02115

Department of Biology

Massachusetts Institute of Technology

Cambridge, Massachusetts 02139

Summary

Multipotent neural cell lines were generated via retrovirus-mediated *v-myc* transfer into murine cerebellar progenitor cells. When transplanted back into the cerebellum of newborn mice, these cells integrated into the cerebellum in a nontumorigenic, cytoarchitecturally appropriate manner. Cells from the same clonal line differentiated into neurons or glia in a manner appropriate to their site of engraftment. Engrafted cells, identified by *lacZ* expression and PCR-mediated detection of a unique sequence arrangement, could be identified in animals up to 22 months postengraftment. Electron microscopic and immunohistochemical analysis demonstrated that some engrafted cells were similar to host neurons and glia. Some transplant-derived neurons received appropriate synapses and formed normal intercellular contacts. These data indicate that generating immortalized cell lines for repair of, or transport of genes into, the CNS may be feasible. Such lines may also provide a model for commitment and differentiation of cerebellar progenitor cells.

Introduction

Little is known about the molecular and cellular mechanisms underlying development of the mammalian central nervous system (CNS). If one could study the properties of individual progenitors, perhaps by immortalizing such cells, it may be possible to unravel some of the complexities of cell-type determination and plasticity in the immature CNS. We (Ryder et al., 1990) and others (Fredericksen et al., 1988; Bartlett et al., 1988; Geller and Dubois-Dalq, 1988; Evrard et al., 1990; Birren and Anderson, 1990) previously reported the establishment of immortalized clonal neural cell lines using retrovirus vectors to transduce oncogenes. Our lines were generated by retrovirus-mediated *v-myc* transfer into progenitors cultured from neonatal mouse cerebellum. Lines were established at a time when glia and neurons—the two major classes of cell type in the CNS—were being generated from the cerebellar external germinal layer (EGL). The EGL is a transient zone of small mitotic cells coating the

external surface of the developing cerebellar cortex. Arising on embryonic day 13 by migration of cells from the fourth ventricle onto and over the external surface of the cerebellum, the EGL was viewed by classical neuroanatomists as a persistent primitive ventricular zone. It has often been used as a test tissue for hypotheses on histogenesis in the nervous system (Schaper, 1987; Male and Sidman, 1961) owing, in part, to its relatively late development and accessibility. Present at birth in mammals, the EGL continues to proliferate postnatally, reaching a maximum 8-cell thickness at the end of the first postnatal week and disappearing by the end of the third postnatal week in rodents.

Our *v-myc*-immortalized cerebellar cell lines, established from the mouse EGL, evinced different morphologies and different cell type-specific antigens, even within a given clone. These results suggested that the original immortalized progenitor cells were multipotent, in keeping with results from *in situ* lineage analysis in a number of CNS locations (Turner and Cepko, 1987; Turner et al., 1990; Holt et al., 1988; Wetts and Fraser, 1988; Gray et al., 1988; Galileo et al., 1990; Leber et al., 1990). Not only was there diversity within clones, but lines were also observed to change during passage *in vitro*, alternating apparently spontaneously between predominantly neuronal and predominantly glial phenotypes. While changes in differentiation status may have simply reflected an instability in genome structure and/or expression, the heterogeneity and lability observed *in vitro* could in fact reflect the potential of progenitors *in vivo* in terms of their responsiveness to microenvironmental signals. To test whether the lines could respond appropriately when presented with the normal developmental cues of the cerebellar environment, as well as to probe the feasibility of using such lines for transduction of genes and/or functions into the *in vivo* environment, the lines were transplanted into the EGL of developing mouse cerebellum. The engrafted cells were then examined to determine whether they could participate in normal cerebellar development.

To identify the cell lines, they were marked by infection with a second retrovirus encoding the *lacZ* reporter gene (Price et al., 1987), the product of which forms a blue, electron-dense precipitate. During cerebellar histogenesis and at adulthood, the cerebella of transplant recipients were processed for identification of donor cells at the light and/or EM level. We now report that transplanted cells integrated into developing cerebellum in a nontumorigenic, cytoarchitecturally appropriate manner. Cells from the same clonal line differentiated into at least two neuronal types or into glia consistent with their site of engraftment. Derivation of engrafted cells from the clonal cell line was confirmed not only by its expression of the *lacZ* gene product but also, in some cases, by identity of the viral integration site between the donor cell line and labeled cells (portions of whose genome were amplified via the polymerase chain reaction [PCR]). Exogenous Escherichia coli β -galactosidase could be transduced and expressed within the cytoarchitectonics of the mammalian

CNS for prolonged periods, at least 22 months posttransplant. In a recent, independent study using a temperature-sensitive SV40 T antigen-immortalized hippocampal cell line, Renfranz et al. (1991) report engraftment and differentiation 3–6 weeks posttransplant.

The strategy of using retrovirus-immortalized lines as transduction agents for exogenous factors or as integral members of the cytoarchitecture of CNS tissue may be feasible for both clinical and research applications.

Results

Characteristics of Multipotent Neural Cell Lines prior to Transplantation

The establishment and *in vitro* characterization of these cerebellar progenitor cell lines has been detailed previously (Ryder et al., 1990). Briefly, retroviruses encoding *v-myc*, transcribed from the viral long terminal repeat (LTR) (plus the *neo* gene transcribed from an internal SV40 early promoter) were introduced into primary cultures of dissociated neonatal mouse cerebellum. Drug-resistant colonies were picked on the basis of morphology and passaged to establish separate lines that were then characterized using antisera to cell type-specific antigens.

Lines were established from G418-resistant colonies that exhibited different morphologies and that reacted with different cell type-specific antisera, suggesting either neuronal or glial lineages. However, some of these lines were found to have identical viral integration sites, suggesting that they derived from infection and immortalization of the same progenitor cell in the primary culture. For example, two lines that shared a common integration site, C17 and C36, were from the same primary culture and presumably derived from sibling cells that formed independent colonies upon initial expansion of the infected primary culture. Both colonies were selected because they contained cells that bore processes, an uncommon phenotype in the cultures. Though both colonies were process bearing, the morphology of the cells was different in the two, as was, on occasion, their antibody reactivity, suggesting that they might represent different cell types. Another line, C27, derived from an independent colony in the same culture, had a distinct integration site in addition to another distinct process-bearing morphology. Some lines thus could be categorized into clonally related "families" based on the location of their respective viral insertion sites. Nevertheless, all three of the above mentioned lines displayed similar qualities of neuronal–glial multipotency, heterogeneity, and lability. Periods of dual cell type–marker positivity or the transient expression of some markers was common, and antibody staining was rarely homogeneous. Subclones of all three lines were made and were found to exhibit these same properties.

As reported in Ryder et al. (1990), the two families of lines used in the following experiments (i.e., the C17/C36 family, the C27 family, and their respective subclones) each had the potential *in vitro* for expression of markers specific for oligodendrocytes (galactocerebroside C [Raff et al., 1978]) and neurons (neurofilament [NF; Wood and Anderton, 1981]). Subclones of C27 also expressed a

marker for astrocytes (glial fibrillary acidic protein [GFAP; Bignami et al., 1972]). Subclones of the C17/36 family, generated for the transplantation experiments, also began to show expression of GFAP subsequent to publication of Ryder et al. (1990). When carried for prolonged periods in culture, some lines (e.g., C27 and C36) became dominated by cells of a flat, non-process-bearing morphology and lost the ability to stain for markers of differentiated cell types in culture.

To define further the similarity of the cerebellar lines to primary cerebellar tissue, C27-3, a subclone of C27 infected with the *lacZ*-encoding retrovirus BAG (Price et al., 1987), was reacted with a battery of antibodies reported to stain within cerebellum for defined cell types, both of neuronal and glial classifications. In addition to the previously mentioned markers, subsets of the same culture of C27-3 stained for the following markers: neuron-specific enolase, the neurotransmitter glutamate, and the monoclonal antibody Q600 (Gravel et al., 1987). All three of these antibodies are specific to neurons, primarily granule cells (GCs), when applied to the cerebellum; their reactivity with noncerebellar cells has not been defined. In addition, F41 (Smith et al., 1990, Soc. Neurosci., abstract), which is reactive with GCs and Purkinje cells, and Q111 (Gravel et al., 1987), which is reactive with cerebellar oligodendrocytes, showed positive staining. C27-3 also stained for microtubule-associated protein 1, a neuronal marker, and myelin basic protein, an oligodendrocyte-specific marker.

As a preliminary assessment of whether the lines were responsive to cues from bona fide cerebellar cells, an *in vitro* coculture experiment was performed. C17-2 and C27-3 were cocultured with primary dissociated cells from the newborn mouse cerebellum. They were then identified by X-gal histochemistry and evaluated for changes in growth properties and morphology. Both cerebellar lines stopped proliferating in the coculture and underwent dramatic alterations in morphology. When cultured alone, both lines were dominated by large, flat, epithelial-like cells (Figure 1A). In the presence of primary cerebellar cells, the soma of C27-3 and C17-2 became compact and small with long, usually bipolar but occasionally multipolar processes present on the majority of X-gal⁺ cells (Figure 1B).

Integration into Developing Cerebellum

Cells from a given line were marked by infection *in vitro* with a replication-incompetent retroviral vector transducing the histochemically detectable E. coli *lacZ* gene (BAG virus) (Price et al., 1987). Subclones were picked, expanded, and tested for β -galactosidase expression, as detailed in the Experimental Procedures. Subclones that contained >90% β -gal⁺ cells were further maintained. These were tested for the presence of helper virus and characterized immunocytochemically for cell type-specific markers prior to transplantation.

Approximately 2×10^4 to 6×10^4 cells of a given line were injected into the EGL of the cerebellum of newborn mice. Animals were sacrificed either during the first postnatal week (6 hr to 7 days posttransplant) when cerebellar histogenesis is active and the EGL is most prominent, or at

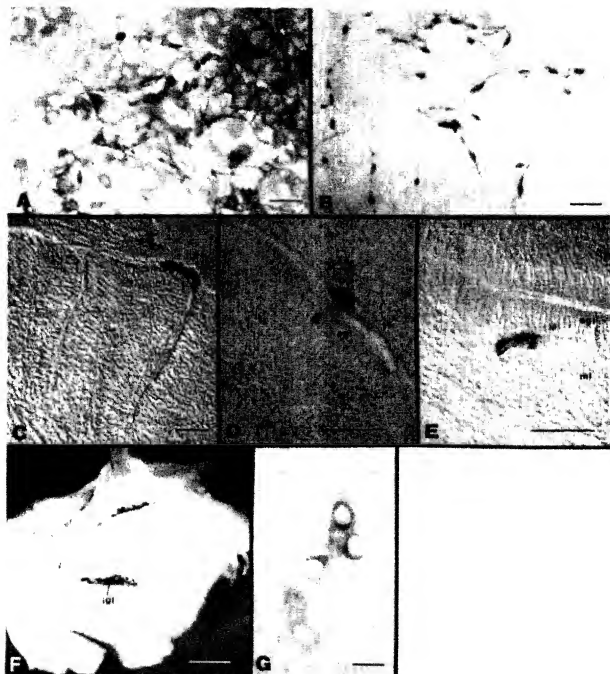


Figure 1. Cerebellar Cell Line C27-3 Can Respond to Environmental Cues In Vitro and Can Engraft into Developing Cerebellum

(A–B) Cerebellar cell line C27-3 cocultured with primary dissociated mouse cerebellum. After 8 days in vitro, C27-3 (blue, X-gal⁺ cells) stopped proliferating and sent out processes in the cocultures (B) but not in the control, noncocultured wells (A).

(C–E) Cerebellar cell line transplants analyzed during cerebellar histogenesis. Parasagittal sections of cerebella from pups processed for *lacZ* expression during cerebellar histogenesis in the first week of life, shortly following transplantation of line C27-3. A relatively small number of cells actually apposed the EGL. Initially (8 hr posttransplant; [C], arrow), began integrating, and appeared to migrate (72 hr posttransplant; [D] and [E], respectively). Arrow in (C) indicates pial surface. (E) illustrates the typical spindle-shaped migratory pattern of a cell leaving the lower EGL and entering the nascent molecular layer (ml).

(F–G) Cerebellar cell line transplant, analyzed at adulthood. (F) shows dense incorporation of blue cells within the internal granular layer (igl) of the cerebellum from a 22 month old mouse who, as a newborn, received a transplant of line C27-3. The cerebellum as pictured in (F) was processed for *lacZ* histochemistry as an ~0.5 mm thick parasagittal floating section in preparation for electron microscopy. (G) shows a 1 µm semithin section of the IGL from the tissue pictured in (F). The blue histochemical precipitate created by the X-gal reaction formed a perinuclear ring around labeled transplanted cells.

Scale bars: (A) and (B), 50 µm; (C)–(E), 100 µm; (F), 500 µm; (G), 10 µm. Photographed using Nomarski optics in (A)–(E) and (G) and bright-field optics in (F).

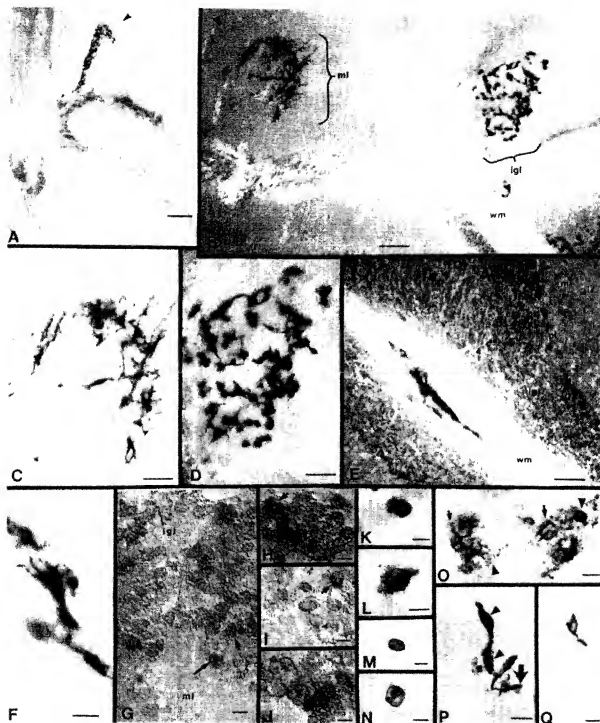


Figure 2. Differentiation of Cerebellar Lines into Neurons and Glia after Stable Engraftment into the Developing Cerebellum

(A) Cerebellar cell line transplant recipient, analyzed at adulthood. Blue cells occupying the IGL of the top-most folium (arrowhead) are cells from line C27-3 transplanted into a newborn mouse and visualized in this 50 μ m thick parasagittal section of cerebellum by X-gal histochemistry at 8 months of age (arrowhead positioned at pial surface).

(B-D) Shown in (B) is a 60 μ m section from the same cell line and same animal pictured in (A), ~1 mm away parasagittally. The group of X-gal⁺ cells on the right of (B) are located in the IGL (layer closest to white matter tracts [wm]) and possess neuronal (GC) morphology, as seen at higher power in (D); the cells in the IGL of (A) also look like this at high power. The group of X-gal⁺ cells on the left of (B) are primarily located in and virtually span the molecular layer (ml; farthest from wm) and possess glial (astrocytic) morphology, as seen at higher power in (C). Arrowhead in (B) indicates pial surface.

(E) X-gal⁺ cells located along white matter tracts (wm) in a 30 μ m section of adult cerebellum from another C27-3 transplant recipient.

(F) High power view of cells pictured in (E). This animal also contained X-gal⁺ cells of the two types pictured in (B) (not shown). pl, Purkinje cell layer, a discontinuous, single layer of large cells oriented between the IGL and the ML.

adulthood (1–22 months of age), by which time cerebellar development and differentiation are complete. Sections of the cerebellum (either 60 μ m cryostat sections affixed to gelatin-coated slides or 100–500 μ m floating sections) were processed using X-gal histochemistry to locate labeled cells.

Analysis in First Week

Analysis of pups during the first week of life revealed engraftment of transplanted cells into the EGL, occasionally as early as 6 hr posttransplantation, but clearly by 72 hr. Between 3 and 7 days posttransplantation, engrafted cells in the EGL could often be seen assuming the spindle-shaped morphology previously described as indicative of migration of endogenous, newly postmitotic EGL-derived cells (Miale and Sidman, 1961; Smeys and Goldowitz, 1989). The labeled cells appeared to migrate from the lower EGL into and across the molecular layer (ML) toward the widening internal granular layer (IGL), the layer where mature GC neurons reside. Of the large number of cells injected for transplantation, a relatively small number actually apposed the EGL initially (Figure 1C) (4.6% of the inoculum 6 hr posttransplant, averaged from two representative animals), and an even smaller number could be seen actually within the EGL and/or appearing to migrate from it (Figures 1D and 1E) (1.8% of the inoculum 72 hr posttransplant, averaged from two representative animals); most of the cells either immediately escaped along the injection tract out the injection hole, entered intermeningeal spaces, or became otherwise inaccessible to neural tissue for engraftment (not shown). Occasionally, large foci of cells were noted intraparenchymally, clearly deposited there by an excessively deep injection.

Analysis at Adulthood

Sections of cerebellum processed at adulthood revealed appropriate integration of labeled cells into that structure's cytoarchitecture with no evidence of tumor formation. In the animal pictured in Figure 2A, sacrificed at 8 months of age, $\sim 10^4$ cells from C27-3 spanning 1.7 mm (medial-lateral dimension) were incorporated. They were predominantly in the IGL and primarily in the vermis (subdivision of the cerebellum located in the midline) and posterior lobules. In the animal pictured in Figure 1F, sacrificed at

22 months of age, approximately twice as many cells (from C27-3) spanning twice that distance were detected.

Within the animal pictured in Figure 2B, some cells from C27-3 were located within the IGL and possessed neuronal morphology, suggestive of GCs (Figure 2D); other cells from that line were located within the ML and possessed glial morphology, suggestive of astrocytes (Figure 2C). Others from that line, e.g., in the animal pictured in Figures 2E and 2F, were found to reside along white matter tracts, assuming the location and morphology characteristic of a different glial cell type (oligodendrocytes). Multiple morphologies suggestive of multiple fates were observed in 5 adult animals transplanted with C27-3 and in 2 adult animals transplanted with C17-2. Further analysis of the nature of engrafted cells using ultrastructural and immunohistochemical criteria will be presented below. A fibroblast cell line expressing the *lacZ* gene, transplanted as a control, always failed to engraft.

Lack of Tumorigenicity

No tumors have ever been seen in more than 200 animals receiving transplants of various neural cell lines and various passages of those lines, often followed for more than 2 years posttransplant. Furthermore, animals with successful cerebellar transplants were never ataxic or otherwise motorically impaired.

Efficiency of Long-Term Engraftment

To date, there have been 34 animals in which X-gal* cells have been found within the cerebellum following transplantation (Table 1). Of these, 14 were present in adults; of these adult cerebella, 10 contained what appeared to be neurons (8 of these in combination with glia); 4 contained what appeared to be glia alone. The number of engrafted cells noted at adulthood varied widely, though attempts were always made to keep the initial inoculum constant in terms of concentration and amount across experiments (as described in the Experimental Procedures). There were many experiments (18) in which no engraftment was observed. In addition to the 34 positive animals presented in the Table 1, there were 172 animals in which no cerebellar engraftment was detected (16 pups, 156 adults).

Two out of three clonal lines examined (C17 and C27),

(G) Cerebellum stained with a cerebellar neuronal nuclear marker. A paraffin-embedded section of cerebellum (1 μ m thick) was reacted with the cerebellar neuronal nuclear antibody Q502 (courtesy of R. Hawkes) and visualized at high power. Neuronal nuclei are stained. The staining is located principally in the IGL, where GCs (e.g., short arrow) are abundant, is seen in the Purkinje cell layer (long arrow), and is virtually nonexistent in the ML, where neurons are sparse.

(H–J) Dual staining for β -galactosidase and the Q502 cerebellar neuronal nuclear marker. Three 1 μ m thick paraffin-embedded sections from the IGL of the C27-3 transplant recipient pictured in Figures 1F and 1G reacted with Q502 as in (G). When immunoperoxidase staining followed X-gel processing, these double-labeled cells (arrows) had a brown bull's eye appearance within a blue perinuclear ring. Nuclei of endogenous GCs also exhibited the brown antibody stain but did not have the blue perinuclear precipitate.

(K–N) Shown are GC neurons mechanically dissociated and visualized as isolated individual cells following X-gal and/or immunocytochemical processing of 1 μ m paraffin-embedded sections. (K) and (L) show double-labeled transplant-derived GC neurons from a recipient of C17-2 with blue perinuclear ring and brown bull's eye appearance following reaction with Q502 (alkaline phosphatase-conjugated secondary antibody). (M) illustrates endogenous GC exhibiting brown Q502 antibody stain but without the blue perinuclear precipitate. (N) shows negative control: an endogenous GC cell stained with an irrelevant antibody.

(O–Q) Transplant-derived cells from the ML stained for the glial (astrocytic) marker GFAP. In (O), cells from the ML of the C17-2 transplant recipient studied in (K) and (L) were stained *in situ* for GFAP as per (H)–(J). Robust staining was noted, primarily of processes (arrows) and occasionally of cell bodies (arrowhead). In (P), blue cells from ML of this animal mechanically dissociated as per (K)–(N) following GFAP staining. Arrowhead indicates GFAP-labeled brown-blue cell bodies. Arrow indicates anti-GFAP-labeled brown process that appeared to emanate from a blue cell. (Q) shows a negative control: transplant-derived GC from the same animal as in (K), (L), (O), and (P) stained instead for the glial marker GFAP. Scale bars: (A), 300 μ m; (B) and (E), 100 μ m; (C) and (D), 50 μ m; (F), 20 μ m; (G)–(Q) and (Q), 5 μ m; (P), 25 μ m. Photographed using Nomarski optics in (B), (D), and (G)–(J); bright-field optics in (A), (C), (F), and (K)–(Q); and dark-field optics in (E).

Table 1. Cell Line Transplant Recipients with Successful Engraftment in Cerebellum

Cell Line ^a	Age at Analysis ^b	Approximate Number of Cells Engrafted ^c	Efficiency of Experiment ^d	Neurons	Glia	EGL/ML ^e
C27-3 ^f	22 months	4+	2/4	x ^{g,h}	x	
C27-3 ^f	8 months	4+	2/4	x ^g	x	
C27-3 ^f	3 months	2+	5/12	x	x	
C27-3	1.25 months	2+	1/5	x	x	
C17-2	2.7 months	3+	2/3	x ^g	x	
C17-2	2.7 months	4+	2/3	x ^g	x	
C27-3	1.5 months	2+	1/1	x	x	
C17-2	6.25 months	1+	1/4	x		
C17-2	3.5 months	1+	3/4	x		
C27-3	1.25 months	1+	1/3		x	
C27-3	1.25 months	1+	1/6		x	
C27-3	1.25 months	1+	1/6		x	
C36-4	6 months	1+	1/5	x	x	
C27-16	2.3 months	1+	3/3		x	
C27-3	P3	1+	5/12			x
C27-3	P3	1+	5/12			x
C27-3	P7	2+	5/12			x
C27-3	P7	2+	5/12			x
C27-3	P8	2+	1/14			x
C27-3	P8	2+	1/5			x
C27-3	P6	1+	1/2			x
C27-3	P4	2+	1/3			x
C27	P6	2+	1/1			x
C27	P4	1+	1/6			x
C27	P4	1+	2/4			x
C27	P14	2+	2/4			x
C27-11	P7	2+	1/7			x
C27-16	P7	2+	3/3			x
C27-16	P7	2+	3/3			x
C27-5	P3	1+	3/9			x
C27-5	P3	1+	3/9			x
C27-5	P7	1+	3/9			x
C17-2	P8	2+	3/4			x
C17-2	P8	2+	3/4			x

^a A given cell line is designated by the number following "C", e.g., C27; a number following a dash refers to a subclone of that cell line, e.g., C27-3.

^b Animals less than 1 month of age (adulthood) are designated by postnatal day of life (e.g., "P3") where day of birth = P0.

^c Approximate number of *lacZ*⁺ cells found at the indicated harvest date: 4+ = >10⁴; 3+ = 10³-10⁴; 2+ = 10²-10³; 1+ = <10².

^d Efficiency of engraftment in the particular experiment of which this animal was a member; numerator = number of positive animals in that experiment; denominator = total number of animals analyzed in that experiment.

^e EGL = external germinal layer; ML = molecular layer (see text for details).

^f Confirmation that the viral insert in blue cells from a transplant recipient brain is identical to that of the donor cell line.

^g Confirmed by electron microscopic evaluation of ultrastructure.

^h Synapses on transplant-derived granule cell neurons identified by electron microscopy.

have shown multiple instances of engraftment. Of these, the respective subclones, C17-2 and C27-3, have proven the most successful and are therefore the best studied. However, the efficiencies vary greatly and, at present, inexplicably. They range from 0%-100% per experiment for the former (mean: 16%) and 25%-75% per experiment for the latter (mean: 55%); failure to engraft being the most common overall outcome at this point. However, since engraftment has been scored by expression of β -galactosidase, it is possible that engraftment rates are much higher, but that frequency of detectable β -galactosidase expression is significantly lower than the actual engraftment rate (see Discussion).

It should be noted that not all cell lines—even subclones of the same line—engraft (although given the low frequency of success with even the best lines, lack of en-

graftment by any line must be interpreted with caution). Furthermore, not all passages of even a competent line (e.g., C27-3) engraft with equal efficiency. We have not yet been able to determine which variables insure the greatest number of engrafted cells per animal with the greatest efficiency per litter. While the precise "engraftability" factor(s) remains elusive, it appears that periods during which the lines are process bearing in culture and display some percentage of differentiated neural markers (NF and/or GFAP) correlate with more reliable engraftment, as opposed to a flat morphology with no cell marker expression. While uniformly flat, non-marker-expressing cells almost never engraft, the converse, i.e., expression of markers, does not necessarily insure engraftment. The first 24-48 hr of life appeared the most "engraftable" age for a recipient newborn mouse pup; while efficiency of engraftment

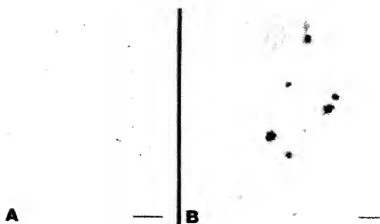


Figure 3. Distribution and Morphology of Host Cerebellar Cells after Transduction of the *lacZ* Gene

To generate X-gal-labeled host cerebellar cells for comparison with X-gal-labeled engrafted cells, neonatal mouse cerebellum of a nonengrafted host was infected by an injection of the BAG virus; the cerebellum was processed for X-gal histochemistry at adulthood.

(A) X-gal⁺ host cells in perisagittal section of adult cerebellum are located primarily in the IGL (borders outlined by small arrows; pial surface is at the top of the photomicrograph). Compare with engrafted C27-3 X-gal⁺ cells in Figure 2A.

(B) Higher power view of X-gal⁺ host cells from cerebellum pictured in (A). Compare with engrafted X-gal⁺ C27-3 cells in Figure 2D.

Scale bars: (A), 100 μ m; (B), 20 μ m. Photographed using bright-field optics in (A) and (B).

was only slightly better (18% at <P2 vs. 15% at <P2), there tended to be a larger number of engrafted cells seen in positive animals transplanted at the younger age.

Endogenous Granule Cells Observed In Situ

To compare the morphology and distribution of cells derived from transplanted lines with those derived from endogenous cerebellar progenitors, the BAG vector was injected directly into neonatal mouse cerebellum, labeling endogenous mitotic progenitors and their progeny in situ. After the cerebella were fully differentiated, sections of the tissue were processed to locate the marked cells. Blue cells were located principally in the IGL, consistent with their having been born postnatally in the EGL and having descended to terminate in the IGL (Figure 3A). Cell bodies were small and round with a few fine dendritic processes barely filled with the blue precipitate (Figure 3B). In contrast, the processes and cytoplasm of IGL cells derived from transplants were "plumper" and better defined (compare Figure 3B with Figure 2D). Parallel fibers of endogenous GCs, the axonal projections that form the ML, were never observed to be labeled by precipitate. Similarly, transplant-derived IGL cells did not exhibit labeled projections. This finding is not unexpected, as the X-gal precipitate has frequently failed to fill the processes of infected neurons and/or glia.

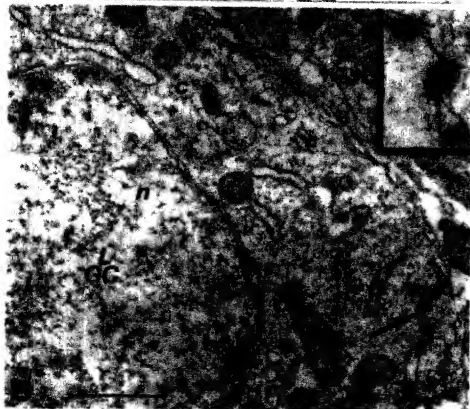
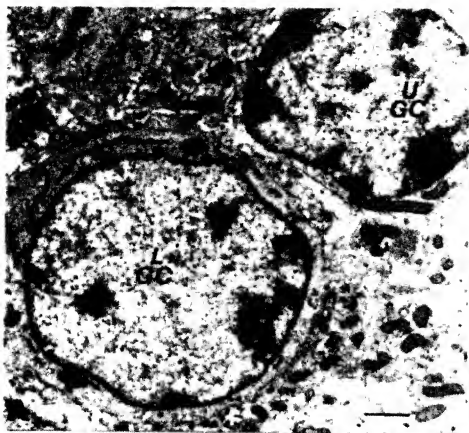
Although newly born GCs migrate from EGL to IGL down columns along radial glial fibers (Rakic, 1971), blue cells derived from either the cell lines or endogenous progenitors were seen not to be columnarily arrayed at adulthood, and cells in columns were far from uniformly blue. Rather, there was enormous scatter of blue cells derived from endogenous progenitors (Figure 3A). A more clustered but still nonradial pattern of distribution of cells derived from the cell lines was seen. Occasionally, from either endogenous progenitors or from transplanted cells, different cell types (e.g., glia and neurons) were juxtaposed. Although a significant percentage of the endogenously derived labeled cells were no doubt clonally related, the extensive

migration of labeled cells made it impossible to delineate clonal boundaries reliably.

Immunohistochemical Analysis of Engrafted Cells

Returning to examination of transplanted, exogenous cells, as shown in Figures 1 and 2, several morphologies and locations consistent with a variety of cell types were observed among stably engrafted cells. To characterize further the engrafted cells, antibodies directed against neuronal and glia cell types were used to stain X-gal⁺ cells. When applied to tissue sections containing X-gal⁺ cells, this approach was slightly hampered by the arrangement of cells within the adult cerebellum. For example, the IGL is an area of extremely high GC density. It is thus difficult to assess reliably whether X-gal⁺ cells are positive or negative for a GC antigen, owing to the high endogenous antigen density. To circumvent this problem partially, two approaches were taken. Cryostat sections (60 μ m) containing X-gal⁺ cells were embedded in paraffin so that thinner, 1 μ m sections, could be made. As the diameter of a GC is 5–8 μ m, 1 μ m sections partially relieved the problem of superposition of endogenous and transplant-derived cells. Second, after immunohistochemical processing of the section, cells within the section were mechanically dissociated. Individual cells could then be scrutinized.

Antibodies that react with cerebellar neurons were directed against the IGL from X-gal-processed tissue of transplant recipients, including those pictured in Figures 1F, 1G, and 2D. As in the semithin sections for electron microscopic (EM) analysis (Figure 1G), the perinuclear ring of the *lacZ* reaction product within the labeled cell left a clear nucleus; a nuclear anti-neuronal monoclonal antibody, detected with a conjugate of horseradish peroxidase or alkaline phosphatase, could be directed against such a cell, conferring a "bull's eye" appearance if successfully double labeled. The monoclonal antibody Q502, when directed against paraffin-embedded 1 μ m sections of mouse cerebellum, stained most neuronal nuclei in the IGL (Figure 2G), as previously reported (Gravel et al.,



1987). Cells within the IGL varied in their intensity of staining, and it appeared that cells within the Purkinje cell layer stained most intensely. Blue cells in the IGL of recipient animals, examined in this fashion, also stained positively with Q502 (Figures 2H–2J); they stained with a variety of intensities, some definitively positive (e.g., Figure 2J), and some less so (e.g., Figure 2I). Dissociated blue cells revealed brown nuclear staining (Figures 2K and 2L) similar to that of isolated endogenous GCs (Figure 2M), but distinguishable from blue GCs stained with an irrelevant antibody (Figure 2N) or with an antibody directed against the astrocyte marker GFAP (Figure 2Q).

A similar procedure using anti-GFAP antibody was performed for transplant-derived cells with glial morphology in the ML. Anti-GFAP stained blue cells in the ML *in situ* (Figure 2O) in a manner similar to that of endogenous cells (not shown). When the tissue was mechanically dissociated, staining of GFAP on individual blue cells was detectable and resembled staining of dissociated endogenous astrocytes (Figure 2P). The cell body, as well as processes, of some blue cells exhibited colocalization of the GFAP and X-gal stains. As previously noted, GFAP did not stain presumptive GCs, which stained for Q502 (Figure 2Q).

Ultrastructural Analysis

As the cerebellum has been extensively characterized at the ultrastructural level using electron microscopy, an assessment of the differentiation state (and thus functional potential) of engrafted cells is most reliably made using these criteria. Ultrastructural features also reliably confirm cell type identification (Palay and Chan-Palay, 1974).

Four positive recipient mouse cerebella were prepared for EM examination (Table 1). Floating sections (100–500 μm thick) of cerebella at adulthood were processed for X-gal histochemistry (Figure 1F). As seen in 1 μm semithin sections of the IGL (Figure 1G), the most obvious location of the blue histochemical precipitate created by dimerization of the X-gal product is in the perinuclear region of transplanted cells, distinguishing them from endogenous GC neurons. This precipitate is electron dense (Bonnerot et al., 1987), allowing engrafted labeled cells to be distinguished from endogenous GC, which they otherwise resemble ultrastructurally (Figure 4A). The precipitate is localized not only to the nuclear membrane but also to cytoplasmic, subcellular organelles such as the endoplasmic reticulum (ER) (Figures 4A and 4B, arrows). Individual particles, when examined under high power, appear crystalline (Figure 4B, inset).

GC neurons are identified ultrastructurally as small

round or oval cells (5–8 μm diameter) in the IGL with meager cytoplasm forming a rim around a large round nucleus. The cytoplasm contains few mitochondria and short tubules of ER, sometimes squeezed into a small space within the cytoplasm created by dimpling of the nucleus. The nucleus contains large blocks of condensed chromatin usually distributed along the inner side of the nuclear envelope forming a characteristic “clock face appearance”; a small nucleolus is usually hidden within one of these chromatin blocks (Eccles et al., 1967; Palay and Chan-Palay, 1974; Peters et al., 1991; S. Palay, personal communication).

A second type of labeled, transplant-derived neuron was also identified, the basket cell (BC) neuron (Figures 5A and 5B). BCs are also born in the postnatal period, although their origin is somewhat controversial (Eccles et al., 1967; Altman, 1982; Miale and Sidman, 1961; Palay and Chan-Palay, 1974; Hallonet et al., 1990). In the normal cerebellum, BCs are very few in number, comprising 20-fold fewer cells than the extremely abundant GCs, and thus were seen labeled only rarely. BCs are defined ultrastructurally as larger cells (12–20 μm diameter) in the lower ML with ample cytoplasm and a distinctive large, indented (often deeply) irregular nucleus with dispersed, nonaggregated, less dense chromatin. The prominent ER cisternae are roughly parallel with the nuclear envelope (Eccles et al., 1967; Palay and Chan-Palay, 1974; S. Palay, E. Mugnaini, personal communication). As in the transplant-derived GCs, label was located within the nuclear envelope and in the ER.

Glial cells with label were also identified (Figures 5C–5E). One type of glial cell, an oligodendrocyte (Figures 5C and 5E), though somewhat similar in size and shape to a GC neuron, is identified by its distinctively dark cytoplasm, an appearance created in the mature cell by numerous fine granules. Because the nucleus lies somewhat eccentrically, a large mass of cytoplasm, while not voluminous, may occur at the poles of the cell. The contour of the perikaryon is smooth and regular. Unlike in the GC, the nuclear chromatin tends to marginate and flatten against the nuclear membrane and/or clump centrally, allowing a prominent nucleolus to be visualized in IGL oligodendrocytes. The mitochondria are short and round and the ER are usually well developed, long, meandering, and distended. Oligodendrocytes are usually located near myelinated fibers or near blood vessels (Palay and Chan-Palay, 1974; Peters et al., 1991). In Figure 5C, precipitate was seen in the nuclear membrane and ER of an ultrastructurally identified oligodendrocyte.

Evidence for label within a second type of glial cell, an

Figure 4. Engrafted Cells, Identified by Electron-Dense X-Gal Precipitate, Resemble Host Granule Cells at the Ultrastructural Level. Electron micrographs from the IGL of the C27-3 transplant recipient pictured in Figures 1F and 1G, 22 months posttransplant. (A) The blue perinuclear histochemical precipitate is electron dense, allowing engrafted labeled cells (LGC) to be distinguished from endogenous unlabeled granule cell neurons (UGC), which they otherwise resemble ultrastructurally. Compare with light microscopic picture of a semithin section from a similar field in Figure 1G. The precipitate is localized in cytoplasmic, subcellular organelles (arrow)—the ER. Scale bar, 1 μm . (B) A transplant-derived, labeled granule cell (LGC) in which the precipitate forms a discontinuous, more discrete pattern around the nucleus and in subcellular organelles (arrow). n, nucleus; c, cytoplasm; m, mitochondrion. Scale bar, 1 μm . (B, inset) The three precipitate particles at the tip of the arrow in (B) are enlarged in order to demonstrate their crystalline character.

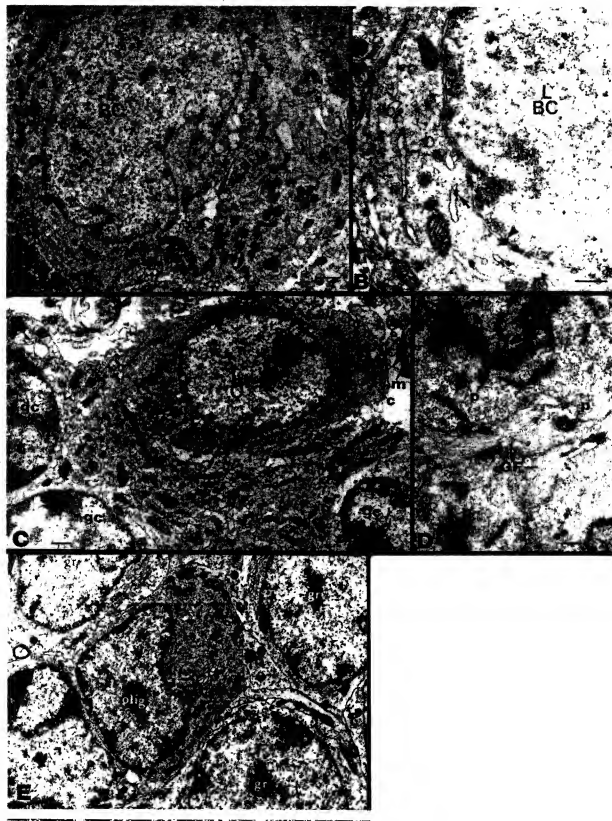


Figure 5. Engrafted Cells Resemble the Host BCs and Two Types of Glia at the Ultrastructural Level

(A) and (B) show a labeled basket cell neuron.

(A) Labeled BC neuron (LBC) in the lower ML displays defining ultrastructural features listed in the text, most prominently the deeply clefted nucleus and the ER coursing roughly parallel to the nuclear membrane. Label precipitate is seen in the nuclear membrane and in the ER. Scale bar, 1 μ m.

(B) Blocked area in (A) at higher power. Note the label within the nuclear envelope (arrowhead) and adherent to the ER (arrow). Scale bar, 0.5 μ m.

astrocyte, was also noted. Mature astrocytes are defined ultrastructurally by the presence of glial filaments (GFs) (the main constituent of which is defined by GFAP antibodies) (Palay and Chan-Palay, 1974; Peters et al., 1991; Big-nami et al., 1972). Figure 5D demonstrates precipitate-bearing processes with GFs, defining them as astrocytic. GFs are defined and distinguished ultrastructurally from neurofilaments (NFs) by several criteria. In appearance, GFs are fine, smooth, uniform in size, closely packed, and unmyelinated. In contrast, NFs are coarse, "bumpy," of multiple sizes, widely spaced, loosely bundled, and often myelinated. GFs and NFs are also distinguished by their size. The labeled GFs (Figure 5D) measured on average 8.4 nm in width, appropriately ~76% of the diameter of NFs (Peters et al., 1991) in the same field.

The synaptic unit in the IGL is the glomerulus: incoming large, mossy fibers synapse on small dendrites from multiple GC neurons. When sliced transversely, as in an EM section, dendrites usually look like small, occasionally elongated, ovals containing a single mitochondrion and often a single ER vacuole, around which a mossy fiber envelops (Eccles et al., 1967; Palay and Chan-Palay, 1974). Figure 6A, obtained from the cerebellum pictured in Figures 1F and 1G, offers a low powered electron micrograph of a labeled, transplant-derived GC neuron (LGC). Near it (blocked area) are a number of synapses, indicated by arrows in the higher power overview of that region (Figure 6B). Further magnification of the blocked areas in Figure 6B (Figures 6C and 6D) demonstrate oval GC dendrites (gd) with label precipitate (p), which, as in the cell bodies, respects membrane boundaries (compare with Figure 4B, inset). Endogenous, unlabeled, multi-vesicle-filled mossy fibers (mf) synapse on them (arrows). The GC dendrites also make adhesive contacts ("puncta adherentia") (Figure 6C, arrowheads) (Palay and Chan-Palay, 1974) with other GC dendrites. Evidence of synapse formation was seen in several other areas within this engrafted animal.

Identity of Proviral Integration Site

Up to this point, identification of donor cells was by virtue of the X-gal histochemical reaction. Escape of the BAG genome from donor cells or contamination of the mice with BAG virus derived from any source could lead to infection of endogenous host cells and subsequent misidentification of host cells as donor cells. Therefore, several steps were taken to confirm that the X-gal⁺ cells were donor derived. First, multiple tests for production of BAG virus by the donor cells were negative in all lines used for trans-

plantation. Second, we sought to identify a unique genetic tag for donor cells that would allow confirmation that the blue cells within a recipient cerebellum were indeed donor derived. This was done by recovery of the sequence at the viral integration site in cell line C27-3 by an inverse PCR (see Experimental Procedures). Oligonucleotides complementary to stretches of sequence constituting the integration site were synthesized to serve as primers in direct PCR against opposing primers within the LTR. When the reaction was performed on genomic DNA from the C27-3 cell line, fragments of predicted size were obtained using all possible primer pairs. These products were specific for C27-3; amplification products were not obtained using genomic DNA from non-clonally related, BAG-infected cell lines generated from the same primary culture that generated C27-3. From the three recipient cerebella pictured in Figures 1G, 2A–2D, and 2E–2F, multiple pieces of tissue, each containing 1–20 blue cells, were dissected from diverse regions, digested with proteinase K, and subjected to PCR. When the amplification products were examined by electrophoresis, tissue containing blue cells yielded fragments of the predicted size, identical to that from the C27-3 cell line. Ninety percent of samples containing blue cells (27/30) successfully amplified. The 10% of samples that failed to amplify (3/30) contained only 1 blue cell each. Samples containing only 1 blue cell amplified 57% of the time (4/7), an efficiency in keeping with that observed for single BAG-infected cells dissected from rodent cortex (C. Walsh and C. L. Cepko, unpublished data). Lanes that contained either no tissue, cerebellar tissue from a littermate in which engraftment failed (i.e., no blue cells), or tissue from an uninfected cerebellum usually demonstrated no amplification product (Figure 7). The rare falsely positive samples (2/24 or 8.3%) presumably resulted from cross-contamination, a common finding when high cycle numbers are used in PCR.

Discussion

Stable Engraftment of Retrovirally Immortalized Lines

A number of studies recently have demonstrated that transplanted primary neural tissue, usually of fetal origin, can become successfully engrafted in host parenchyma (reviewed in Gage and Fisher, 1991). Some of these studies have addressed developmental questions—e.g., do grafted cells follow an autonomous program or do they accommodate to their new surroundings (Sotelo and Alvarado-Mallart, 1986, 1987; McConnell, 1985, 1988;

- (C) Labeled glial cell (oligodendrocyte). Labeled oligodendrocyte (LO) present in the IGL displays the defining ultrastructural features that distinguish it from nearby granule cell neurons (gc) (see text). Specifically, there is a distinctively dark cytoplasm (c) that collects at the poles of the cell, a dark nucleus, a prominent nucleolus located near centrally clumped chromatin (arrow) with the remainder of the chromatin marginated as a rim along the inner nuclear membrane. Label is present in the nuclear membrane and in the long meandering ER (arrowhead). The cell is adjacent to a myelinated fiber (mf). Scale bar, 1 μ m. Compare with (E), olig. oligodendrocyte; gr, granule cell.
- (D) Labeled glial (astrocytic) process containing GFs. A process bearing label precipitate (p) also contains GFs, which define that process as glial (astrocytic). (The process lies adjacent to the cytoplasm of labeled glial cells that border it on both sides and that themselves contain precipitate in ER and near poorly filled mitochondria.) The GFs average 8.4 nm in diameter. Their distinctive appearance and size are discussed in the text.
- (E) For comparison with (C), an endogenous IGL oligodendrocyte and granule cell are reproduced (with permission) from the textbook of Palay and Chan-Palay (1974) (their Figure 266).

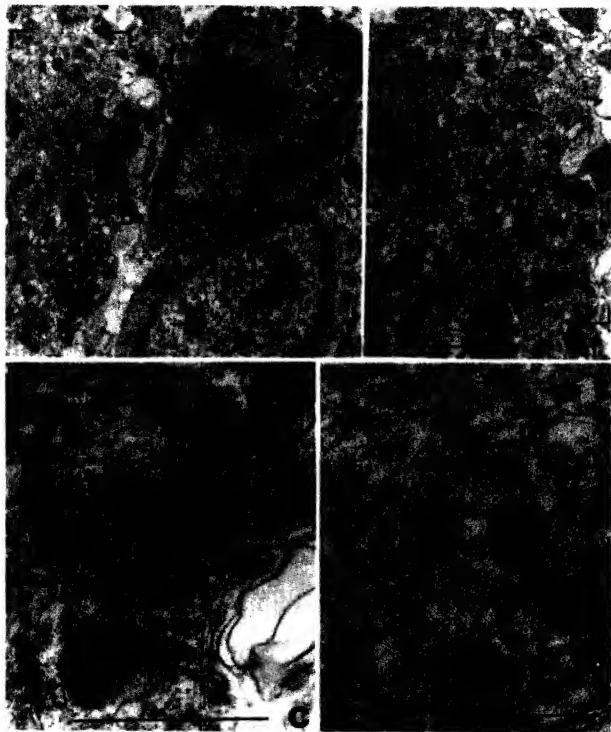


Figure 6. Postsynaptic Specializations on Labeled GC Dendrites

Electron micrograph from the IGL of the C27-3 transplant recipient pictured in Figures 1F, 1G, 4, and 5, 22 months posttransplant. (A) Low power view of a transplant-derived, labeled granule cell neuron (LGC). Scale bar, 1 μ m. Glomerular complexes near it (blocked area) are examined at higher power in (B) (scale bar, 1 μ m), where arrows indicate a number of synapses. The blocked area in (B) is further magnified in (C) (scale bar, 1 μ m; lower block) and (D) (scale bar, 1 μ m; upper block). Both (C) and (D) demonstrate oval granule cell dendrites (gd) with label precipitate (p). Note: the label respects membranes and resembles the precipitate in the GC bodies as seen under high power in Figure 4B, inset. Endogenous, unlabeled, multi-vesicle-filled mossy fibers (mf) synapse on the labeled granule cell dendrites (arrow). In (C), the GC dendrite also makes adhesive contacts (puncta adherentia) (arrowheads) with other granule cell dendrites. m, mitochondrion. See text for further explanation and definitions.

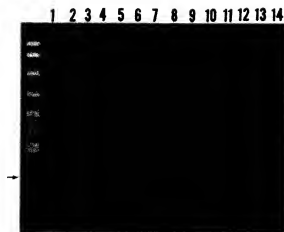


Figure 7. Blue Cells within a Recipient Cerebellum Bear the Same "Genetic Tag" As the Donor Cells

As detailed in the text, oligonucleotides complementary to portions of flanking sequence served as one-half of a set of primers for a PCR against opposing primers within the LTR. This gel shows the amplification products obtained following nested PCR using first primers #1 and #26 and then primers #2 and #21 (see Experimental Procedures). The arrow marks 104 bp, the predicted size of products following the second amplification; the left-most lane contains molecular weight standards obtained from an *MspI* digest of pBR322. Amplification products of the predicted size were obtained using genomic DNA from the C27-3 cell line (lane 1) but not from C17-2 (lane 2) or C38-4 (not shown). Cerebellar tissue from two C27-3 transplant recipients containing blue cells (the animal in Figures 1F and 1G, lanes 3–6, and the animal in Figures 2E and 2F, lanes 7–10) also yielded amplification products of the predicted size, identical to that from the C27-3 cell line (lane 1). Lanes that contained tissue from an uninjected cerebellum demonstrated no amplification product (lanes 11–14). Blue cells from the animal in Figures 2A–2D yielded amplification products identical to those in lanes 3–10. Lanes that contained tissue from a littermate in which engraftment failed (i.e., no blue cells) demonstrated no amplification product (not shown). "Shadow bands" as seen in the lane with genomic DNA from the C27-3 cell line (lane 1) do not appear when only 45 cycles of un-nested PCR are performed with primers #2 and #21 alone (not shown).

Stanfield and O'Leary, 1985; O'Leary and Stanfield, 1989; Lund et al., 1987). Reconstitution of lost function has also been achieved through transplantation, using either primary fetal- or tumor-derived tissue (Barry et al., 1987; Isacson et al., 1986; Gage et al., 1983; Fisher et al., 1991; Bjorklund et al., 1982; Buzsaki et al., 1988; Rosenberg et al., 1988; Sotelo and Alvarado-Mallart, 1986, 1987; Labbe et al., 1983; O'Leary and Stanfield, 1989; Freund et al., 1985). The transplantation data presented in this article and in a recent report by Renfranz et al. (1991) represent a demonstration of cytoarchitecturally and, perhaps, functionally appropriate engraftment by exogenous mammalian central neural tissue that is neither tumorigenic nor of tumor or primary fetal origin. The potential would seem to exist for transplanting such lines for repair in lesioned or mutant animals or for the transport of genes of developmental or therapeutic interest into the CNS. Furthermore, the techniques for generating transplant material in this manner may conceivably someday circumvent concerns over the use of primary fetal tissue. However, since prob-

lems with efficiency of stable engraftment remain poorly understood and thus difficult to control, much work remains prior to the use of such lines for clinical applications.

Resemblance to Endogenous Cerebellar Progenitors

Following the progeny derived from a single progenitor maintained in culture has been useful for defining a range of potentials for a subset of neuroblasts (Baroffio et al., 1988; Temple, 1989). Immortalization and cloning of individual progenitors represents another approach to the question of potency. While both approaches suffer from inherent limitations, such as removal of a cell from its *in vivo* context, it was hoped that the availability of an unlimited number of cells derived from a single progenitor would offer some advantages over primary cultures. One hope was that the act of immortalization would freeze a progenitor cell in a particular state, providing a source of homogeneous cells that could be manipulated to alter the fate of its progeny. However, in this case, as in many others in which CNS cells were immortalized, homogeneity has been observed only rarely (Ryder et al., 1990; Cepko, 1988; Evrard et al., 1990; Fredericksen et al., 1988; Bartlett et al., 1988; Birren and Anderson, 1990; Geller and Dubois-Dalcq, 1988). Instead, immortalization of single progenitors yields clonal lines that are both heterogeneous and plastic (i.e., changing over time in culture). Subsets of the same line often express both neuronal and glial phenotypes concurrently and/or alternate "spontaneously" between the two. It is unclear whether these observations are the result of a self-renewing "pool" of uncommitted precursors responding specifically to changing signals or of stochastic changes, perhaps including transdifferentiation.

To determine whether lines are bona fide representatives of endogenous cells or are simply an artifact, one can compare their behavior to that of their counterparts left *in situ*. *In situ* lineage mapping using retroviral vectors and injection of tracers has allowed an examination of the potency of individual progenitors of the vertebrate CNS. In the retina (Turner and Cepko, 1987; Turner et al., 1990; Holt et al., 1988; Wetts and Fraser, 1988), tectum (Gray et al., 1988; Galileo et al., 1990), and spinal cord (Leber et al., 1990), individual endogenous neural progenitors were found to give rise to multiple neural cell types of both neuronal and glial phenotype. This assessment was enabled by the fact that clonally derived cells in these regions remained as identifiable clusters into adulthood. The ability to extend this technique and its conclusions, however, to mammalian CNS as a whole has been confounded by the observation of extensive migration of clonally related cells in several other regions, including cortex (Walsh and Cepko, 1988; Austin and Cepko, 1990), striatum (Halliday and Cepko, unpublished data), and, as illustrated here, cerebellum. Thus, currently there are no interpretable data on the potency of an individual EGL cell *in situ*, although efforts are underway in our laboratory to solve these problems (E. F. Ryder and C. L. Cepko, unpublished data).

However, one can use other methods to assess how closely immortalized cerebellar cells resemble primary

cells in culture and/or differentiated cerebellar cells *in situ*. C27-3, for example, exhibits a number of cerebellar antigens. C17-2, cocultured with primary astrocytes or with the U251 human astrocytoma cell line, has the ability to inhibit proliferation and induce differentiation of these cells (Weinstein et al., 1990), as has been described for cultured primary GCs (Hatten et al., 1986). Both C17-2 and C27-3 induce neurite outgrowth in cultured primary cerebellar neurons (J. R. Madsen, unpublished data). Finally, the lines express other cerebellar-specific proteins. En-1 and En-2 constitute a murine homeodomain family homologous to *Drosophila engrailed*. En-1 has been localized throughout the neuraxis in developing embryos; En-2 is restricted to a subset of En-1⁺ cells specifically in the hindbrain of the embryo and, ultimately, the IGL of adult cerebellum (Davis et al., 1988; Davidson et al., 1988; Joyner et al., 1991). The lines express these proteins to various degrees (A. Joyner, personal communication). All of these features suggest that these lines at least resemble primary cerebellar tissue.

An additional way to investigate the authenticity of the lines, however, is to demonstrate incorporation of these cells into the cytoarchitecture of the appropriate brain region at the appropriate host age. When newborn mouse cerebella were transplanted with cell lines, it was seen that transplanted cells derived originally from the EGL had reincorporated into the EGL. At adulthood, cells of these lines were observed to have differentiated into multiple cell types classically thought to be derived from the EGL (Miale and Sidman, 1961; Palay and Chan-Palay, 1974; Altman, 1982), including GC and BC neurons as well as glia (oligodendrocytes and astrocytes). However, since a recent report (Hailonnet et al., 1990) has called into question the classical view of the EGL progenitor-progeny relationships, it is difficult to interpret whether the cell types recovered after transplantation offer evidence of an EGL cell line or of a cerebellar or CNS progenitor with broader potential.

Comparison with Mature, Endogenous Cerebellar Cells

Although engrafted cells in the first week resemble endogenous EGL cells, at adulthood, many transplant-derived GCs appear "plumper" at the light microscopic level than their endogenous GC counterparts labeled directly with the BAG virus (e.g., Figures 3A and 3B). Processes and cytoplasm of transplanted cells appear more "distended" with precipitate. We cannot explain this difference in labeling pattern. At the EM level, however, transplant-derived cells resembled their endogenous unlabeled cell-type counterparts, indicating that they had differentiated into GC and BC neurons and glia. The value of the transplanted lines for addressing developmental and/or clinical issues hinges on their functional fidelity to endogenous neural cells. EM analysis provided evidence that some transplanted cells that differentiated into ultrastructurally identifiable GC neurons developed dendrites that were postsynaptic to the appropriate presynaptic areas on mossy fibers (Figure 6), suggesting functional as well as anatomic integration. This is based on the observation that some dendrites contained the characteristic X-gal precipitate. The

X-gal reaction product could theoretically have diffused from donor cell bodies onto dendrites of host cells. However, the fact that the precipitate was usually membrane bound within cell bodies, respected dendritic membranes, and was not seen in inappropriate locations (e.g., the presynaptic mossy fibers) would seem to argue against this potential problem. Additional observations of a greater number of animals that bear large numbers of engrafted cells and thus allow EM analysis of synaptic structures is required to confirm and extend these findings.

The Engraftment Process

We cannot yet distinguish among several scenarios regarding the nature of the cells that actually engraft. For example, engraftment by mitotic, uncommitted progenitors may produce progeny that differentiate in response to position-dependent microenvironmental cues. Alternatively, committed mitotic progenitors may engraft and produce progeny that differentiate following migration. Engraftment may also occur by differentiated postmitotic cells that migrate to their appropriate loci, or there may be a selection by the microenvironment among many postmitotic cells that randomly distribute. Our analyses of animals shortly following transplantation suggest that a scenario in which postmitotic cells are the only cells that engraft is rather unlikely. When the animals were examined within a few days of transplantation, a relatively small number of cells actually seemed to appose the EGL. Furthermore, a small percentage of the inoculum actually integrated and appeared to migrate. In situations in which large numbers of transplanted cells were ultimately seen at adulthood, we favor the hypothesis that mitotic cells, rather than many postmitotic cells, engrafted, replicated, and differentiated in response to particular microenvironmental cues. However, because injections may vary from animal to animal, it is possible that animals with large numbers of engrafted cells, by chance, received an inoculum that was in some way more efficient with respect to placement and/or survival of postmitotic cells. Furthermore, there is some indication that even cells that express differentiation-specific markers, including NF, may continue to divide (Flyder et al., 1990). As efficiency and uniformity of transplantation increase, these possibilities may be better distinguished by paired experiments wherein markers or inhibitors of mitotic activity are administered to cultures prior to transplantation and the number and phenotype of successfully engrafted cells are compared.

Ruling Out Viral Contamination

That staining at the microscopic level of transplant-derived cells, as well as their distribution, differs from that of cells labeled directly by injected virus actually provides some evidence that blue cells in transplant recipient brains are not due to viral contamination. Further reassurance was the demonstration that the viral insertion site in the donor cell line was identical to that in blue cells recovered from the engrafted animals. In addition, multiple tests for production of BAG virus by C27 and C17 were run and found to be uniformly negative.

Long-Term Expression of an Exogenous Gene

Implicit in these studies is evidence for successful expression of an exogenous gene (*lacZ*) following incorporation of transplanted neural tissue. In some cases, expression could be demonstrated after 22 months (e.g., Figures 1F and 1G; Figures 4–6). While histochemistry allows us to infer positive expression in blue cells, we cannot rule out the possibility that some “white” cells are also transplanted derived but fail to express the *lacZ* gene at levels detectable using the X-gal histochemistry. White cells appear within dishes of clonal *lacZ* cells spontaneously over time in the culture and appear to correlate with lack of expression from the viral LTR (S. Fields-Berry and C. L. Cepko, unpublished data). One interpretation of the higher apparent engraftment rate after short survival (56%) vs. long survival (8%) is that inactivation of β -galactosidase expression occurs at a significant frequency over time. Of course, alternative explanations, such as cell death, may also pertain. The availability of a genetic tag detectable by PCR will allow for an independent test of whether the cells are indeed present, but undetectable by X-gal histochemistry. The recent availability of an alternative marker gene that shows less loss of expression in culture may also circumvent the problem (e.g., alkaline phosphatase [Fields-Berry et al., 1992]).

myc Expression in the Cerebellum

The proto-oncogene *c-myc* is expressed in mouse cerebellar neurons at different levels during different developmental stages (Ruppert et al., 1986). It appears that progenitor cells accumulate *c-myc* message during proliferation and/or in preparation for differentiation. Down-regulation of *myc* expression is correlated with differentiation (Grip and Westphal, 1988; Morse et al., 1986). While it is obvious that tumors do not form, we do not know whether *v-myc* continues to be expressed following transplantation and differentiation of C27-3 or C17-2. However, studies in other systems (La Rocca et al., 1989; Palmieri et al., 1983) indicate that interaction of *v-myc*-transformed cells with normal cells in mixed cultures suppresses the transformed phenotype. In these cases, proliferation is suppressed and reexpression of the differentiated cellular program occurs, even without down-regulation of *v-myc* expression. Our experiments wherein cerebellar cell lines were cocultured with primary cerebellar cells seem to reproduce this phenomenon. The same phenomenon may occur *in vivo* following transplantation. Future studies will seek to determine the extent of *v-myc* expression in engrafted cells.

Future Directions

The potential of C27-3 and C17-2 can be further explored using a variety of transplantation recipients and protocols. The availability of murine mutants with specific cell-type deficiencies in the cerebellum will allow an additional test of the competence, potential, and fidelity of these lines via complementation experiments. Since the present studies did not examine whether these cells are committed or restricted to cerebellar fate, examination of engraftment of

lines in regions and at developmental periods other than those from which they were generated are being carried out to allow an assessment of this property. Preliminary evidence indicates that these lines may engraft in regions of the CNS outside the cerebellum (E. Y. Snyder, S. A. Arnold, and C. L. Cepko, unpublished data). Whether genes of reportedly site-specific expression are expressed by these lines in new locations might help to test hypotheses that hold that specification of the spatial domains of different cell populations during CNS development proceeds by the progressive expression or loss of expression of various regulatory genes. Availability of engraftable lines that can be stably transduced with exogenous genes and presumably manipulated by homologous recombination techniques to achieve other alterations of regulatory genes may facilitate functional tests of these regulatory events.

Experimental Procedures

Propagation of Cerebellar Cell Lines

Cerebellar cell lines were generated as previously described [Ryder et al., 1990]. Lines were grown in Dulbecco's modified Eagle's medium supplemented with 10% fetal calf serum (Gibco), 5% horse serum (Gibco), and 2 mM glutamine on poly-L-lysine (PLL) (Sigma) (10 μ g/ml)-coated tissue culture dishes (Corning). While the lines grew well on uncoated tissue culture dishes, the most successful differentiation and subsequent engraftment may be associated with prior plating on a PLL substrate. The lines were maintained in a standard humidified, 37°C, 5% CO₂-air incubator and were either fed weekly with one-half conditioned medium from confluent cultures and one-half fresh medium or split (1:10 or 1:20) weekly or semiregularly into fresh medium. Changes in brand of tissue culture plastic, type of substrate coat, and type and concentration of serum might change the phenotypes displayed by the lines. Lines appeared to engraft most successfully when, prior to transplantation, they were in an active growth phase; yielded process-bearing cells; displayed immunocytochemical neural cell type-specific markers (e.g., NF and/or GFAP); and, for purposes of detection, when they had >50% of their cells positive with X-gal.

Immunocytochemistry

The markers routinely chosen were those that have been well-associated with differentiated neurons—NF (Wood and Anderton, 1981; monoclonal antibody BA1, courtesy of C. Barnstable)—and with differentiated glial cells—galactosyltransferase C for oligodendrocytes (Raff et al., 1978; hybridoma supernatant courtesy of B. Renshaw) and GFAP for astrocytes (Bignami et al., 1972; monoclonal antibody from Boehringer). Dilutions of NF (1:100) and GFAP (1:4) were in Dulbecco's modified Eagle's medium supplemented with 10% goat serum, 0.3% Triton X-100, and 0.05% azide; anti-galactosyltransferase C hybridoma supernatant was used undiluted. The secondary antibody was fluorescein- or biotin-conjugated goat α -mouse. A monoclonal antibody directed against an irrelevant antigen served as a negative control for nonspecific staining. Immunofluorescence methodology was outlined in Ryder et al. (1990). When immunoperoxidase or immunohistochemical phosphatase staining was desired, the ABC kit and procedures from Vector Laboratories were used (Fields-Berry et al., 1992). For staining of tissue sections, tissue was first dehydrated through graded alcohols and xylenes, embedded in paraffin at 60°C, sliced into 1 μ m sections on a Reichert-Jung BIOCUT microtome, transferred to heated (80°C) 1%–3% gelatin-coated slides, deparaffinized and rehydrated through reverse-graded xylenes and alcohols, and stained for immunocytochemistry as for cultured cells using the immunoperoxidase or immunohistochemical phosphatase method. If double labeling of X-gal⁺ cells and cell type-specific markers was desired, the X-gal reaction was performed first on glutaraldehyde-fixed tissue, prior to embedding in paraffin. To examine isolated, individual cells from a 1 μ m tissue section that had been analyzed immunohistochemically, the section was mechanically dissociated by “squashing,” i.e., placing gently but firm,

concentrated pressure on the portion of coverslip overlying the section, in planes both perpendicular and parallel to the section.

Transduction of Cerebellar Progenitor Lines with IecZ Gene
A recent 1:10 split of the cell line of interest was plated onto 60 mm tissue culture plates. Between 24 and 48 hr after plating, the cells were infected with the replication-incompetent retroviral vector BAG (10^6 colony-forming units [c.f.u.]) plus 8 μ M polybrene for 1–4 hr. Cells were then cultured in fresh feeding medium for approximately 3 days until they appeared to have undergone at least two doublings. The cultures were then trypsinized and seeded at low density (500–5000 cells on a 100 mm tissue culture dish). After approximately 2 weeks, well-separated colonies were isolated by brief exposure to trypsin within plastic cloning cylinders. Colonies were plated in 24-well PLL-coated Costar plates. At confluence, these cultures were passaged to 60 mm tissue culture dishes and expanded. A representative dish from each subclone was stained directly in the culture dish using X-gal histochemistry (see Price et al., 1987; Cepko, 1989a, 1989b). The percentage of blue cells was counted under the microscope. Subclones with the highest percentage of blue cells (ideally >90%; at least >50%) were maintained, characterized, and used for transplantation.

Tests for Virus Transmission

The presence of helper virus was assayed by measurement of reverse transcriptase activity in supernatants of cell lines as described by Goff et al. (1981) and by testing the ability of supernatants to infect NIH 3T3 cells and generate G418-resistant colonies or X-gal⁺ colonies (detailed in Cepko, 1989a, 1989b). All cerebellar cell lines used for transplantation were helper virus-free as judged by these methods.

Coculture of Neural Cell Lines with Primary Cerebellar Tissue

Primary dissociated cultures of neonatal mouse cerebellum were prepared as in Ryder et al. (1990) and seeded at a density of 2×10^4 to 4×10^4 cells per PLL-coated alpha-chamber LabTek glass or plastic slide (Miles). After the cells settled (usually 24 hr), 10% of a nearly confluent 10 cm dish of the neural cell line of interest was seeded, following trypsinization, onto the slide. The coculture was re-fed every other day and grown in a 5% CO₂-air, humidified incubator until 8 or 14 days of coculture. It was then fixed and processed for X-gal histochemistry (detailed in Price et al., 1987; Cepko, 1989a, 1989b).

Preparation of Cell Lines for Transplantation

Cells from a nearly confluent but still actively growing dish of donor cells were washed twice with phosphate-buffered saline (PBS), trypsinized, gently triturated with a wide-bore pipette in serum-containing medium (to inactivate the trypsin), gently pelleted (1100 rpm for 1 min in a clinical centrifuge), and resuspended in 5 ml of PBS. Washing by pelleting and resuspension in fresh PBS was repeated twice, with the cells finally resuspended in a reduced volume of PBS to yield a high cellular concentration (at least 1×10^6 cells per μ l). Trypan blue (0.05% [w/v]) was added to localize the inoculum. The suspension was kept well triturated, albeit gently, and maintained on ice prior to transplantation to minimize clumping.

Injections Into Postnatal Cerebellum

Newborn CD-1 or CF-1 mice were cryoanesthetized, and the cerebellum was localized by transillumination of the head. Cells were administered either via a Hamilton 10 μ l syringe with a beveled 33-gauge needle or a drawn glass micropipette with a 0.75 mm inner diameter and 1.0 mm outer diameter generated from borosilicate capillary tubing (FHC, Brunswick, ME) by a Fleming Brown Micropipette Puller (Model p-87, Sutter Instruments) using the following parameters: heat 750, pull 0, velocity 60, time 0. Best results were achieved with the glass micropipette. The tip was inserted through the skin and skull into each hemisphere and vermis of the cerebellum where the cellular suspension was injected (usually 1–2 μ l per injection). Typically, the following situation existed: 1×10^6 cells per ml of suspension; 1×10^4 to 2×10^4 cells per injection; one injection in each cerebellar hemisphere and in the vermis. Importantly, the cellular suspension, maintained on ice throughout, was gently triturated prior to each injection in order to diminish clumping and to keep cells suspended.

The injection of BAG virus was performed as described for the cell

suspension. The BAG virus stock (8×10^4 G418-resistant c.f.u./ml) contained, in addition to trypsin buffer, polybrene at 8 μ M/ml.

Processing of Tissue for β -Galactosidase Histochemical Detection by Light Microscopy

Mice were killed by barbiturate or ketamine overdose and perfused first with 10 ml of PBS (pH 7.3), MgCl₂ (2 mM), EGTA (2 mM) followed by 30 ml of 2% paraformaldehyde in 0.1 M PIPES buffer (pH 8.9), MgCl₂ (2 mM), EGTA (2 mM) for over 30 min. β -Galactosidase activity was detected by incubation of the tissue in 5-bromo-4-chloro-3-indolyl β -D-galactoside (X-gal) as detailed in Cepko (1989a, 1989b). Cellular location and morphology in tissue sections were enhanced as needed with Nomarski optics permitting reliable cell-type identification within cerebellum (Paley and Chan-Petey, 1974).

Electron Microscopy of Tissue Reacted for X-Gal Histochemistry

Processing of tissue for X-gal histochemistry was as previously described (Cepko, 1989a, 1989b), except that all fixation of experimental tissue, including the fix for perfusion of animals, was performed with a modified Karnovsky's Fixative (2% paraformaldehyde, 2.5% glutaraldehyde, 4.1% sucrose in PIPES) without the addition of detergents but with MgCl₂ (2 mM) and EGTA (2 mM). Rather than embedding frozen tissue in OCT embedding compound for cryostat sectioning, the tissue was sliced into 100 μ m coronal sections using a McIlwain tissue chopper (Brinkmann) or into 0.2–0.5 mm parasagittal sections under a dissecting scope using razor blades. These tissue slices were processed as floating sections using X-gal histochemistry. It was possible, under these conditions, to obtain adequate staining of labeled cells with no background if embedded as soon as possible (within 3 days). The cells were located under a dissecting scope (50 \times), and the appropriate tissue slice was selected for further processing for electron microscopy, using standard techniques. Briefly, the tissue was reacted with 1% osmium tetroxide in PBS (w/v), washed well in PBS followed by distilled water, stained en bloc in 1% uranyl acetate in distilled water (pH), dehydrated through graded alcohols, exposed for 10 min to propylene oxide and to propylene oxide plus accelerated (DMP-30) epon-araldite (1:1) for a length of time from 15 min to overnight (shorter times optimal), and embedded in accelerated epon-araldite from which ultrathin sections were cut and transferred to Formvar-coated slot grids. (Multiple absolute ethanol washes was an alternative dehydration technique.) The grids were not further reacted with lead citrate or uranyl acetate. They were observed on a Joel 1000C electron microscope, and photomicrographs were taken at 80 kV and spot size 1 with the smallest objective aperture. The X-gal reaction product (5-bromo-4-chloro-3-indolyl precipitate) examined in this fixation was electron dense, allowing identification of transplanted cells (Bonnerot et al., 1987). Cells were evaluated only if they contained label that was confined to subcellular organelles and/or respected membranes. Excellent fixation is required to identify postsynaptic specializations on GC dendrites. One of the 4 positive animals examined ultrastructurally (Table 1) met this criterion, permitting the successful identification of synapses. Fixation in the remaining 3 animals was inadequate to assess the presence or absence of synapses. To measure the width of such intermediate filaments as GFs and NFs, fibers were magnified to the equivalent of 74,000 \times , printed on photographic paper, and measured directly. As an internal control for calibration error within the microscope, the populations of GFs and NFs measured were from the same negative. The average width of GFs was 8.4 nm (expected: 8–9 nm), the average width of NFs was 11.1 nm (expected: 10–12 nm), values acceptable within the 10%–20% calibration error of the microscope. The width ratio of GFs to NFs was within the expected 70%–80% range, verifying internal consistency.

Determination of Integration Sites in Engrafted Cells by the PCR

Genomic DNA from the cell line C273 was prepared by standard techniques (Maniatis et al., 1982). Because the integrated proviral LTR contained no recognition sites for TaqI, digestion with TaqI endonuclease yielded fragments that included the LTR and unique portions of the host flanking sequences. DNA fragments were then ligated into circles using T4 DNA ligase (New England Biolabs) at a final DNA concentration of 1 ng/ μ l in ligation buffer. The DNA (10 ng) was then

emplified by an "inverse PCR" (Ochman et al., 1988): the ligated DNA circles were religated by digestion with XbaI (New England BioLabs), which cuts once in the LTR, and the fragments were then amplified using two oppositely oriented oligonucleotide primers within the LTR on opposite sides of the XbaI site (primer #21: TCTCTCTGAGT-GATTGACTACCCGTCAGC; primer #22: TGATCTGAACCTCTCTCT-TATTTCTCAGTTATGT). The amplified fragment was sequenced following introduction into the Msp18 site of an M13 cloning vector (Pharmacia), and the flanking sequences were identified. Two oligonucleotides of 27 bp, complementary to portions of this now known flanking sequence and progressively closer to the LTR, were synthesized on an Applied Biosystems Oligonucleotide Synthesizer (primer #1: GGCCTACTTCTTCTCTCCGAGTGG; primer #2: GAGCAGTGC-CAGGATTTCTGATTTCTCAGC). These served as one-half of a set of primers for subsequent direct nested PCR against opposing primers within the LTR (primer #21: sequence as above; primer #2: AGTTGCATCC-GACTTGTGGTCTCGCTGTTT).

After histochemical processing of a transplant recipient's cerebellum for X-gel⁺ cells, small pieces of tissue, each containing 1–20 blue cells, were dissected from various regions and transferred to separate wells of a Falcon Microtest III Flexible Assay Plate, containing 10 μ l of a mixture of 200 μ g/ml proteinase K, 0.5% Tween 20, 1.5 mM MgCl₂, 50 mM KCl, and 10 mM Tris buffer (pH 8.3). After incubation at 65°C for 30 min, the protease was inactivated at 85°C for 20 min. The following were then added: PCR buffer (1.2 mM MgCl₂, 10 mM Tris buffer (pH 8.3), 50 mM KCl), deoxyribonucleotides (final concentration, 200 μ M each), 0.5 U of Taq DNA polymerase (Cetus), and 1 μ M each of a pair of oppositely oriented oligonucleotide primers (one in the flanking region [primer #1], the other within the LTR [primer #26]). Following 45 cycles of PCR amplification (1 cycle consisted of 94°C for 45 s, 60°C for 45 s, and 72°C for 2 min), a 5 μ l aliquot from each of the first reaction products was used in a second PCR amplification (25–35 cycles) employing a second set of oligonucleotides internal to the first (a "nested amplification") (primer #2 and primer #21) (Mullis and Faloona, 1989). Samples of genomic DNA from the cell line served as positive controls. Cerebella from littermates in which engraftment failed (no blue cells), unengrafted cerebella, and samples containing no tissue served as negative controls. At least 10 μ l of amplified product from the second amplification was electrophoresed on a 3% NuSieve-1x⁺ SeaKem agarose gel plus 1 μ g/ml ethidium bromide with Tris-acetate-EDTA or Tris-borate-EDTA buffer (as per Maniatis et al., 1982). Bands of the appropriate size were identified using ethidium bromide staining.

Acknowledgments

This work was supported in part by grants to E. Y. S. from the National Institute of Neurological Disorders and Stroke (Clinical Investigator Development Award 5-K08-NS01403-02) and from the William Randolph Hearst Foundation. Support also came from the Seerle Scholars Program to C. L. C. and the Dana Foundation to C. W.

We thank Drs. Elizabeth Hay at Harvard Medical School and Marian DiFiglia at the Neuroscience Center at Massachusetts General Hospital who kindly made available their EM facilities. We are deeply indebted to Dr. Sanford L. Palay for generously sharing with us his expertise in the ultrastructure of the cerebellum, helping us to evaluate our EM material, and aiding us in the identification of cerebellar structures. We are also grateful to Dr. Elio Ravits for invaluable advice on the preparation and assessment of our material.

The costs of publication of this article were defrayed in part by the payment of page charges. This article must therefore be hereby marked "advertisement" in accordance with 18 USC Section 1734 solely to indicate this fact.

Received June 27, 1991; revised October 23, 1991.

References

Altman, J. (1982). Morphological development of the rat cerebellum and some of its mechanisms. In *The Cerebellum: New Views*, S. L. Palay and V. Chen-Palay, eds. (Heidelberg: Springer-Verlag), pp. 8–49.

- Austin, C. P., and Cepko, C. L. (1990). Cellular migration patterns in the developing mouse cerebellar cortex. *Development* 110, 713–732.
- Baroffio, A., Dupin, E., and Le Douarin, N. M. (1988). Clone-forming ability and differentiation potential of migratory neural crest cells. *Proc. Natl. Acad. Sci. USA* 85, 5325–5329.
- Barry, D. I., Kikavade, I., Brundin, P., Bolwig, T. G., Björklund, A., and Lindvall, O. (1987). Grafted noradrenergic neurons suppress seizure development in kindling-induced epilepsy. *Proc. Natl. Acad. Sci. USA* 84, 8712–8715.
- Bartlett, P. F., Reid, H. H., Bailey, K. A., and Bernard, O. (1968). Immortalization of mouse neural precursor cells by the c-myc oncogene. *Proc. Natl. Acad. Sci. USA* 65, 3255–3259.
- Bignami, A., Eng, L. F., Dehl, D., and Uyeda, C. T. (1972). Localization of the glial fibrillary acidic protein in astrocytes by immunofluorescence. *Brain Res.* 43, 429–435.
- Birren, S. J., and Anderson, D. J. (1990). A v-myc-immortalized sympathetic progenitor cell line in which neuronal differentiation is initiated by FGF but not NGF. *Neuron* 4, 189–201.
- Björklund, A., Steneli, U., Dunnett, S. B., and Gage, F. H. (1982). Cross-species neural grafting in a rat model of Parkinson's disease. *Nature* 298, 652–654.
- Bonnerot, C., Rocencourt, D., Briand, P., Grimmer, G., and Nicolas, J.-F. (1987). A β -galactosidase hybrid protein targeted to nuclei as a marker for developmental studies. *Proc. Natl. Acad. Sci. USA* 84, 6795–6799.
- Buzsáki, G., Ponomareff, G., Bayardo, F., Shaw, T., and Gage, F. H. (1988). Suppression and induction of epileptic activity by neuronal grafts. *Proc. Natl. Acad. Sci. USA* 85, 9327–9330.
- Cepko, C. L. (1988). Retrovirus vectors and their applications in neurobiology. *Neuron* 1, 345–353.
- Cepko, C. L. (1989a). Retrovirus-mediated immortalization of neural cells. *Annu. Rev. Neurosci.* 12, 47–65.
- Cepko, C. L. (1989b). Lineage analysis and immortalization of neural cells via retrovirus vectors. In *Neuron methods*, vol. 16, Molecular Neurobiological Techniques, A. A. Boulton, G. B. Baker, and A. T. Campagnoni, eds. (Clifton, New Jersey: Humana Press), pp. 177–219.
- Davidson, D., Graham, E., Sime, C., and Hill, R. (1988). A gene with sequence similarity to *Drosophila engrailed* is expressed during the development of the neural tube and vertebrate in the mouse. *Development* 104, 305–316.
- Davis, C. A., Noble-Topham, S. E., Rossant, J., and Joyner, A. L. (1988). Expression of the homeobox-containing gene *En-2* delineates a specific region of the developing mouse brain. *Genes Dev.* 2, 361–371.
- Ecclies, J. C., Ito, M., and Szentogothai, J. (1967). *The Cerebellum As a Neuronal Machine* (New York: Springer-Verlag).
- Evrad, C., Borge, I., Marin, P., Gellana, B. E., Premont, J., Gros, F., and Rouget, P. (1990). Immortalization of bipotential and plastic glial-neuronal precursor cells. *Proc. Natl. Acad. Sci. USA* 87, 3062–3066.
- Fields-Berry, S. C., Halliday, A. L., and Cepko, C. L. (1992). Novel recombinant retrovirus encoding alkaline phosphatase confirms clonal boundary assignment in lineage analysis of murine retina. *Proc. Natl. Acad. Sci. USA*, in press.
- Fisher, L. J., Jinnah, H. A., Kale, L. C., Higgins, G. A., and Gage, F. H. (1991). Survival and function of intrastrially grafted primary fibroblasts genetically modified to produce L-dopa. *Neuron* 6, 371–380.
- Fredericksen, K., Jat, P. S., Valtz, N., Levy, D., and McKay, R. (1988). Immortalization of precursor cells from the mammalian CNS. *Neuron* 1, 439–448.
- Freund, T. F., Bolam, J. P., Björklund, A., Steneli, U., Dunnett, S. B., Powell, J. F., and Smith, A. D. (1985). Efferent synaptic connections of grafted dopaminergic neurons reinnervating the host neostriatum: a tyrosine hydroxylase immunocytochemical study. *J. Neurosci.* 5, 603–616.
- Gage, F. H., and Fisher, L. J. (1991). Intracerebral grafting: a tool for the neurobiologist. *Neuron* 6, 1–12.

- Gege, F. H., Dunnnett, S. B., Stenevi, U., and Bjorklund, A. (1983). Aged rats: recovery of motor impairments by intrastriatal nigral grafts. *Science* 221, 966-968.
- Gallioe, D. S., Gray, G. E., Owens, G. C., Mejors, J., and Sanas, J. R. (1990). Neurons and glia arise from a common progenitor in chicken optic tectum: demonstration with two retroviral and cell-type specific antibodies. *Proc. Natl. Acad. Sci. USA* 87, 458-462.
- Geller, H. M., and Dubois-Dalq, M. (1988). Antigenic and functional characterization of a rat central nervous system-derived cell line immortalized by a retroviral vector. *J. Cell Biol.* 107, 1977-1986.
- Goff, S., Traktman, P., and Baltimore, D. (1981). Isolation and properties of Moloney murine leukemia virus mutants: use of a rapid assay for release of virion reverse transcriptase. *J. Virol.* 38, 239-248.
- Greval, C., Leclerc, N., Refrafi, J., Sasseville, R., Thivierge, L., and Hawkes, R. J. (1987). Monoclonal antibodies reveal the global organization of the cerebellar cortex. *J. Neurosci. Meth.* 21, 145-157.
- Grey, G. E., Glover, J. C., Mejors, J., and Sanas, J. R. (1988). Radial arrangement of clonally related cells in the chicken optic tectum: lineage analysis with a recombinant retrovirus. *Proc. Natl. Acad. Sci. USA* 85, 7356-7360.
- Grieg, A. E., and Westphal, H. (1988). Antisense myc sequences induce differentiation of F9 cells. *Proc. Natl. Acad. Sci. USA* 85, 6806-6810.
- Hellonot, M. E. R., Treille, M.-A., and Le Douarin, N. M. (1990). A new approach to the development of the cerebellum provided by the quail-chick marker system. *Development* 108, 19-31.
- Hetten, M. E., Liem, R. K. H., and Mason, C. A. (1986). Weever mouse cerebellar granule neurons fail to migrate on wild-type astroglial processes. *In vitro*. *J. Neurosci.* 6, 2678-2683.
- Holt, C. E., Bertsch, T. W., Ellis, H. M., and Harris, W. A. (1988). Cellular determination in the Xenopus retina is independent of lineage and birth date. *Neuron* 1, 15-26.
- Isacson, O., Dunnnett, S. B., and Bjorklund, A. (1986). Graft-induced behavioral recovery in an animal model of Huntington disease. *Proc. Natl. Acad. Sci. USA* 83, 2728-2732.
- Joyner, A. L., Herrup, K., Auerbach, B. A., Davis, C. A., and Rossant, J. (1991). Subtle cerebellar phenotype in mice homozygous for a targeted deletion of the *En-2* homeobox. *Science* 251, 1239-1243.
- Labbe, R., Firt, A., Mufson, E. J., and Stein, D. G. (1983). Fetal brain transplants: reduction of cognitive deficits in rats with frontal cortex lesions. *Science* 221, 470-472.
- La Rocca, S. A., Grosel, M., Felcone, G., Alem, S., and Tatò, F. (1989). Interaction with normal cells suppresses the transformed phenotype of v-myc-transformed quail muscle cells. *Cell* 58, 123-131.
- Laber, S. M., Brediova, S. M., and Sanas, J. R. (1990). Lineage, arrangement, and death of clonally related motoneurons in chick spinal cord. *J. Neurosci.* 10, 2451-2462.
- Lund, R. D., Rao, K., Henkin, M. H., Kunz, H. W., and Gill, T. J., III (1987). Transplantation of retinal and visual cortex to rat brains of different ages. Maturation, connection patterns, and immunological consequences. *Ann. NY Acad. Sci.* 495, 227-241.
- Menietti, T., Fritsch, E. F., and Sambrook, J. (1982). *Molecular Cloning: A Laboratory Manual* (Cold Spring Harbor, New York: Cold Spring Harbor Laboratory).
- McConnell, S. K. (1985). Migration and differentiation of cerebral cortical neurons after transplantation into the brains of ferrets. *Science* 229, 1268-1271.
- McConnell, S. K. (1986). Fate of visual cortical neurons in the ferret after isochronic and heterochronic transplantation. *J. Neurosci.* 6, 945-974.
- Mila, I., and Sidman, R. L. (1961). An autoradiographic analysis of histogenesis in the mouse cerebellum. *Exp. Neurol.* 4, 277-296.
- Morse, H. C., Hartley, J. W., Fredrickson, T. N., Yetter, R. A., Majumder, C., Cleveland, J. L., and Rapp, U. R. (1986). Recombinant murine retroviruses containing avian v-myc induce a wide spectrum of neoplasms in newborn mice. *Proc. Natl. Acad. Sci. USA* 83, 6868-6872.
- Mullis, K. B., and Faloone, F. A. (1989). Specific synthesis of DNA in vitro via a polymerase catalyzed chain reaction. *Math. Enzymol.* 155, 335-350.
- Ochman, H., Gerber, A. S., and Hartl, D. L. (1988). Genetic applications of an inverse polymerase chain reaction. *Genetics* 120, 821-823.
- O'Leary, D. D. M., and Stanfield, B. B. (1989). Selective elimination of axons extended by developing cortical neurons is dependent on regional locale: experiments utilizing fetal cortical transplants. *J. Neurosci.* 9, 2230-2248.
- Paley, S. L., and Chan-Palay, V. (1974). *Cerebellar Cortex, Cytology and Organization* (Heidelberg: Springer-Verlag).
- Palmieri, S., Kahn, P., and Gref, T. (1983). Quail embryo fibroblasts transformed by four v-myc-containing virus isolates show enhanced proliferation but are nontransforming. *EMBO J.* 2, 2385-2389.
- Peters, A., Paley, S. L., and Webster, H. D. (1991). *The Fine Structure of the Nervous System, Neurons and Their Supporting Cells*, third edition (Oxford: Oxford University Press).
- Price, J., Turner, D. L., and Cepko, C. L. (1987). Lineage analysis in the vertebrate nervous system by retrovirus-mediated gene transfer. *Proc. Natl. Acad. Sci. USA* 84, 158-160.
- Raff, M. C., Mirsky, R., Fields, K. L., Lisak, R. P., Dorfman, S. H., Silberberg, D. H., Gregson, N. A., Leibowitz, S., and Kennedy, M. C. (1978). Galactocerebroside is a specific cell-surface antigenic marker for oligodendrocytes in culture. *Nature* 274, 813-816.
- Rakic, P. (1971). Neuron-glia relationship during granule cell migration in developing cerebellar cortex. A Golgi and electron microscopic study in *Macaca rhesus*. *J. Comp. Neurol.* 141, 283-312.
- Renfranz, P. J., Cunningham, M. G., and McKay, R. D. G. (1991). Region-specific differentiation of the hippocampal cell line HB5 upon implantation into the developing mammalian brain. *Cell* 66, 713-729.
- Rosenberg, M. B., Friedmann, T., Robertson, R. C., Tuszynski, M., Wolff, J. A., Breakefield, X. O., and Gage, F. H. (1988). Grafting genetically modified cells to the damaged brain: restorative effects of NGF expression. *Science* 242, 1575-1578.
- Ruppert, C., Goldowitz, D., and Wille, W. (1986). Proto-oncogene c-myc is expressed in cerebellar neurons at different developmental stages. *EMBO J.* 5, 1897-1901.
- Ryder, E. F., Snyder, E. Y., and Cepko, C. L. (1990). Establishment and characterization of multipotent neural cell lines using retrovirus vector-mediated oncogene transfer. *J. Neurobiol.* 21, 356-375.
- Schaper, A. (1987). The earliest differentiation in the central nervous system of vertebrates. *Science* 5, 430-431.
- Smeyne, R. J., and Goldowitz, D. (1989). Development and death of external granular layer cells in the weaver mouse cerebellum: a quantitative study. *J. Neurosci.* 9, 1608-1620.
- Sotelo, C., and Alvarado-Mallart, R. M. (1986). Growth and differentiation of cerebellar suspensions transplanted into the adult cerebellum of mice with hereditary degenerative ataxia. *Proc. Natl. Acad. Sci. USA* 83, 1135-1139.
- Sotelo, C., and Alvarado-Mallart, R. M. (1987). Embryonic and adult neurons interact to allow Purkinje cell replacement in mutant cerebellum. *Nature* 327, 421-423.
- Stanfield, B. B., and O'Leary, D. D. M. (1985). Fetal occipital neurons transplanted to the rostral cortex can extend and maintain a pyramidal tract axon. *Nature* 313, 135-137.
- Temple, S. (1989). Division and differentiation of isolated CNS blast cells in microculture. *Nature* 340, 471-473.
- Turner, D. L., and Cepko, C. L. (1987). A common progenitor for neurons and glia persists in rat retina late in development. *Nature* 328, 131-136.
- Turner, D. L., Snyder, E. Y., and Cepko, C. L. (1990). Lineage-independent determination of cell type in the embryonic mouse retina. *Nature* 4, 833-845.
- Wahle, C., and Cepko, C. L. (1988). Clonally-related cortical cells show several migration patterns. *Science* 241, 1342-1345.
- Weinstein, D. E., Sholanski, M. L., and Liem, R. K. (1990). C17, a retrovirally immortalized neuronal cell line, inhibits the proliferation of

astrocytes and astrocytoma cells by a contact-mediated mechanism. *Glia* 3, 130-139.

Wetts, R., and Fraser, S. E. (1988). Multipotent precursors can give rise to all major cell types of the frog retina. *Science* 239, 1142-1145.

Wood, J. N., and Anderton, B. H. (1981). Monoclonal antibodies to mammalian neurofilaments. *Biosci. Rep.* 1, 263-268.

Note Added in Proof

Please direct inquiries to the present address of E. Y. Snyder: Harvard Medical School, c/o Children's Hospital, 300 Longwood Avenue, 248 Enders, Boston, Massachusetts 02115.

Immortalizing oncogenes subvert the establishment of granule cell identity in developing cerebellum

Wei-Qiang Gao* and Mary E. Hatten

The Rockefeller University, 1230 York Avenue, New York, NY 10021-6399, USA

*Present Address: Department of Neuroscience, Genentech, Inc., South San Francisco, CA 94080, USA

SUMMARY

After implantation into the external germinal layer of early postnatal cerebellum, primary external germinal layer progenitor cells gave rise exclusively to granule neurons. In contrast, all major classes of cerebellar cells were observed following implantation of embryonic day 13 cerebellar precursor cells into the external germinal layer. These results suggest that granule cells arise from precursors with a restricted potential. In contrast to results with the primary external germinal layer population, cell lines established from external germinal layer cells, by infection with a retrovirus containing the SV40 large T-antigen

oncogene, gave rise to several cerebellar cell types upon implantation. These included granule neurons, one subclass of stellate interneurons, Golgi cells, Bergmann glia and astrocytes. From these results, we conclude that early postnatal external germinal layer progenitors are normally fated to a granule cell identity and that expression of the SV40 large T-antigen oncogene subverts mechanisms that control granule neuron fate.

Key words: granule neuron, cerebellum, oncogene, cell lines, transplantation

INTRODUCTION

Current models of vertebrate neural fate specification derive from the hematopoietic system, where cell fate is established by the proliferation of pluripotent stem cells (Spangrude et al., 1988; Till and McCulloch, 1961), partial commitment of precursor cells to sublineages, amplified division of partially committed cells (Metcalfe, 1987), and final differentiation of cells within a given sublineage (Nicola and Johnson, 1982; Ogawa et al., 1983). Evidence for a hemopoiesis-like model for vertebrate neural cells has been obtained in studies on the neural crest cell population, including the sympathoadrenal sublineage (reviewed by Anderson, 1989). A general role for local signals in the establishment of CNS neural identity has been inferred from studies on neurological mutant mice (Heintz et al., 1993; Sidman, 1972), from CNS precursor cell transplantation studies (McConnell and Kaznowski, 1991), from the identification of diffusible factors that influence cell specification (Jessell and Melton, 1992) and from *in vitro* studies showing that close appositions among CNS precursor cells promote precursor cell division and restrict cell fate (Gao et al., 1991).

The cerebellar cortex is perhaps the best studied region of the CNS. For nearly a century, all of the cerebellar cell types have been recognized and their pattern of synaptic connections known. Much of this wealth of information was described by Ramon y Cajal from Golgi studies (1911), with information on the development (Altman and Bayer, 1978; Miale and Sidman, 1961; Altman and Bayer, 1985), anatomy (Palay and Chan-Palay, 1974), fiber tracts (Brodal, 1993) and circuitry (Llinas

and Hillman, 1969) of the cerebellum emerging over the past several decades. The basic plan of the cerebellar cortex includes three layers—two neuronal layers, the Purkinje cell layer (PCL) and the internal granule cell layer (IGL), and a superficial, plexiform layer, the molecular layer (ML). The PCL consists of a single row of Purkinje neurons situated at the upper margin of the IGL. The Purkinje neuron is easily distinguished by its large cell soma, elaborate, ascending dendrites, and single, descending axon. The IGL contains a vast number of granule neurons, calculated in the human cerebellar cortex to number 10^{11} (Kandel et al., 1991). The numerous, small granule neurons elaborate short, radiating dendrites in the IGL and project a unique 'T-shaped' axon up into the ML. The granule cell axons, termed parallel fibers, are densely stacked through the depth of the ML.

Within each of three cerebellar layers, interneurons can be discerned by their location and pattern of neuritic arborization. In the ML, as described by Ramon y Cajal (1911), the small, stellate interneurons can be seen. There are two subtypes of stellate cells, horizontally oriented stellate cells in the most superficial aspect of the ML and spiny stellate cells within the core and deeper aspect of the ML. In the PCL, the medium-sized basket cells radiate long, slender dendrites up into the ML and project horizontal axons across the PCL, forming dense pericellular baskets around Purkinje cell bodies. In the IGL, two types of interneurons can be seen. One, the Lugaro cell, is situated just beneath the Purkinje cells, extending long, horizontal processes that contact the descending Purkinje cell axons. The other, the Golgi cell, projects thin, ascending dendrites into the ML, and a thick skirt of axons down into the

IGL. In addition to these six types of cerebellar neurons, two classes of astroglial cells can be seen - the Bergmann glia, located just above the PCL with numerous, radial processes coursing to the pial surface, and astrocytes of the IGL. Although cerebellar glial cells (Hatten and Liem, 1981) and Purkinje cells (Ross et al., 1989) can be readily identified by cellular antigen markers, other cerebellar cells are classically identified by their size, laminar position and pattern of neuritic arborization.

Among cerebellar neurons, the granule cell presents an opportune model for studying CNS neuronal specification. Unlike the other five cerebellar neurons, the granule cell arises in a displaced proliferation zone, the external germinal layer (EGL) (Ramon y Cajal, 1911). Experimental chick/quail chimeras provide evidence that, whereas the other cerebellar neurons originate from the caudal aspect of the mesencephalon, the EGL arises from the rostral portion of the metencephalon via a complex series of transverse migrations. The distinct origin of the EGL (Hallonet et al., 1990; Hallonet and Le Douarin, 1992; Martinez and Alvarado-Mallart, 1989) raises the question as to whether granule cell identity is specified by regulatory factors, localized to the superficial germinal zone. In vitro studies with purified EGL precursors support the conclusion that the close apposition of granule cell precursors within the EGL restricts the fate of these progenitor cells to a granule cell identity (Gao et al., 1991). In the present study, we have further examined whether the EGL provides local signals that restrict precursor cells to a granule cell identity, by re-implanting labeled EGL precursors into the EGL and examining their laminar positioning and neuritic arborization after short survival times (1-7 days).

Another general approach to understanding the control of neural fate is to study progenitor cells immortalized by oncogene transfer. Although experiments in non-neuronal systems, including the hemopoietic system (Klinken et al., 1988), have cautioned against the use of immortalized cells in lineage analyses, the demonstration that immortalized CNS neuronal precursors would incorporate into developing brain, and differentiate into identifiable cell classes has suggested that immortalized CNS cells provide a convenient means of studying developmental processes in brain (for reviews see Cepko, 1988; Lendahl and McKay, 1990). However, as previous CNS cell lines have been generated by immortalizing a mixture of progenitor cells (e.g. Renfranz et al., 1992), it has not been possible to assess the effects of oncogene expression on the specification of the primary cell of a given CNS sub-lineage.

In the current study, we transferred the tsA58 allele of the SV40 large T antigen oncogene into purified early postnatal EGL precursor cells and compared the development of primary EGL cells with infected cells both in vitro and in vivo. To compare the fate of the cells, we implanted primary EGL cells and immortalized EGL cells into cerebellar EGL on postnatal day 6. After implantation, whereas primary EGL cells gave rise exclusively to granule neurons, immortalized cells gave rise to granule neurons, stellate interneurons, neurons and astroglia. In the same transplantation assay, precursor cells taken from the cerebellar primordium on embryonic day 13 (E13) generated Purkinje neurons, interneurons, granule neurons and astroglia after implantation into the early postnatal EGL. These results indicate that whereas E13 cells show multiple fates,

early postnatal EGL cells have a restricted potential, giving rise only to granule neurons. The control of precursor cell potential is apparently subverted by the expression of the SV40 large T-antigen oncogene as immortalized cells generate multiple programs of cell differentiation.

MATERIALS AND METHODS

Preparation of early postnatal EGL precursor cells and astroglia of embryonic day 13 cerebellar cells

The present experiments were carried out with primary cells from C57Bl/6j mouse cerebella harvested on the 5-6 postnatal days (P5-P6). EGL cells were purified as described previously (Gao et al., 1991; Hatten, 1985). Astroglial cells were purified from the same preparations used to harvest EGL cells, as described by Hatten, (1985). Cells from the E13 cerebellar analogue were prepared as described by Hatten and Sidman, (1978). Briefly, cerebella were incubated sequentially in 0.08% and 0.25% trypsin in CMF-PBS containing 0.02% EDTA for 15 minutes at 37°C each, after which soybean trypsin inhibitor (0.05 mg/ml in CMF-PBS containing 0.05 mg/ml DNase) was added. The tissue was then triturated and dissociated into single cells.

Implantation of EGL cells, astroglia, E13 cerebellar cells and immortalized EGL cells into P6 cerebellum

Prior to implantation, purified EGL cells, astroglial cells, E13 cerebellar cells or GC-B6 cells (see below) were labeled with green fluorescent latex microbeads (Lumafuor, Inc., NJ) in vitro for 1 hour at a dilution of 1:300 in the culture medium. The cells were then washed with medium or CMF-PBS for several times, collected in a test tube and stained with PKH-26 at a concentration of 4 μ M for 5 minutes (Zynaxis, Inc.; see Gao et al., (1992)). The labeled cells were then washed several times and suspended in DMEM + 9 mg/ml glucose in the presence of 20 mM Hepes buffer (pH 7.4). Approximately 25,000 cells were implanted into the EGL of P5-6 C57Bl/6j mice (Gao and Hatten, 1993). Prior to the cell implantation procedure, P6 mouse pups were rendered unconscious by chilling the animals at 4°C for 1-2 minutes and placed in a Stoelting stereotaxic device fitted with a neonatal rat adapter and a vertical holder for a Hamilton syringe (Wood Dale, IL). The skin overlying the midbrain and hindbrain was rinsed with alcohol, a small incision was made in the skin and the Hamilton syringe needle was lowered gently through the incision to a position just beneath the meninges (just above the EGL). The animals insensitivity to the surgical procedure was judged by their lack of movement. Approximately 1 μ l of the cell suspension (2.5 $\times 10^7$ cell/ml) was injected slowly on each side of the cerebellum, after which the syringe was removed, the skull was rinsed with a solution of penicillin-streptomycin (0.25%), and the skin was replaced and sealed with Vetbond (Henry Schein Inc). The animal was then warmed to 35.5°C and returned to the litter.

After survival of 1-7 days, animals were anaesthetized with ketamine prior to perfusion with 4% paraformaldehyde in 0.1 M phosphate buffer (pH 7.4). The cerebella were removed by dissection and post fixed in the same fixative prior to being washed in PBS and embedded in 3% agar gel. Serial sections (90-100 μ m) were cut with a vibratome and labeled cells were visualized with epifluorescence microscopy using a Zeiss Axiophot microscope fitted with phase contrast, Nomarski and epifluorescent illumination, Plan-neofluor 20x and 40x objectives and an Axiophot camera module.

To examine the extent of PKH-26 dye leakage and re-uptake, we double labeled cells with PKH-26 and microbeads and followed the incorporation of labeled cells. In a cell sample of several thousand cells, we did not observe a cell that was not double labeled, suggesting that the dye was not transferred from implanted, double-labeled cells to endogenous, unlabeled cells. As a further control, we labeled primary EGL cells with PKH-26, killed them by freezing and thawing

four times at -80°C , and implanted the dead, labeled cells into the P6 EGL. In those experiments, no PKH-26 labeled cells were seen distal to the site of injection, confirming previous findings (Gao et al., 1992; Gao and Hatten, 1993; Horan and Slezak, 1989) that the PKH-26 dye does not transfer to other cells in intact tissue.

In some experiments, cells were visualized with an Axiovert 135 microscope with DIC and epifluorescent illumination, Plan-Neofluor 20x objective, and a computer-driven (z-axis, Ludl system) stage. Images were acquired with a high-sensitivity Biorad MRC-600 scanning, imaging head controlled with an 80386 host computer with scan control and imaging acquisition and analysis system, using two detectors for acquisition of simultaneous Nomarski and fluorescence imaging. A 15 mW argon/krypton mixed gas multi-line mode laser with lines at 488, 568 and 647 was used for imaging of blue line excitation (FITC, Rhodamine 1,2,3). Images were stored on an optical disk, Ethernet-linked to a Silicon Graphics Iris computer system and printed on a Sony U-811 Video Printer System.

Immortalization of EGL cells using retroviral constructs

Purified EGL cells from P5-6 mouse cerebella were infected with conditioned medium from psi 2 cells packaging the retrovirus encoding *AS18/U197* antigen and neomycin, at a density of $10^6/\text{ml}$ in the presence of $8 \mu\text{g}/\text{ml}$ polybrene (Sigma) in a untreated culture dish. The virus-producing cells were kindly provided by R. McKay (NIH). After being infected twice (6 hours each time), the virus-containing medium was replaced with BME plus 10% horse serum, 5% fetal bovine serum, 9 mg/ml glucose, and cells were placed at 35°C for 2 days then transferred to a polylysine coated dish ($500 \mu\text{g}/\text{ml}$). Several days later, cultures were selected in the above medium containing G418 ($200 \mu\text{g}/\text{ml}$). The selection medium was replaced every 2 days, and G418-resistant colonies were observed in 2 weeks and picked with cloning rings. The clones were then expanded, frozen, subcloned, and cultured in DMEM plus 10% newborn calf serum. In the present experiments, although similar results were obtained from one of the other clones, only the data from subclone GC-B6 were described and used for transplantation.

Immunocytochemistry

Immunocytochemical labeling of primary EGL cells was as described previously (Gao et al., 1991). In the present experiments, GC-B6 cells were plated in 16-well lab-tak slides coated with poly-D-lysine ($0.1 \text{ mg}/\text{ml}$) (35°C , overnight) in either DMEM plus 10% newborn calf serum or serum-free medium (Redu-Ser II from Upstate Biotech Inc.) at 39°C for 16-24 hours before being fixed with 4% paraformaldehyde for 30 minutes. The cells were then incubated with antibodies against N-CAM (Thiery et al., 1977), kindly provided by Dr Christo Goridis (Marseilles), L-1 (Rathjen and Schachner, 1984), provided by Dr Carl Lagenauer (Pittsburgh), TAG-1 (Dodd et al., 1988), provided by Drs Jane Dodd and Thomas Jessell (Columbia), antibodies against the glial filament protein (GFAP; Hatten and Liem, 1981), provided by Dr Ronald Liem (Columbia), or with monoclonal antibody R24s, which is against GD3, generously provided by Dr James Goldman (Columbia). Antibodies were applied at 4°C overnight at 1:2-1:1000 in the presence of 3% normal goat serum, after which the cells were washed three times with CMF-PBS, then incubated with rhodamine or FITC-conjugated second antibodies (1:100) (Tago, Inc.) for 30 minutes at room temperature. For cytoplasmic antigens, 0.1% Triton X-100 was added to the staining saline. The preparations were then mounted in Gel/Mount (Bio-Medical Corp.) and visualized with a Zeiss Axiophot microscope fitted with phase contrast, Nomarski and epifluorescent illumination and Plan-neofluor 20x, or 40x objectives and an Axiophot camera module.

Co-culture of the immortalized EGL cells with the primary EGL cells

EGL cells were purified (Hatten, 1985) from P5-6 mouse cerebella and plated as a monolayer on a poly-D-lysine ($500 \mu\text{g}/\text{ml}$) coated 16-

well Lab-tak slide (1×10^6 cells/well) in serum-free medium (Redu-Ser II from Upstate Biotech Inc.) for 1 day. The GC-B6 cells were removed from the culture dish with trypsin-EDTA (Gibco), labeled with PKH-26 (Gao et al., 1992), washed, and plated ($3,000$ cells/well) on the top of the monolayer culture of primary EGL cells at low density in serum-free medium. 24-48 hours later, the culture was fixed with 4% paraformaldehyde in phosphate buffer (pH 7.4) for 30 minutes, and mounted in gel/mount (Biomedical Co.). The implanted cells were visualized with a Zeiss Axiophot microscope fitted with phase contrast, Nomarski and epifluorescent illumination and Plan-neofluor 40x objectives and an Axiophot camera module.

RESULTS

Previous in vitro analyses of primary EGL cells in reaggregate cultures (Gao et al., 1991; Gao et al., 1992) demonstrated that local interactions among EGL precursor cells promote granule cell neurogenesis and differentiation. A striking aspect of these studies was the finding that proliferating cells in homotypic reaggregate cultures had a restricted cell fate, expressing cellular antigen markers and morphological features of granule cells, but not other classes of cerebellar neurons (Gao et al., 1991). To examine the fate of purified EGL cells in vivo, we double-labeled purified EGL cells with fluorescent microbeads and PKH-26, injected them just beneath the pia of P6 animals, allowed the animals to survive for short periods of time (1-7 days), and examined the morphology and location of labeled cells in the cerebellar cortex. Using fluorescent and confocal microscopy it was found that labeled cells remained at the injection site during the first 1-24 hours in vivo, with some cells undergoing mitosis in the superficial aspect of the EGL, as evidenced by labeled, mitotic figures (not shown). 24-48 hours after implantation, primary EGL cells, characterized by their small ($4-6 \mu\text{m}$) size and globular shape, descended into the deeper aspect of the EGL, where they extended long fibers, $100-200 \mu\text{m}$ in length, parallel to the surface of the anlage (Fig. 1A). This sequence of developmental events confirmed the hypothesis of Ramon y Cajal, who suggested that granule cell axon extension precedes the inward migration of the cell soma (Ramon y Cajal, 1911).

A second stage of development commenced 48 hours after implantation, the polarization of the cell soma to extend a descending process perpendicular to the plane of parallel fiber extension (Fig. 1B). Following extension of this descending or 'leading process' (Edmondson and Hatten, 1987; Rakic, 1971; Ramon y Cajal, 1911), many of the implanted cells started to migrate along Bergmann glial fibers, requiring approximately 10-12 hours to reach the internal granule cell layer (IGL). During migration, the trailing process of labeled cells displayed an ascending 'T-shape' (Fig. 1C), characteristic of the granule cell axon. At low magnification, in a coronal plane of section, several dozen labeled cells could be seen migrating through the molecular layer (ML) and settling in the IGL (Fig. 1D). All of these cells expressed the morphology described in classical studies of Golgi-impregnated tissue (Ramon y Cajal, 1911).

After settling within the IGL, labeled cells extended four to six, short radiating dendrites, with branched claw-like endings, characteristic of mature granule cells. Among the more than 80 animals injected with several thousand labeled EGL cells each,

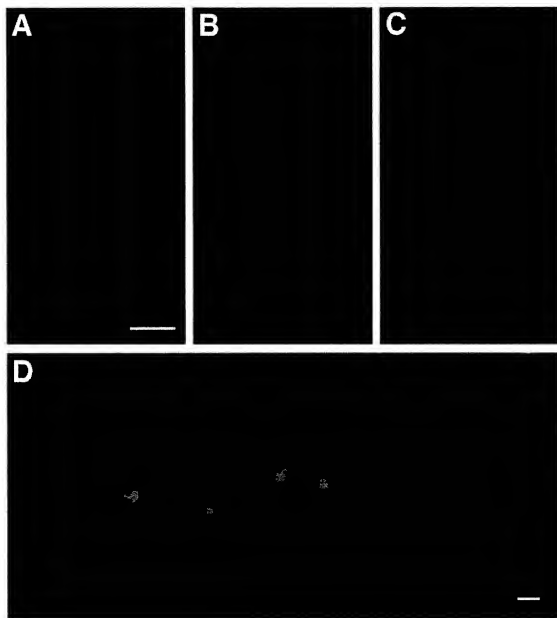


Fig. 1. Primary EGL cells differentiated exclusively into granule cells after re-implantation into the EGL of P6 mouse cerebellum. (A) 2 days after implantation, labeled cells extended long parallel fibers. (B) 3-4 days after implantation, labeled cells extended a descending migratory process and began to transit the molecular layer (ML), displayed morphological features of migrating cells (C). 6 days after implantation, labeled cells are positioned beneath the Purkinje cell layer, in the internal granule cell layer (IGL). The ascending axon of the labeled neuron formed a 'T-shape' characteristic of mature granule cells. Within the IGL, the cell extended 4-6 short, dendritic processes. (D) At lower magnification, all labeled cells in the field showed features of developing granule neurons. Fluorescence microscopy. Bar, 15 μ m.

and analyzed by serial sectioning of the brain, more than 99% of the cells that underwent differentiation expressed a granule neuron identity, positioning their soma in the IGL, forming 4-6 short dendrites, and extending an ascending 'T-shaped' parallel fiber into the molecular layer. Less than 0.5% of the differentiated cells we counted assumed the glial phenotype, consistent with the level of contamination of the cell preparation with glial cells. No other classes of cerebellar neurons

were observed after injection of labeled EGL cells (Table 1), suggesting that EGL precursor cells were normally fated to a granule cell identity.

By confocal microscopy, approximately 10-20% of the cells we injected into the host tissue differentiated as described. The same general distributions of cell types, were obtained in each of the 80 animals we injected with labeled cells. As a control, we implanted labeled, primary astroglial cells purified from

Table 1. Differentiation of implanted cells in developing cerebellum

Cells implanted	Classes of labeled cells observed			
	Granule neuron	Purkinje neuron	Interneurons	Bergmann glia
Primary EGL cells	99	0	0	<1
Primary astroglial cells	0	0	0	20-30
GC-B6 cells*	5-10	0	10-15	20-30
E13 cerebellar cells	10-15	30-40	10-20	10-20

Primary P6 EGL cells, P6 astroglia, GC-B6 or E13 cerebellar cells were implanted into the EGL on postnatal day 6 as described in the text. After 1-7 days in vivo, the morphology and position of labeled cells was used to classify them as granule neurons, Purkinje neurons, interneurons, Bergmann glia or astrocytes. The percentage of dye-labeled cells with the morphology and laminar position of specific cerebellar cell types is indicated.

* Approximately 30% of the implanted cells could not be identified.

P4-6 cerebellum, identified by their expression of GFAP, into the developing cerebellum. Purified glial cells differentiated into Bergmann glial cells (20-30%) and astrocytes (40-60%) after implantation into P6 cerebellar cortex. None of the labeled glial cells we injected differentiated into granule neurons or other types of cerebellar neurons (Table 1), suggesting that glial cell fate was specified prior to P6.

Implantation of primary E13 cerebellar cells generates all major classes of cerebellar cells

To test whether the early postnatal EGL contains local factors that inhibit the development of other classes of cerebellar neurons, including the Purkinje cell, we injected embryonic precursors of other types of cerebellar cells into the EGL and followed their development. As all other classes of cerebellar cells are thought to arise from the ventricular zone lining the IVth ventricle, between embryonic days 11 and 13 (Altman and Bayer, 1985; Miale and Sidman, 1961), we used the E13 cerebellar anlage as a source of cells. At this age, the anlage contains a mixture of postmitotic and proliferating Purkinje cell precursors, as well as proliferating precursors of other neurons, the emerging EGL, and glial precursor cells. To test whether this complex population of cells would generate all classes of cerebellar cells if placed in the EGL, we labeled the dissociated E13 cells with PKH-26, and injected them just beneath the pia of the cerebellar cortex of P6 animals. Implantation of E13 cerebellar precursor cells resulted in the appearance of all cerebellar cell types, including granule neurons with ascending, T-shaped axons (Fig. 2A), Bergmann glial cells with multiple, slender, ascending processes (Fig. 2B), Purkinje neurons with several thick ascending processes and one descending axon (Fig. 2C,D), and multiple classes of interneurons and astrocytes of the IGL and white matter (Table 1). Moreover, most of these differentiated implanted, primary precursor cells were positioned in the correct layer (Fig. 2). Immature Purkinje cells seen after implantation of E13 precursor cells resembled both young Purkinje cells in the process of migration (Fig. 2C) and cells that were settling into the Purkinje cell zone (Fig. 2D).

Among the E13 cells that differentiated after incorporation into the early postnatal EGL, approximately 10-15% of the cells expressed the features of granule neurons, 30-40% resembled Purkinje neurons, 10-20% formed interneurons and

20-40% astroglia. The granule cells we observed most likely originated in the lateral aspect of the E13 anlage, as the EGL is just beginning to emerge across the rhombic lip at this age. The observation of Purkinje neurons, interneurons and glial cells, after implantation of the cells harvested from the E13 cerebellar anlage suggests that local signals within the early postnatal EGL can support the differentiation of precursors of all of the principal classes of cerebellar neurons.

Infection of primary EGL cells with a replication-deficient retrovirus containing the *tsA58* allele of SV40 large T antigen oncogene

In order to examine the role of oncogene expression in the specification of granule cells, we infected purified, granule cell progenitors with a retrovirus carrying the *tsA58* allele of SV40 large T antigen oncogene and the neomycin gene (Renfanz et al., 1992). Retroviral transfer was carried out in reaggregated cultures under conditions where EGL cell proliferation occurs (Gao et al., 1991). As a first step, G418-resistant colonies were picked, expanded, and subcloned by standard limited dilution methods. Among several dozen clonal cell lines established, most generated cells that expressed neuronal antigen markers at the non-permissive temperature. We next tested the cell lines for their ability to differentiate in co-culture with primary neurons (see below) and their ability to rescue *weaver* granule neuron differentiation (not shown). As one of the clonal lines, GC-B6, expressed both of these properties of 'normal' granule neurons, this line was chosen for further study. As shown by immunostaining with a monoclonal antibody against large T antigen, all GC-B6 cells showed nuclear labeling of the large T antigen, demonstrating expression of the *tsA58* allele of SV40 large T antigen oncogene in EGL precursor cells (Fig. 3A,B).

At the permissive temperature, GC-B6 cells had either a flat or bipolar morphology when cultured on a surface treated with polylysine, laminin or Matrigel, and expressed low levels of neuronal or glial markers (see below). These cells underwent rapid proliferation with a cell generation time of approximately 12-14 hours. Shifting the cells to the non-permissive temperature (to allow differentiation) slowed proliferation to generation times of 48-72 hours. Although a large number of the cells became elongated at 39°C, neurite formation was not evident. Addition of growth factors (basic fibroblast growth factor, epithelial growth factor, insulin-like growth factor-1, nerve growth factor, brain-derived neurotrophic factor and neurotrophin 3) or medium conditioned by either granule cells or astroglia, did not induce neurite formation (not shown). Maximal differentiation, including the extension of slender, bipolar neurites, was seen when the cells were plated on a monolayer of purified, primary EGL cells (Fig. 4A,B), suggesting that EGL cells induce differentiation of the GC-B6 cell line by a mechanism that involves close cell apposition. This is consistent with previous findings on primary EGL cells (Gao et al., 1991).

Immunocytochemical characterization of the expression of cellular antigen markers by GC-B6 cells, cultured for 16-24 hours at the non-permissive temperature to allow differentiation of the cells, revealed heterogeneity within the population, with a subpopulation of cells expressing the germinal zone antigen GD3 (Goldman et al., 1984) (Fig. 3C,D). While all of the cells expressed the neuronal cell adhesion molecule

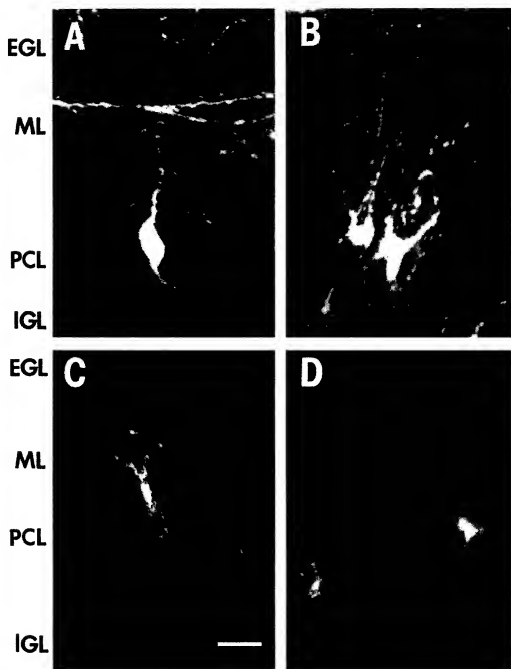


Fig. 2. Differentiation of embryonic cerebellar precursor cells after implantation into postnatal cerebellar EGL. (A) An implanted E13 cell differentiated into a cell with the morphological characteristics of a granule neuron, 3 days after implantation. (B) Several implanted cells extended multiple, ascending processes toward the pial surface, characteristic of Bergmann glial cells. (C,D) Cells resembling immature Purkinje neurons were evident. In C a cell resembling a migratory Purkinje cell, having thick ascending processes and a single, descending axon can be seen. D shows more differentiated forms of immature Purkinje cells, resembling those settling in the PC zone. In both cases, the cells were differentiating in an outside-in direction, backwards to the usual pattern seen when cells arise in the VZ and migrate inward to establish the Purkinje cell layer. Bar, 10 μ m.

(NCAM) (Thiery et al., 1977) (Fig. 3E,F), fewer than 5% expressed markers for differentiated granule cells, including the axonal glycoproteins L1 (Rathjen and Schachner, 1984) and TAG-1 (Dodd et al., 1988), the neuron-glia ligand astro-

tactin (Edmondson et al., 1988) (Fig. 3G,H), or the neurofilament protein (see Table 2). Instead, 20-30% of the cells within a given culture expressed the glial filament protein (GFAP), while a subpopulation of GFAP+ cells co-expressed the neu-

rofilament protein. Cells that expressed both neurofilament protein and GFAP were process-bearing cells, resembling astroglia. Thus, within clonal populations of immortalized EGL cells, a range of differentiated marker proteins were expressed by the cells in culture. The results with GC-B6 cells contrast with previous results on primary EGL precursor cells in which cells undergo neuronal differentiation, including neurite extension, cell migration in a number of different culture systems (Fishell and Hatten, 1991; Gao et al., 1991, 1992), and express neuronal but not glial cell markers in vitro (Gao et al., 1991).

Twenty-eight cell lines established by immortalizing purified EGL cells with retroviruses containing the temperature-sensitive large T antigen showed similar immunocytochemical heterogeneity. Although this was not investigated in detail, in the several cases where subcloning of clonal lines was carried out, heterogeneous populations of cells resulted. In addition, immortalization with E1A constructs containing the *v-myc* oncogene gave rise to clones of cells that generated both neuronal and glial progeny, as judged by cellular antigen marker expression (not shown).

Immortalized EGL cells have multiple fates after implantation into the EGL

We next examined the fate of GC-B6 cells in vivo, under environmental influences where primary EGL fate was restricted to a granule cell identity. As seen for primary cells, 24 hours after implantation many of the GC-B6 cells appeared to undergo proliferation at the superficial aspect of the EGL. Thereafter, GC-B6 cells descended into the deeper layers of the EGL and integrated into the host cerebellar cortex. In contrast to the primary EGL cells, which generated granule neurons exclusively, GC-B6 cells differentiated into several types of cells (see Table 2). A minority of the cells (5–10%) were identified as granule cells by their globular morphology, extension of parallel fibers, migratory profiles, and/or formation of an ascending T-shaped axon (Fig. 5A,B). In addition to granule neurons, interneurons, including stellate cells in the upper aspect of the ML (Fig. 5C) and Golgi neurons (Fig. 5D), could be identified by their laminar position and morphology (see Introduction).

A larger number of the immortalized cells, 20–30% of the differentiated population, differentiated into Bergmann glia, as evidenced by a somata 8–10 μ m in diameter, positioned just above the Purkinje cell layer, and the extension of multiple discrete fibers ascending vertically to the pial surface (Fig. 5F), giving the typical 'candelabrum' appearance of Bergmann cells. In addition, approximately 10–20% of the implanted cells were identified as astroglia within the IGL and the white matter, based on morphology and position (Fig. 5E and Table 2).

Although the GC-B6 cells differentiated into multiple types of cells after implantation, they did not generate all of the classes of neurons seen in P6 cerebellar cortex. Most notable was the absence of Purkinje neurons, small stellate cells in the deeper layers of the EGL, basket and Lugaro cells. The same subset of cells—granule cells, stellate cells of the upper aspect of the ML, Bergmann glial cells and astrocytes in the IGL—were obtained in each of the injection experiments we carried out, totalling more than 25 animals. Approximately 0.5–1% of the immortalized cells we implanted incorporated into

Table 2. Immunocytochemical characterization of GC-B6 cells

Markers	Immunopositive cells (%)
Germinal zone antigens	
R24a (GD3)	20–30
Neuronal antigens	
N-CAM	100
LI	0
TAG-1	0
Astroctactin	5–10
Neurofilament protein	2–5
Glial antigens	
Glial filament protein	20–30

Immortalized cerebellar granule cells were plated in 500 μ g/ml polylysine-coated 8-well Lab-Tek culture slides (1×10^4 cells/well) in serum-supplemented medium (Gao et al., 1991) for 24–48 hours and were then immunostained with the antibodies listed above.

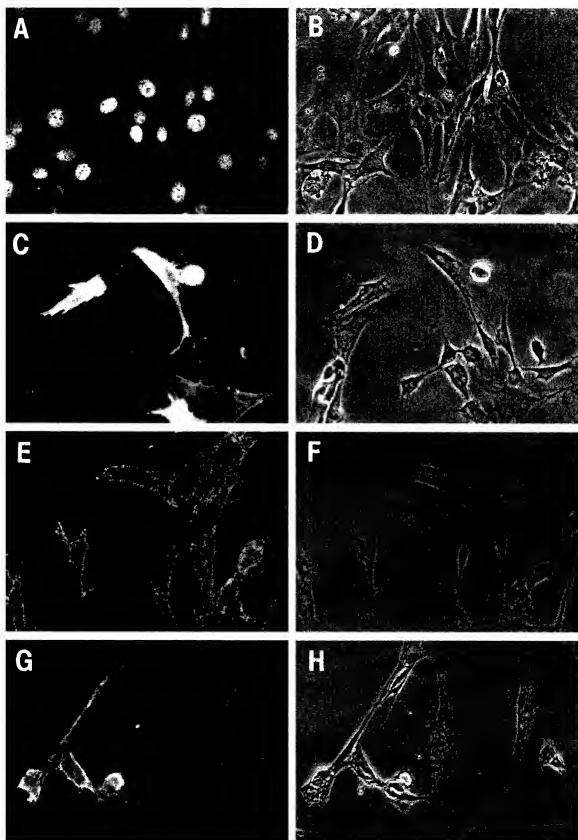
the host tissue. As stated above, 10–20 times more primary cells incorporated into developing cerebellar cortex than did immortalized GC-B6 cells. The levels of GC-B6 cell incorporation are consistent with the results of Renfranz et al. (1992) and Snyder et al. (1992). The incorporation rates of both primary and immortalized cells probably underestimated the capacity of the cells to integrate into host brain, as we used short survival times to chronicle the developmental steps followed by implanted cells.

DISCUSSION

Granule neurons arise from precursors with a restricted potential

The re-implantation of purified EGL precursors into early postnatal EGL provided a test of the role of local signals in the EGL to the development of cerebellar granule neurons. In an *in vivo* transplantation assay, cells taken from the cerebellar primordium on embryonic day 13 generated multiple fates, with each of the major classes of cerebellar cells evident. E13 was chosen because it is the time point when precursors of all of the principle neuron classes are present (Altman and Bayer, 1978, 1985) with EGL precursors just emerging across the rhombic lip to establish the external germinal layer. The demonstration that EGL cells purified in the early postnatal period give rise to cells with the laminar position and neuritic profile of granule neurons, and not other cerebellar cell types, after implantation into the EGL suggests that the fate of EGL cells is normally restricted (Fig. 6). Thus granule cells appear to arise from precursor cells with a restricted potential.

The homotypic transplantation experiments support the conclusion that the EGL is normally fated to produce granule neurons. This result is consistent with our finding that EGL cells have a restricted fate when cultured in homotypic cellular aggregates (Gao et al., 1991) and with studies on chick-quail chimeras (Martinez and Alvarado-Mallart, 1989; Hallonet et al., 1990; Hallonet and Le Douarin, 1992) showing that EGL precursors give rise to granule neurons and not other cerebellar cell types. The present study extends our previous findings by demonstrating that the entire program of granule cell development, including axon extension, laminar position, and



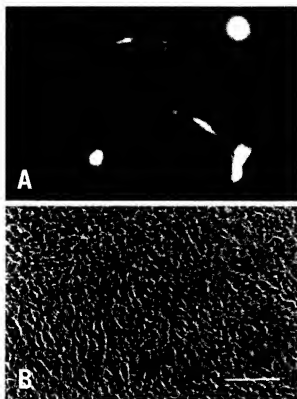


Fig. 4. Co-culture of GC-B6 cells with primary EGL cells induces neurite formation. GC-B6 cells were labeled with PKH-26 and cultured on a monolayer of primary EGL cells for 24 hours *in vitro*. Two cells were seen extending long, slender, bipolar neurites characteristic of granule neurons, suggesting differentiation of GC-B6 cells on a monolayer of primary EGL cells. (A) Fluorescence microscopy and (B) phase contrast microscopy of the same field. Bar, 50 μ m.

dendritic development, is realized after re-implantation of the cells. These findings do not exclude the possibility that EGL precursors would express a different potential after transplantation to heterotypic brain regions.

The finding that EGL cells give rise only to granule neurons suggests that segregation of this population of precursor cells, from the time of their origin in the primordium (Hallonet et al., 1990; Hallonet and Le Douarin, 1992), and continued proliferation in displaced germinal zone, sets forth the pattern of cell fate restriction leading to a granule cell identity. Interestingly, the granule neuron is the only class of CNS neurons to arise from a displaced germinal zone, and also the only CNS neurons

to appear in such extreme abundance, accounting for nearly 20% of the total neuronal population of human brain (Kandel et al., 1991). The vast numbers of EGL cells suggest that these cells represent a sublineage of CNS cells that undergo amplification after commitment, in a hemopoietic model. In this model, granule cell identity would be specified, either at the site of origin in the primordium, or during the segregation of these precursor cells into an external zone (embryonic days 13 and 17). Evidence for partial commitment of the cells comes from studies on the neurotransmitter uptake systems of EGL cells. As early as E13, EGL cells do not show any ability for uptake of GABA, the neurotransmitter system used by other cerebellar neurons (Hatten et al., 1983). In the mouse, the amplified proliferation of EGL cells occurs between P0 and P10 (Miale and Sidman, 1961), when the EGL thickens from a thin, unicellular layer to a layer 8–10 cells deep. *In vitro* studies suggest that local signals promote the continued proliferation of EGL precursor cells (Gao et al., 1991).

Immortalized EGL cells do not show a restricted cell potential

In contrast to the results obtained with primary EGL cells, EGL cells infected with retroviral constructs containing the *tsA58* allele of SV40 large T antigen oncogene did not retain a granule neuron specification. Our observation that immortalized cells gave rise to multiple types of cells after implantation into the cerebellum (Fig. 6) is consistent with the findings of Renfranz et al. (1992), who showed that immortalized progenitor cells differentiated into a variety of cerebellar cell classes after implantation into early postnatal cerebellar cortex. This result is also consistent with the results of Snyder et al. (1992), who showed that immortalized cerebellar cells can participate in formation of the cerebellum. A major difference between the previous studies and the present analysis is that we have directly compared the fate of a single class of purified CNS primary precursor cells with immortalized precursor cells. Our finding that immortalized EGL cells did not express the fate seen for their primary counterparts suggests that introduction of the *tsA58* allele of the SV40 large T antigen oncogene into EGL precursor cells altered the response of the cells to regulatory components needed to specify a granule cell identity.

In spite of the failure of immortalized EGL cells to retain a granule cell commitment after implantation into developing cerebellar cortex, EGL cell lines should prove useful for a number of other experiments, as they express selected features of granule cells. These include the ability to differentiate upon close apposition with primary EGL cells, shown here, and the ability to rescue *weaver* granule cell differentiation (Gao et al., 1992). Comparison of these and other EGL cell lines might also provide insights to the molecular determinants of pluripo-

Fig. 3. Immunocytochemical characterization of GC-B6 cells. Immunocytochemical staining of GC-B6 cells, grown at the permissive temperature *in vitro* for 16–24 hours, with a monoclonal antibody against large T-antigen (A,B) reveals nuclear expression of the large T antigen by all cells in the population. Immunocytochemical labeling of cells, grown at the non-permissive temperature *in vitro* for 16–24 hours, with the germinal zone marker GD3, the monoclonal antibody R24a (C,D) revealed staining of a subpopulation of the cells. Staining of GC-B6 cells grown at the non-permissive temperature *in vitro* for 16–24 hours, with antibodies against the neural cell adhesion molecule N-CAM (E,F) labeled all cells, and antibodies against the neuron–glial adhesion system astrocytin (G,H) labeled a small number of cells. Thus, although all cells expressed the large T antigen and NCAM, more restricted neuronal markers were expressed by a subset of cells within the cell population. (A,C,E,G) Fluorescence microscopy. (B,D,F,H) Phase contrast microscopy of paired fields. Bar, 50 μ m.

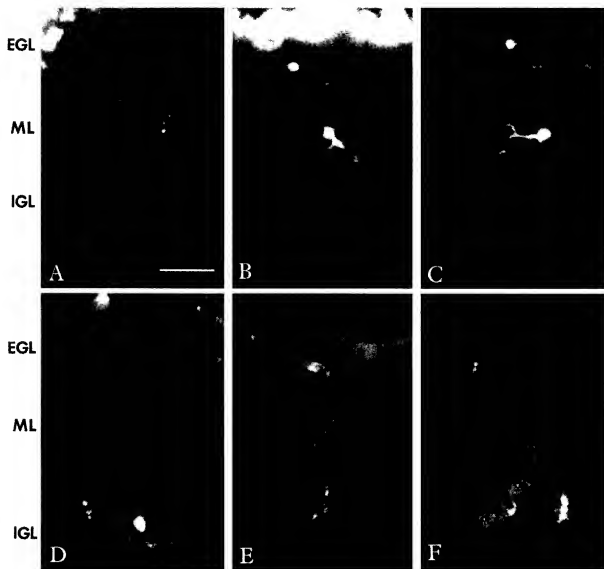


Fig. 5. Immortalized EGL cells differentiated into multiple types of cells after implantation into P6 EGL. (A) 4 days after implantation, one of the implanted GC-B6 cells assumed the profile of a migratory granule cell (A), another cell displayed an ascending T-shaped axon, typical of granule neurons (B) A GC-B6 cell, shown in C, developed into a stellate neuron, positioned its cell body in the outer third of the molecular layer and extended a short tuft of dendrites horizontal to the plane of granule cell migration. (D) A Golgi II-like neuron with a cell soma deep to the Purkinje cells and an abundant array of axons descending into the IGL. E shows several cells with astrocytic morphology. F shows a group of Bergmann glial cells, each with a 'candelabrum' shape, extending multiple, slender ascending processes to the pial surface. Bar, 25 μ m.

tency versus a restricted fate; to primary EGL cells or other CNS cells.

Effects of SV40 large T oncogene on neuronal fate specification

In previous studies, immortalized CNS cell lines have been proposed to represent multipotential stem cells, owing to the diversity of cells seen after their implantation into developing brain (Renfranz et al., 1992; Snyder et al., 1992). In this model, immortalization of the cells is thought to capture cells that have entered a neural sublineage, but remain multipotential. As

these cell lines were generated from a mixture of uncharacterized progenitor cells, it was difficult to assess the effect of the transfected oncogene to cell specification. The present experiments suggest that, although the cells retain a neural character, immortalization subverts the specification of granule cells. The most striking feature of the GC-B6 cell line was the odd variety of types of cerebellar cells generated after implantation of GC-B6 cells. For example, although we observed one subclass of inhibitory stellate cells, those located in the upper aspect of the molecular layer, we did not observe the more common stellate cells seen in deeper aspects of the molecular layer. As the par-

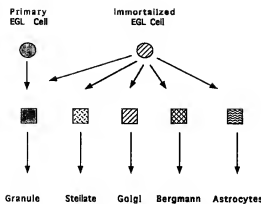


Fig. 6. Oncogene expression subverts granule cell lineage specification. On postnatal day 6, a variety of factors present in the developing cerebellar cortex support cell differentiation (represented by squares). When implanted into the EGL of the P6 cerebellar cortex, primary EGL precursor cells (stippled circles) are committed to a granule neuron fate, proceeding through all of the steps of granule cell development seen *in vivo*. By contrast, immortalized EGL cells (hatched circles) give rise to a variety of cell types, suggesting they are not committed to a granule cell fate.

ticular variety of cell types generated by GC-B6 cells have not been suggested to arise from a common precursor or even the same germinal zone, it seems unlikely that the GC-B6 cell line represents a restricted progenitor found *in vivo*.

Although the EGL is not inhibitory for Purkinje cell differentiation, as evidenced by the ability of E13 cells to differentiate into Purkinje cells following transplantation into the EGL, it may not contain local signals required for the specification of Purkinje cells (or the classes of interneurons not seen). The failure of the GC-B6 cell line to form Purkinje cells after implantation into the EGL may therefore be due to the absence of Purkinje cell determinants in the EGL zone. It will be interesting to examine, in future experiments, if transplantation of GC-B6 progenitors to the site of origin of the Purkinje neuron, the embryonic VZ lining the fourth ventricle, results in the generation of a Purkinje cell. This would be in agreement with the cortical transplantation studies of McConnell and Kazanietz (1991), showing that environmental cues in the cortical VZ influence the laminar fate of neural progenitor cell.

The interpretation that immortalizing oncogenes subvert normal mechanisms of cell fate commitment is supported by studies on non-neural cells. In the hematopoietic system, overexpression of the *v-ras* oncogene leads to lineage switching, converting B lineage cells, from either lymphomas or preleukemic bone marrow cells of Eμ *myc* transgenic mice, to macrophages. As the B cell and macrophage lineages are not closely related, *v-ras* expression appears to subvert normal mechanisms of lineage specification (Klinken et al., 1988). More generally, lineage instability is common among transformed cell populations. Many tumors, including a tumor which is thought to arise from EGL progenitor cells, the medulloblastoma, give rise to multiple cell types *in situ* (Russell and Rubenstein, 1977). These general features of CNS neural tumors, together with our current findings, point to the potential for oncogenes to subvert normal cell fate specification.

The model that emerges from our studies is one where a

variety of local signals can provide components of a program of neuronal differentiation, with primary EGL precursor cells showing a restricted response to local signals, having a program of gene expression leading to a granule cell identity (Kuhar et al., 1993). Our experiments suggest that this is due to a prior specification of the cells, rather than regulatory signals localized to the EGL. This view is supported by the fact that all classes of cerebellar cells, including Purkinje cells, could develop after implantation into the EGL. What seems to be restricted is the response of a given class of progenitor cells to a particular environment, with primary cells showing restricted responses to local cues for differentiation and immortalized cells showing unrestricted responses (Fig. 6). These mechanisms that restrict the response of precursor cells to a subset of local signals, i.e. direct them to particular sublineage, are critical to the establishment of different cell types in brain.

At present, the regulation of nuclear transcription in the response of any given class of CNS precursors to specific local signals in the developing brain remains to be described. The general approach presented here, of altering the fate of a purified population of CNS cells and then implanting those cells into brain to follow specific steps in their development *in situ*, should provide an analysis of the function of genes that specify neuronal fate during CNS development. Indeed careful analysis of the control of neuronal fate specification of primary cells may ultimately lead to the replacement of particular classes of neurons in developing or injured brain.

We are grateful to Drs Kathy Zimmerman and Sally Temple for critically reading the manuscript, and to our colleagues Drs Nathaniel Heintz, Gord Fishell, Rodolfo Rivas, Carol Mason and Jane Dodd for helpful discussions. We also thank Dr L. Feng for assistance with the preparation of Figs 1 and 4, and J. Zheng for excellent technical assistance. This work was supported by Program Project P01 30532 (MEH).

REFERENCES

- Aitman, J. and Bayer, S. A. (1978). Prenatal development of the cerebellar system in the rat. *Cytogenesis and histogenesis of the deep nuclei and the cortex of the cerebellum*. *J. Comp. Neurol.* 179, 23-48.
- Aitman, J. and Bayer, S. A. (1985). Embryonic development of the rat cerebellum. *J. Comp. Neurol.* 231, 1-64.
- Anderson, D. J. (1989). The neural crest lineage problem: Neoploids? *Neuron* 3, 1-12.
- Brodal, P. (1993). *Neurological Anatomy in Relation to Clinical Medicine*. New York: Oxford University Press.
- Cepko, C. L. (1988). Immortalization of neural cells via oncogene transduction. *Trends Neurosci.* 11, 6-8.
- Dodd, J., Morton, S. B., Karagoev, D., Yamamoto, M. and Jessell, T. M. (1988). Spatial regulation of axonal glycoprotein expression on subsets of embryonic spinal neurons. *Neuron* 1, 105-116.
- Edmondson, J. C. and Hatten, M. E. (1987). Glial-guided granule neuron migration *in vitro*: A high-resolution time-lapse video microscopic study. *J. Neurosci.* 7, 1928-1934.
- Edmondson, J. C., Liem, R. K. H., Kuster, J. E. and Hatten, M. E. (1988). Astrocytes, a novel cell surface antigen that mediates neuron-glia interaction in cerebellar microcultures. *J. Cell Biol.* 106, 505-517.
- Fishell, G. and Hatten, M. E. (1991). Astrocytes form a receptor system for CNS neuronal migration. *Development* 113, 755-765.
- Gao, W.-Q., Heintz, N. and Hatten, M. E. (1991). Cerebellar granule cell neurogenesis is regulated by cell-cell interactions *in vitro*. *Neuron* 6, 705-715.
- Gao, W.-Q., Liu, X. L. and Hatten, M. E. (1992). The weaver gene encodes a non-autonomous signal for CNS neuronal differentiation. *Cell* 68, 841-854.
- Gao, W.-Q. and Hatten, M. E. (1993). Neuronal differentiation rescued by

- implantation of weaver granule cell precursors into wild-type cerebellar cortex. *Science* 260, 367-369.
- Goldman, J. E., Hirano, M., Yu, R. K. and Seyfried, T. N. (1984). GD3 ganglioside is a glycolipid characteristic of immature neuroectodermal cells. *J. Neuroimmunol.* 7, 179-192.
- Hallonet, M. E. R., Teillet, M.-A. and Le Douarin, N. M. (1990). A new approach to the development of the cerebellum provided by the quail-chick marker system. *Development* 108, 19-31.
- Hallonet, M. E. R. and Le Douarin, N. M. (1992). Tracing neuroepithelial cells of the mesencephalic and metencephalic alar plates during cerebellar ontogeny in quail-chick chimeras. *Eur. J. Neurosci.* 5, 1145-1155.
- Hatten, M. E. and Sidman, R. L. (1978). Plant lectins detect age and region-specific differences in cell surface carbohydrates and cell reassociation behavior of embryonic mouse cerebellar cells. *J. Supramol. Struct.* 7, 267-278.
- Hatten, M. E. and Liem, R. K. H. (1981). Astroglia provide a template for the positioning of developing cerebellar neurons in vitro. *J. Cell Biol.* 90, 622-630.
- Hatten, M. E., Francois, A. M., Napolitano, E. and Roffler-Tarlov, S. (1983). Embryonic cerebellar neurons accumulate 3H-GABA. Visualization of developing GABA-utilizing neurons in vitro and in vivo. *J. Neurosci.* 4, 1343-1353.
- Hatten, M. E. (1985). Neuronal regulation of astroglial morphology and proliferation in vitro. *J. Cell Biol.* 100, 384-396.
- Heintz, N., Norman, D. J., Gao, W.-Q. and Hatten, M. E. (1993). Neurogenetic approaches to mammalian brain development. In *Genome Analysis*. Cold Spring Harbor: Cold Spring Harbor Laboratory Press. (In press).
- Horan, P. K. and Slezak, S. E. (1989). Stable cell membrane labeling. *Nature* 340, 167-168.
- Jessell, T. M. and Melton, D. A. (1992). Diffusible factors and embryonic induction. *Cell* 68, 257-270.
- Kandel, R., Schwartz, J. and Jessell, T. M. (1991). *Principles of Neural Science*. 3rd ed. Norwalk, CT: Appleton & Lange.
- Klinken, S. P., Alexander, W. S. and Adams, J. M. (1988). Hemopoietic lineage switch: v-ras oncogene converts Emu-myc transgenic B cells into macrophages. *Cell* 53, 857-867.
- Kuhar, S., Feng, L., Vidas, S., Ross, E. R., Hatten, M. E. and Heintz, N. (1993). Developmentally regulated cDNAs define four stages of cerebellar granule neuron differentiation. *Development* 112, 97-104.
- Lendahl, U. and McKay, R. D. G. (1990). The use of cell lines in neurobiology. *Trends Neurosci.* 13, 132-137.
- Llinas, R. and Hillman, D. E. (1969). Physiological and morphological organization of the cerebellar circuits in various vertebrates. In *Neurobiology of Cerebellar Evolution and Development*. (ed. R. Llinas), pp. 43-73. Chicago: AMA-ERF Institute for Biomedical Research.
- Martinez, S. and Alvarado-Mallart, R. M. (1989). Rostral cerebellum originates from the caudal portion of the so-called mesencephalic vesicle: a study using chick/quail chimeras. *Eur. J. Neurosci.* 1, 549-560.
- McConnell, S. K. and Kazanowski, C. E. (1991). Cell cycle dependence of laminar determination in developing neocortex. *Science* 254, 282-285.
- Metcalfe, D. (1987). The molecular control of normal and leukemic granulocytes and macrophages. *Proc. Roy. Soc. (Lond.) B* 230, 389-423.
- Mishe, I. and Sidman, R. L. (1961). An autoradiographic analysis of histogenesis in the mouse cerebellum. *Exp. Neurol.* 4, 277-296.
- Nicola, N. A. and Johnson, G. R. (1982). The production of committed hematopoietic colony-forming cells from multipotential precursor cells in vitro. *Blood* 61, 823-829.
- Ogawa, M., Porter, P. N. and Nakahata, T. (1983). Renewal and commitment to differentiation of hematopoietic stem cells (an interpretive review). *Blood* 61, 823-829.
- Palay, S. F. and Chan-Palay, V. (1974). *Cerebellar Cortex, Cytology and Organization*. Berlin: Springer-Verlag.
- Rakic, P. (1971). Neuron-glia relationship during granule cell migration in developing cerebellar cortex. A golgi and electromicroscopic study in Macacus rhesus. *J. Comp. Neurol.* 141, 283-312.
- Ramon y Cajal, S. (1911). *Histologie du Systeme Nerveux de l'Homme et des Vertebres*. Paris: Maloine (reprinted by Consejo Superior de Investigaciones Cientificas, Madrid, 1955).
- Rathjen, F. G. and Schachner, M. (1984). Immunocytochemical and biochemical characterization of a new neuronal cell surface component (L1 antigen) which is involved in cell adhesion. *EMBO J.* 3, 1-10.
- Renfranz, P. J., Cunningham, M. G. and McKay, R. D. G. (1992). Region-specific differentiation of the hippocampal stem cell line HB3 upon implantation into the developing mammalian brain. *Cell* 66, 713-729.
- Ross, M. E., Fletcher, C., Mason, C. A., Hatten, M. E. and Heintz, N. (1989). Meander trail reveals a developmental unit in mouse cerebellum. *Proc. Natl. Acad. Sci. USA* 87, 4189-4192.
- Russell, D. S. and Rubenstein, L. J. (1977). *Pathology of Tumors of the Nervous System*. 4th ed. Baltimore, MD: Williams and Wilkins.
- Sidman, R. L. (1972). *Cell Interactions*. Proceedings of the Third Lepetit Colloquium, pp. 1-13. Amsterdam: North-Holland Publishing Company.
- Snyder, E. Y., Deitcher, D. L., Walsh, C., Arnold-Aldea, S., Hartwig, E. A. and Cepko, C. L. (1992). Multipotent neural cell lines can graft and participate in development of mouse cerebellum. *Cell* 68, 33-51.
- Spangrude, G. J., Heimfeld, S. and Weissman, I. L. (1988). Purification and characterization of mouse hematopoietic stem cells. *Science* 241, 58-62.
- Thiery, J.-P., Brackenbury, R., Rutishauser, U. and Edelman, G. M. (1990). Adhesion among neural cells of the chick embryo II. Purification and characterization of a cell adhesion molecule from neural retina. *J. Biol. Chem.* 265, 6841-6845.
- Till, J. E. and McCulloch, E. A. (1961). A direct measurement of the radiation sensitivity of normal mouse bone marrow cells. *Radiat. Res.* 14, 213-222.

(Accepted 18 January 1994)

The Adult CNS Retains the Potential to Direct Region-Specific Differentiation of a Transplanted Neuronal Precursor Cell Line

Lamy S. Shihabuddin,^{1,2} Jeffrey A. Hertz,² Vicky R. Holets,^{1,2,3,4,*} and Scott R. Whittemore^{1,2,3,5}

¹Neuroscience Program, ²The Miami Project to Cure Paralysis, and Departments of ³Neurological Surgery, ⁴Cell Biology and Anatomy, and ⁵Physiology and Biophysics, University of Miami School of Medicine, Miami, Florida 33136

The chronic survival and differentiation of the conditionally immortalized neuronal cell line, RN33B, was examined following transplantation into the adult and neonatal rat hippocampus and cerebral cortex. In clonal culture, differentiated RN33B cells express p75^{NTR} and trkB mRNA and protein, and respond to brain-derived neurotrophic factor treatment by inducing c-fos mRNA. Transplanted cells, identified using immunohistochemistry to detect β -galactosidase expression, were seen in most animals up to 24 weeks posttransplantation (the latest time point examined). Stably integrated cells with various morphologies consistent with their transplantation site were observed. In the cerebral cortex, many RN33B cells differentiated with morphologies similar to pyramidal neurons and stellate cells. In the hippocampal formation, many RN33B cells assumed morphologies similar to pyramidal neurons characteristic of CA1 and CA3 regions, granular cell layer neurons of the dentate gyrus, and polymorphic neurons of the hilar region. Identical morphologies were observed in both adult and neonatal hosts, although a greater percentage of β -galactosidase immunoreactive cells had differentiated in the neonatal brains. These results suggest that RN33B cells have the developmental plasticity to respond to local microenvironmental signals and that the adult brain retains the capacity to direct the differentiation of neuronal precursor cells in a direction that is consistent with that of endogenous neurons.

[Key words: neuronal cell line, immortalization, transplantation, differentiation, hippocampus, cerebral cortex]

Spontaneous regeneration in the mammalian CNS is limited, so injury or disease usually results in permanent loss of function. Neural transplantation is one potential therapeutic approach to restore function in the injured, degenerating, or aging CNS (Björklund, 1991; Emerich et al., 1992). Transplanted fetal CNS

tissue can integrate within the host brain and promote functional recovery in animal models of neurodegenerative disease (Perlow et al., 1979; Björklund and Stenevi, 1984; Gash et al., 1985; Segal et al., 1986; Lindvall et al., 1990). However, the use of fetal tissue for transplantation is complicated by logistical, immunological (Seiger, 1985; Widner and Brudin, 1988), and ethical (Hoffer and Olson, 1991) considerations. Several alternative cell types have been used in various transplantation paradigms including peripheral neurons (Freed et al., 1981), PC12 cells (Jaeger, 1985), and neuroblastoma cells (Gash et al., 1986; Kordower et al., 1987). However, these cells have not survived or have proved tumorigenic.

An alternative source of donor cells is genetically modified cells which can be engineered to secrete specific neurotransmitters or trophic factors to replace a lost or defective function (Gage et al., 1987, 1991). Genetically engineered cells have been transplanted after specific CNS lesions and in some cases ameliorate functional deficits (Horellou et al., 1990; Fisher et al., 1991). However, non-neuronal cells are limited in the extent to which they can integrate into the host neuronal circuitry. Several approaches to the development of immortalized neuroepithelial cell lines of CNS origin have been undertaken (Cepko, 1989; Gage et al., 1995; Whittemore et al., 1995). Results from transplanting such cell lines into the neonatal CNS suggest that immortalized pluripotent cell lines undergo both neuronal and glial differentiation that is dependent upon their location in the host tissue (Renfranz et al., 1991; Snyder et al., 1992; Gao and Hatton, 1994). Importantly, the neuronally differentiating cells sent projections to appropriate target sites and formed synapses with host-derived afferent fibers. A recent study demonstrates that engraftment of neural progenitor cells genetically engineered to secrete β -glucuronidase corrects the lysosomal storage disorder throughout the MPS VII mouse brain (Snyder et al., 1995), but this did not require the transplanted cells to differentiate with a neuronal phenotype. If immortalized CNS cell lines are to be used therapeutically as donor material to replace lost neurons, it may be advantageous for specific applications that they are restricted to a neuronal lineage *in vivo*. This is of importance in allogeneic grafts, as neuronal differentiation of CNS precursor cell lines results in down regulation of cell surface molecules necessary for recognition by cytotoxic T-lymphocytes (White et al., 1994).

The conditionally immortalized cell line, RN33B, constitutively differentiates only with neuronal properties and does not demonstrate any non-neuronal phenotypes (Whittemore and White, 1993). In initial studies, Onifer et al. (1993) demonstrated

Received April 5, 1995; revised May 24, 1995; accepted May 31, 1995.

We thank Dr. Ellen Barrett for critically reviewing the manuscript, Linda A. White for her expertise with the organotypic cultures and her insightful suggestions throughout the course of the work, Deyanira Santiago for her help with animal care, Dr. John Klose and Dr. Mary Eaton for their assistance with the statistical analysis, and Robert Camerona for his photographic excellence. This work was supported by The Miami Project to Cure Paralysis, General Reinsurance, The Daniel Heuman Fund for Spinal Cord Injury, and NS26887.

Correspondence should be addressed to Scott R. Whittemore, Ph.D., The Miami Project, University of Miami School of Medicine, 1600 NW 10th Avenue, R-48, Miami, FL 33136.

*Present address: National Tuberous Sclerosis Association, 8000 Corporate Drive, Suite 120, Landover, MD 20785.

Copyright © 1995 Society for Neuroscience 0270-6474/95/156666-13\$05.00/0

that at two weeks posttransplantation into the adult rat hippocampus and spinal cord some RN33B cells morphologically differentiated with multiple neuritic processes. In the present study, we describe the developmental capacity of RN33B cells and their ability to respond to local microenvironmental cues following chronic transplantation into various regions of the adult and neonatal CNS.

Materials and Methods

Animals and chemicals. Timed-pregnant and adult female Lewis rats (175–200 gm) were purchased from Charles River Laboratories (Wilmington, MA). Rabbit polyclonal antisera to β -galactosidase (β -gal) was obtained from 5 Prime–3 Prime, Inc. (Boulder, CO); normal rabbit serum and Vectastain ABC kits were purchased from Vector Laboratories, Inc. (Burlingame, CA). Fluorescein di- β -D-galactopyranoside (FDG) was purchased from Molecular Probes, Inc. (Eugene, OR).

Cell culture. RN33B cells were grown at permissive temperature (33°C) as described previously (Whittemore and White, 1993).

Preparation of RN33B cells for transplantation. Prior to transplantation, undifferentiated RN33B cells were labeled in vitro by retrovirus-mediated transfer of the *E. coli* Lac Z gene as described (Shimohama et al., 1989; Onifer et al., 1993). Cells were then incubated with FDG, and β -galactosidase immunoreactive (β -gal-IR) RN33B cells enriched by fluorescent activated cell sorting (Nolan et al., 1988; Whittemore and White, 1993) and expanded. Using this method, over 80% of the RN33B cells were β -gal-positive as detected histochemically or immunohistochemically. When roughly 80% confluent, proliferating RN33B cells were washed with ice-cold PBS containing 0.5 mM ethylenediaminetetraacetic acid (EDTA), gently scraped in PBS containing EDTA, pelleted at 1500 rpm for 3 min, and resuspended in ice-cold, sterile Earle's balanced salt solution (EBSS). The pellets were washed twice and resuspended in EBSS at a density of 100,000 cells/ μ l and stored on ice until use. Only cell suspensions demonstrating greater than 80% viability, as determined by Trypan blue exclusion, were used for transplantation. RN33B cells express RT1.A* haplotypes at the class II major histocompatibility complex (MHC) A locus (White et al., 1994) while Lewis rats are RT1.A* (Gill et al., 1987). Thus, these are allogeneic cell transplants. At the conclusion of the transplantation procedures, the viability of the suspended cells was reassessed and was always $\geq 70\%$. For control transplants, a cell suspension of lysed (non-viable) RN33B cells of similar density was prepared by five repeated cycles of freezing and thawing.

Transplantation of RN33B cells into adult and neonatal brain. Adult rats were anesthetized by intraperitoneal injection of Equithesin (0.3 ml/100 gm body weight), prepared for surgery, and placed in a stereotaxic instrument (Narishige, Scientific Instrument Lab.). Postnatal day 5 female Lewis rats were anesthetized by placing them on ice for 5 min and then maintaining hypothermia during the injection into one hemisphere using a stereotaxic instrument. After craniotomy, the exposed dura was cut over the transplantation site. Each animal received a unilateral injection of 1.0 μ l of RN33B cell suspension (10^5 cells) into the hippocampus, white matter, and cerebral cortex along one injection track in the right hemisphere. The stereotaxic coordinates used were initially determined from cresyl violet stained cryostat sections of age-matched animals. The transplants were placed 1.7 mm lateral to midline, 2.1 mm posterior to bregma, and 2.0 mm below the dura. In adult rats, the transplantation site was 3.0 mm lateral to midline, 4.0 mm posterior to bregma, and 1.5–3.0 mm below the dura. Stereotaxic coordinates were derived according to Paxinos and Watson (1986). Cell suspensions were slowly injected with a 10 μ l Hamilton syringe over a period of 5 min. The needle was left in place for another 5 min and then slowly pulled up. Because of the backflow of some of the cell suspension while pulling up along the needle track, the precise number of RN33B cells injected into each site was difficult to establish. A total of 38 adults and 48 neonates were used (Table 1). No difference was observed between transplants into female rats and those into male rats in an earlier study (Onifer et al., 1993).

All surgical procedures were carried out in strict accordance with the Laboratory Animal Welfare Act, Guide for the Care and Use of Laboratory Animals (NIH, DHEW Pub. No. 78-23, Revised, 1977) only after review and approval by the Animal Care and Use Committee of the University of Miami School of Medicine.

β -Gal immunohistochemistry. After variable survival times (1, 2, 5,

Table 1. RN33B cell transplant recipients by age group and survival time posttransplantation; transplants containing β -gal immunoreactive cells were classified as positive

Age	Survival time (weeks)	Total # of rats	# of positive transplants
Adult	2	9	9
	5	8	8
	8	10	6
	16	8	3
	24	3	1
Total	2–24	38	28
Neonate	2	11	10
	5	12	8
	8	13	9
	16	10	4
	24	2	2
Total	2–24	48	33

8, 16, and 24 weeks) following RN33B cell transplantation, animals were deeply anesthetized, and then transcardially perfused with Ca^{2+} -free Tyrode's solution followed by a modified Zamboni's fixative containing 4% paraformaldehyde and 10% picric acid in PBS, pH 6.9. Brains were removed, postfixed for 90 min in the same fixative and kept overnight at 4°C in PBS (pH 7.4). Brains were blocked for coronal sectioning through the transplanted region. Serial 50 μ m sections were cut on a vibratome and stored at 4°C in PBS until further processing. Floating sections were processed for β -gal immunoreactivity as previously described (Onifer et al., 1993).

Quantitative analysis of the morphological differentiation of transplanted RN33B cells. Every sixth 50 μ m vibratome section through the transplant site (12 sections per animal) was processed for β -gal immunohistochemistry. Transplanted β -gal-positive RN33B cells were quantified using an IMAGE-1 image analysis system (Universal Imaging Corp., West Chester, PA). Sections were observed by light microscopy at low magnification (50 \times) to localize the integration site of the transplant (neocortex, hippocampus, or white matter). A grid, covering 1.98 mm², was overlaid on the low magnification image of the region of interest. Each square was analyzed at higher magnification (200 \times) to count β -gal-IR cells and assess the degree of morphological differentiation of detected cells in terms of shape of the cell body, the number of processes that these cells extended, and the pattern and orientation of these processes. Only labeled cells where a nucleus and a cytoplasm could be seen were included in the quantitative analysis. Transplanted RN33B cells with sheath-like somas in which a nucleus and cytoplasm, but no processes, were seen were classified as undifferentiated. Cells with an ovoid or spindle-shaped cell body and ≤ 2 processes were classified as bipolar, while cells with ≥ 3 processes and cell bodies with variable morphologies were classified as multipolar. β -gal-IR multipolar cells in the neocortex were classified as pyramidal cells if they had triangular or ovoid cell bodies and a long apical neuritic process extending towards the apical surface and two long basal processes or as stellate cells if they had polymorphic cell bodies and four or more long processes extending radially from the cell body. The criteria used to categorize the labeled cells were based on earlier descriptions of cortical cells stained by the method of Golgi (Ramon y Cajal, 1888). In the hippocampus, β -gal-IR cells were classified as CA3 pyramidal cells if they were located in the pyramidal cell layer of the CA3 region, had large, angular cell bodies with abundant cytoplasm that tapered into one or two apical processes, a small number of wide basal processes and had appropriate structural polarity. Cells were characterized as CA1 pyramidal cells if they were located in the pyramidal layer of the CA1 region, had appropriate structural polarity, had small cell bodies, but otherwise had characteristics similar to CA3 pyramidal cells. β -gal-IR cells located in the granular cell layer that had small round or ovoid cell bodies, unipolar neuritic arbors, and lacked basal processes were classified as granular cells. The classification criteria used are based on

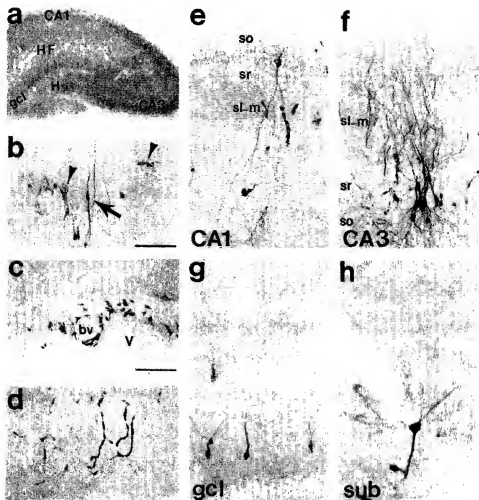


Figure 1. Variable morphologies of β -gal-IR RN33B cells transplanted into the hippocampal formation. Bright-field photomicrographs of β -gal-IR RN33B cells in coronal sections of the hippocampus. *a*, Photomicrograph of the rat hippocampal formation. Abbreviations: fields CA1–3 of Ammon's horn (CA1–CA3), granular cell layer (gcl), hilar region (H), and the hippocampal fissure (HF). *b*, A bipolar β -gal-IR RN33B cell (arrow) in the stratum lacunosum-moleculare, and undifferentiated β -gal-IR cells (arrowheads). *c*, Undifferentiated RN33B cells surrounding a blood vessel (bv) and lining the lateral ventricle (V). *d*, Undifferentiated RN33B cells in the stratum lacunosum-moleculare above the hippocampal fissure. β -gal-IR RN33B cells with their cell bodies embedded in the pyramidal layer of CA1 (*e*) and CA3 (*f*) had somewhat ovoid or angular cell somas with abundant cytoplasm that tapered into an apical process extending through the stratum radiatum (sr) and into the stratum lacunosum-moleculare (sl-m). In the lacunosum-moleculare layer, many secondary and tertiary branches are observed. The basal processes exit from several places along the base of the perikaryon into the stratum oriens (sr-o). *g*, β -gal-IR RN33B cells with ovoid cell bodies embedded in the gcl, with processes extending from the apical end of the cell bodies. At the base of the cell body, one cell has a fine process extending toward the hilar region. *h*, β -gal-IR RN33B cell body embedded in the pyramidal layer of the subiculum (sub), extending an apical process and two basal processes with multiple branches. Scale bars: *b*, *g*, *h*, 50 μ m; *c*, *e*, 100 μ m. The age of host and the intervals between transplants and histology are adult and 5 weeks in *b* and *d*; neonate and 2 weeks in *c* and *e*; adult and 8 weeks in *f*, neonate and 16 weeks in *g*; neonate and 5 weeks in *h*.

detailed descriptions of Golgi-impregnated hippocampal neurons *in situ* (Bayer, 1980; Gähwiler, 1984; Frotscher et al., 1988).

An estimate of the number and extent of differentiation of the transplanted RN33B cells was made by counting all β -gal-IR cells in all sections processed per animal, and categorizing these cells into the different cell types by location, morphology, and structural polarity. These data were used to calculate the percent of the total cells detected that assumed differentiated neuronal morphologies. An exact count of the number of surviving RN33B cells can not be made as not all transplanted RN33B cells were β -gal-IR prior to transplantation ($\sim 80\%$ expressed β -gal immunoreactivity) and down regulation of β -galactosidase expression from viral LTRs *in vivo* may occur (St. Louis and Verma, 1988; Palmer et al., 1991; Onifer et al., 1993). However, similar cell suspensions were used for all animals and these quantitative data can be used as estimates to compare the effect of the age of the host and the survival time posttransplantation on the number of detected RN33B cells and the percentage of differentiated cells.

Results

Survival of transplanted RN33B cells

Following transplantation into adult and neonatal CNS, surviving RN33B cells were detected using β -gal immunohistochemistry. Even though the cell concentration, volume transplanted, and coordinates of transplant were kept constant across experiments, the number and position of the transplanted RN33B cells varied from animal to animal. RN33B cell transplants were found in 100% of adult rats that survived for up to 2 weeks. At longer posttransplant survival intervals, 4–24 weeks, the efficiency of successful transplantation ranged from 33–100% (Table 1). RN33B cell transplants were found in 90% of the neonates that survived for up to 2 weeks posttransplantation. At

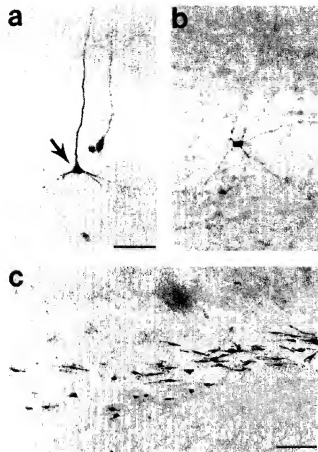


Figure 2. Variable morphologies of β -gal-IR RN33B cells transplanted into the cerebral cortex. Bright-field photomicrograph of β -gal-IR RN33B cells in a coronal section of the cerebral cortex. *a*, β -gal-IR RN33B cell with a pyramidal cell body (arrow), a large apical process extending towards the pial surface and branching basal processes. A fine process can be seen extending from the basal surface towards the white matter. *b*, A β -gal-IR RN33B cell with an ovoid cell body and an apical process can be also seen. *c*, A RN33B cell with a polygonal cell body and five divergent branched neuritic processes. *c*, Bipolar RN33B cells in the corpus callosum. Scale bars: *a* and *b*, 50 μ m; *c*, 100 μ m. The age of host and the intervals between transplant and histology are adult and 2 weeks in *a*; neonate and 16 weeks in *b*; neonate and 2 weeks in *c*.

survival intervals of 5–16 weeks, the efficiency of successful transplantation ranged from 40–67%. RN33B cells can survive up to 6 months posttransplantation in nonimmunosuppressed, histoincompatible adult and neonatal rat hosts (see Fig. 4*a,b*).

Morphological classification of transplanted β -gal-IR RN33B cells

Nearly all of the transplanted, RN33B β -gal-IR cells were found in the neocortex, subadjacent white matter, and hippocampus, although a few cells were also detected in the diencephalon, in the lining of the lateral ventricles, or within the meninges overlying the cortical injection site. In the hippocampal formation, β -gal-IR cells assumed variable morphologies depending on their location within the cellular layers of the hippocampus or hippocampal parenchyma (Fig. 1). The cells varied in size and shape of the cell soma and pattern of neuritic outgrowth. At early time points, undifferentiated β -gal-IR cells with sheath-

like cell somas and no processes were found within all regions and layers of the hippocampus (Fig. 1*d*) and around blood vessels (Fig. 1*c*). Other β -gal-IR cells within the lacunosum molecular layer, radiatum layer, and dentate gyrus had bipolar morphologies (Fig. 1*b*). β -gal-IR cells located in the hippocampal fissure and lining the ventricles assumed both undifferentiated and bipolar morphologies. Most of the β -gal-IR cells whose somata were embedded in the pyramidal layer of CA1 (Fig. 1*e*) or CA3 (Fig. 1*f*) had somewhat angular cell somas with abundant cytoplasm that tapered into an apical process extending through the stratum radiatum and into the stratum lacunosum molecular; many secondary and tertiary branches were seen. In addition, basal processes exited from several places along the base of the perikaryon and repeatedly branched in the stratum oriens. In the granular cell layer of the dentate gyrus, β -gal-IR cells displayed a characteristic monopolar, conically shaped field of processes extending from the apical end of an ovoid cell body to fan out in the host molecular region (Fig. 1*g*), which is the dendritic field of the dentate gyrus granular neurons. In the subiculum, some β -gal-IR cells also had pyramidal morphologies (Fig. 1*h*).

In the cerebral cortex, β -gal-IR cells that assumed neuronal phenotypes were classified as pyramidal-like (Fig. 2*a*) or stellate-like (Fig. 2*b*) cells. Some cortical β -gal-IR cells had ovoid or pyramidal cell bodies, a large apical process extending towards the pial surface and branching basilar processes. In some cells (arrow in Fig. 2*a*), a small caliber process extended from the basal surface towards the white matter. These processes may be axons, since the axons of pyramidal neurons have a smaller diameter than their dendrites. Such β -gal-IR RN33B cells were dispersed through layers II–VI of the cerebral cortex. Other β -gal-IR cells were polygonal or stellate in form and had four or more divergent branched varicose processes extending in all directions (Fig. 2*b*). These cells were few in number, and were seen in layer I underneath the pial surface or in layer VI above the corpus callosum. In white matter, at all intervals posttransplantation, β -gal-IR cells were either morphologically undifferentiated or bipolar, with a spindle-shaped cell body and unbranched short processes extending from opposite sides of the cell soma (Fig. 2*c*). No β -gal-IR cells were detected in animals that received lysed RN33B cells (data not shown).

Time course of survival and differentiation of RN33B cell transplants in adult hippocampus

In the hippocampal formation, β -gal-IR RN33B cells were found within all regions and layers of the hippocampus spanning 1.8–2.5 mm (anterior-posterior dimension) and 0.8–1.5 mm (medial-lateral dimension) from the injection site. At 1 week posttransplantation, the majority of β -gal-IR cells were aligned along the needle track (Fig. 3*a*) and assumed undifferentiated morphologies. Some of the β -gal-IR cells located in field CA3 exhibited some morphological differentiation with ovoid cell bodies and an apical process (arrows in Fig. 3*b*). At 8 weeks posttransplantation, many of the detected β -gal-IR cells were located in the hilar and CA3 region. These cells were morphologically differentiated with elaborate processes and extensive branching (Figs. 3*c,d*). β -gal-IR cells were still detected at 24 weeks posttransplantation (Fig. 4*a*). The β -gal-IR cells in CA3 pyramidal layer had pyramidal cell bodies, extensive apical processes extending in the stratum radiatum toward stratum lacunosum-molecular, and basal processes descending into the stratum oriens.

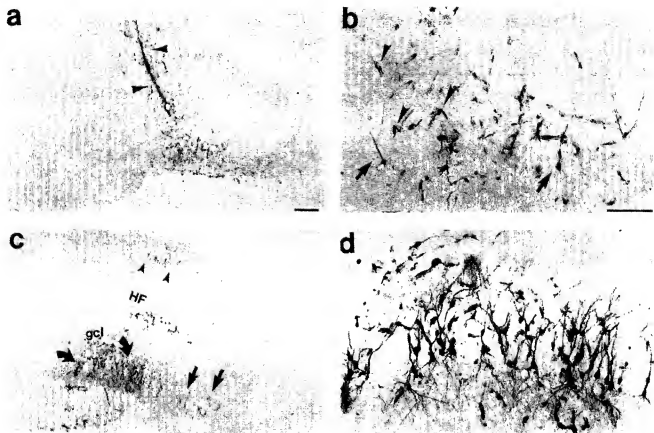


Figure 3. β -gal-IR RN33B cells in the adult hippocampus 1 (*a, b*) and 8 (*c, d*) weeks posttransplantation. *a*, Low-power view of the β -gal-IR RN33B transplant at 1 week posttransplantation. Many labeled cells are aligned along the needle track (arrowheads) and have undifferentiated morphologies. *b*, Higher magnification of β -gal-IR RN33B cells located in the CA3 pyramidal layer; some cells have ovoid cell bodies and extend some apical processes (arrows). Other β -gal-IR cells have undifferentiated morphologies (arrowheads). *c*, Low-power view of β -gal-IR RN33B cells at 8 weeks posttransplantation. Most cells have differentiated morphologies. Some β -gal-IR RN33B cells are located in the CA1 pyramidal cell layer (arrowheads) and extend both apical and basal processes. Most of the cells are located in the hilar region (curved arrows) and send out extensive processes. Some β -gal-IR RN33B cells are located in the CA3 pyramidal cell layer (straight arrows). Some undifferentiated cells are located above the granular cell layer (gcl) and below the hippocampal fissure (HF). *d*, Higher magnification showing β -gal-IR RN33B cells located in the hilar and CA3 regions. These cells are morphologically differentiated with elaborate processes and extensive neuritic branching, exhibiting structural polarity appropriate for neurons of that region. Scale bars: *a* and *c*, 200 μ m; *b* and *d*, 100 μ m.

Time course of survival and differentiation of RN33B cell transplants in adult cerebral cortex

β -gal-IR RN33B cells were dispersed without order throughout the entire thickness of the neocortex (Fig. 5). At 2 weeks posttransplantation, the majority of the detected RN33B cells were undifferentiated (Fig. 5*a, b*). However, a few β -gal-IR cells had morphologies similar to those of endogenous pyramidal and stellate cortical neurons (arrows in Fig. 5*a–f*). After survival intervals of 5 (Fig. 5*c, d*) and 16 (Fig. 5*e, f*) weeks, some of the transplanted RN33B cells remained undifferentiated (arrowheads in Fig. 5*c, e*) or assumed bipolar morphologies. Other β -gal-IR RN33B cells differentiated with morphologies similar to those of endogenous pyramidal cortical neurons (Figs. 5*d, f*). Their ovoid or pyramidal cell bodies ranged from 7 to 16 μ m in diameter, and they had thick apical processes extending towards the pial surface of the brain. Shorter branched, basal processes extended horizontally (Fig. 5*c–f*). At 5 weeks posttransplantation, more β -gal-IR cells were differentiated than observed at 2 weeks, but the total number of cells detected appeared not to change. Similar results were seen, at 8 and 16 weeks posttransplantation.

Quantitative analysis of RN33B cell transplants in the adult CNS

Morphological criteria described above and illustrated in Figures 1 and 2 were used to classify β -gal-IR RN33B cells in the cerebral cortex, hippocampus, and white matter into various cell types. Animals were chosen for quantitation based on the following criteria: (1) evidence of β -gal-IR cells in both hippocampus and cerebral cortex, and (2) that the entire transplant was contained within the sectioned region. To illustrate the quantitation, Table 2 presents data from a representative neonatal animal for each posttransplantation survival interval. It shows that RN33B cells were counted and classified as different cell types depending on the location and the cellular morphology in each region. In adults the total number of β -gal-IR cells in the neocortex and hippocampus did not change with longer survival times (up to 16 weeks, Fig. 6*a*). While there was a trend towards an increased percentage of differentiated β -gal-IR cells in the cerebral cortex and hippocampus with longer survival times (Fig. 6*b*), these differences were not statistically significant. The percent of maximal morphological differentiation at 8 weeks

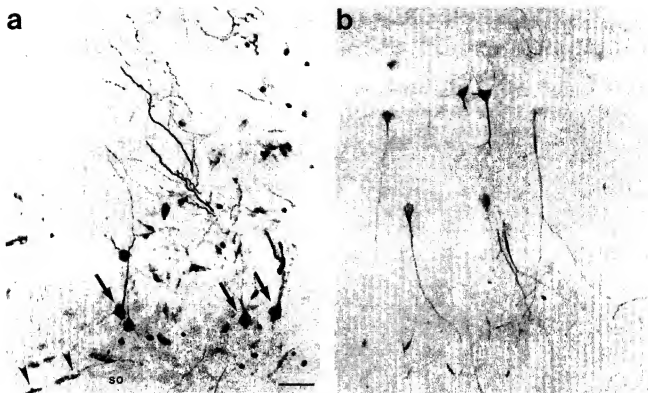


Figure 4. β -gal-RN33B cells in the adult and neonatal hippocampus at 24 weeks posttransplantation. *a*, In adults, β -gal-IR RN33B cells located in the pyramidal cell layer of the CA3 field (arrows) are multipolar with elaborate apical processes and extensive branching. Bipolar β -gal-IR RN33B cells are seen in the stratum oriens (so, arrowheads). *b*, In neonates, β -gal-IR RN33B cells located in the subiculum are pyramidal with elaborate apical and basal processes, and structural polarity appropriate for pyramidal cells of this region. Scale bar: 50 μ m for *a* and *b*.

posttransplantation was roughly 22% of the cells detected in the cerebral cortex and 13% of those in the hippocampus.

Time course of survival and differentiation of RN33B cell transplants in neonatal hippocampus

In neonates, as in adults, β -gal-IR cells were found within all regions and layers of the hippocampus spanning 2.4–3.6 mm (anterior-posterior dimension) and 1.1–2.0 mm (medial-lateral dimension). Two weeks posttransplantation, many β -gal-positive RN33B cells were detected in the neonatal hippocampal formation (Fig. 7*a,b*). Some β -gal-IR cells in the pyramidal layers of CA3 (arrows in Fig. 7*a*) and CA1 (arrowheads in Fig. 7*a*) fields had ovoid cell bodies and extended apical processes into stratum radiatum and towards stratum moleculare, with basal processes into the stratum oriens. However, the majority of β -gal-IR cells were undifferentiated. At 5 weeks posttransplantation, fewer β -gal-positive cells were detected (Fig. 7*c,d*), but more were morphologically differentiated. Figure 7*d* shows an example of cells in the CA3 field. Note the morphological differences between β -gal-IR cells that were located in the pyramidal cell layer where most of the cells assumed pyramidal morphologies, and β -gal-IR cells that were located above or below the pyramidal cell layer. These latter cells remained undifferentiated or assumed bipolar morphologies. By 16 weeks posttransplantation, most β -gal-IR cells assumed phenotypes similar to neurons at the integration site (Fig. 7*e,f*). β -gal-IR cells with cell bodies in the granular cell layer were ovoid with several processes extending into the host molecular region (small arrows in Fig. 7*e*). Other β -gal-IR cells were located in the hilus and

CA3 field. Figure 7*f* shows a higher magnification of polymorphic β -gal-IR cells with multiple processes in the hilus (large arrows in Fig. 7*e*) and cells in the pyramidal layer of the CA3 field with ovoid cell bodies, apical and basal processes, and structural polarity appropriate for pyramidal cells of this region (arrowheads in Fig. 7*e*). β -gal-IR cells were still detected at 24 weeks posttransplantation (Fig. 4*b*).

Time course of survival and differentiation of RN33B cell transplants in neonatal cerebral cortex

In the cerebral cortex of neonates, the temporal progression of RN33B cell differentiation was similar to that seen in the hippocampus. At 2 weeks posttransplantation, a large number of β -gal-IR RN33B cells were detected (Fig. 8*a,b*). Some β -gal-IR cells had morphologically differentiated to resemble cortical pyramidal neurons with long apical processes extending towards the pial surface (Fig. 8*b*), but the majority were undifferentiated. At 5 weeks posttransplantation, fewer β -gal-IR cells were found (Fig. 8*c,d*), but many more were differentiated. A cluster of β -gal-IR cells located in the deeper layers (IV–VI) of the neocortex had pyramidal cell bodies with diameters of 10–16 μ m and extensive branched processes (Fig. 8*d*) resembling endogenous pyramidal cortical neurons. By 16 weeks posttransplantation, most β -gal-IR cells had differentiated phenotypes (Figs. 8*e,f*).

Quantitative analysis of β -gal-IR RN33B cell transplants in the neonatal CNS

Figure 9*a* shows that the total number of β -gal-IR cells in neonatal hosts significantly decreased with longer survival times.

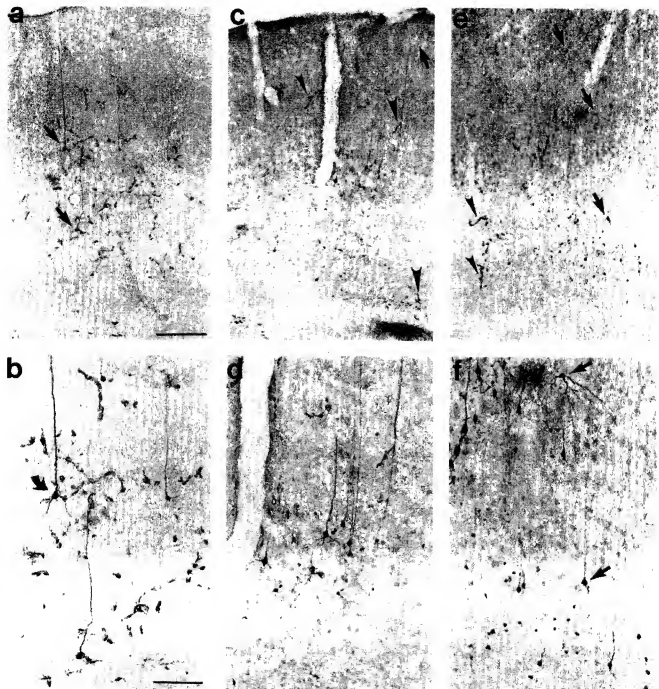


Figure 5. Temporal progression of RN33B differentiation in the adult cerebral cortex. β -gal-IR RN33B cell transplants in coronal sections of adult occipital cerebral cortex at 2 (*a, b*), 5 (*c, d*), and 16 (*e, f*) weeks posttransplantation. *b, d*, and *f* are higher magnification photomicrographs of regions of the fields shown in *a, c*, and *e*, respectively. At 2 weeks posttransplantation (*a, b*) the majority of β -gal-IR RN33B cells are undifferentiated. A few β -gal-IR RN33B cells extended large caliber apical process and extensive basal processes (arrows in *a*), similar to endogenous cortical pyramidal neurons. One of the cells (curved arrow) had a fine axon-like process extending towards the white matter. At 5 weeks, many β -gal-IR RN33B cells were differentiated with morphologies similar to those of medium-sized pyramidal neurons (*c, d*). Note the extensive process outgrowth extending both distally and apically towards the pial surface. The arrow in *c* indicates the terminal arborization in the plexiform layer of processes from an β -gal-IR RN33B cell whose cell body is in another plane of focus. Some undifferentiated cells are seen (arrowheads in *c*) and some cells are observed in close proximity to blood vessels. At 16 weeks (*e, f*), more differentiated β -gal-IR RN33B cells are seen dispersed throughout the thickness of the cerebral cortex (arrows in *e* and *f*). Some β -gal-IR RN33B cells remained undifferentiated (arrowheads in *e*). Scale bars: *a, c* and *e*, 200 μ m; *b, d*, and *f*, 100 μ m.

Table 2. RN33B cell counting and classification used for quantitative analysis

Region		Animal #			
		HCTP2 F	HCTP5 F	HCTP8 H	HCTP16 B
Cortex	Pyramidal cell	73	312	61	279
	Stellate cell	7	30	9	60
	Bipolar	25	21	5	99
	Around vessels	14	34	0	11
	Undefined	13	14	0	25
	Undifferentiated	495	190	14	205
Hippocampus	CA3 pyram. cell	115	70	15	31
	CA1 pyram. cell	45	61	10	15
	Granular cell	1	57	21	19
	Subiculum cell	0	0	10	22
	Hilar region	0	60	67	123
	Bipolar	171	111	106	86
	Around vessels	141	54	14	86
	Undefined	147	238	58	70
White matter	Undifferentiated	1575	1082	551	98
	Bipolar	1880	645	191	97
	Undifferentiated	3483	640	364	37
Total		8185	3630	1496	1295

Each column illustrates a representative neonatal animal for each survival interval. RN33B cells detected were counted and classified into different cell types depending on location of integration and morphology of cells in each region. Animal # abbreviations: hippocampal cortical transplant in postnatal rat (HCTP); the number indicates the survival interval (2, 5, 8, or 16 weeks), and the last letter indicates the animal in a series of transplants (A–J).

Posthoc analysis showed that all time points differed significantly with the exception of 8 and 16 weeks. At 2 weeks post-transplantation 59% of transplanted cells were detected. By 5 weeks 46% of the initial cells detected at 2 weeks remained, while only 13% of those detected at 2 weeks were observed 16 weeks after transplantation. In contrast, the percent of differentiated cells significantly increased with longer posttransplant survival times in the cerebral cortex and in the hippocampus (Fig. 9c), so that at 16 weeks 68% of the remaining RN33B cells exhibited a differentiated phenotype in the cerebral cortex and 63% in the hippocampus. However, the total number of differentiated RN33B cells in the cerebral cortex and the hippocampus at various survival times was not significantly different (Fig. 9b).

Discussion

Transplanted RN33B cell assume complex and variable neuronal phenotypes in the neocortex and hippocampal formation of adult and neonatal rat hosts. As observed *in vitro* (Whittemore and White, 1993), RN33B cells differentiate *in vivo* along a neuronal phenotype. Optimal morphological differentiation into region-specific neuronal phenotypes was seen only following transplantation into the CNS. The classifications of RN33B cells are based on morphological criteria comparable to those described in earlier studies of Golgi-impregnated neurons. RN33B cells in different neuroanatomical sites assumed morphologies characteristic of endogenous neurons at the integration site or remained undifferentiated. In the hippocampus, depending on the cell layer in which RN33B cells were located, some cells assumed morphological characteristics similar to those of endogenous CA1, CA3, and subiculum pyramidal neurons and granule cell neurons in terms of the shapes of their cell bodies

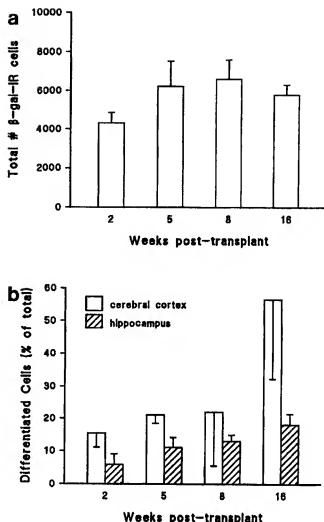


Figure 6. Quantitation of surviving, β -gal-IR RN33B cell in adult CNS. *a*, Counts of total numbers of β -gal-IR cells after variable survival intervals demonstrate that the total number of RN33B cells did not change with longer survival times (ANOVA, $df = 3, 11$, $F = 0.921$, $p = 0.462$). Each bar gives the mean \pm SEM for four animals except at 16 weeks which represents three animals. *b*, The percentage of differentiated β -gal-IR RN33B cells in the cerebral cortex and hippocampus increased with longer survival times. Statistical analysis showed that these increases are not significant (ANOVA, $df = 3, 11$, $F = 1.746$ and 2.842 , $p = 0.215$ and 0.086 in the cerebral cortex and hippocampus, respectively).

and the number, pattern, and orientation of neuritic processes and their structural polarity (Bayer, 1980; Gahwiler, 1984; Frotscher et al., 1988). In the cerebral cortex, the morphologies of differentiated RN33B cells were consistent with those of cortical pyramidal neurons and polygonal cells of the first cortical layer and polymorphic cells of the deep layer of Golgi (Ramón y Cajal, 1988). In white matter, RN33B cells remained undifferentiated or became spindle-shaped, bipolar cells. Double staining for GFAP and X-gal indicated that transplanted RN33B cells did not differentiate to an astrocytic phenotype. Moreover, recent ultrastructural results have detected synapses on β -gal-IR processes in both the cerebral cortex and hippocampus (L. S. Shihabuddin, M. B. Bunge, V. R. Holets, and S. R. Whittemore, unpublished observations), consistent with a differentiated neu-

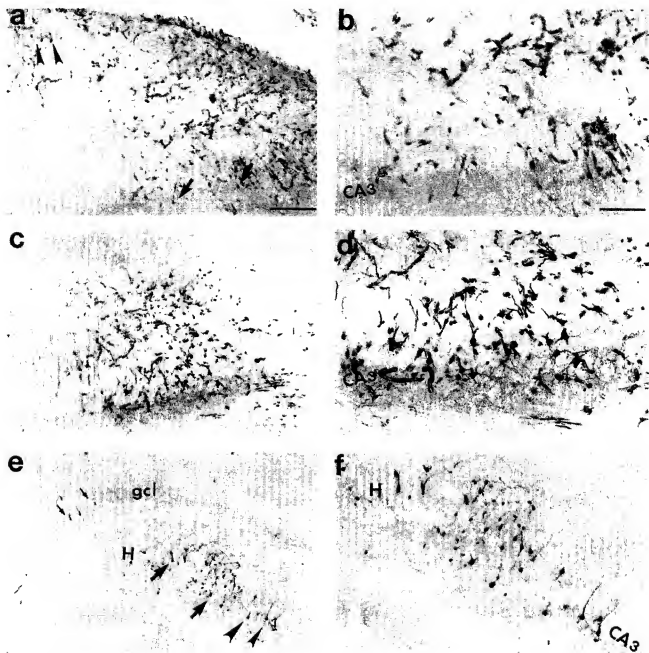


Figure 7. Temporal progression of RN33B cell survival and morphological differentiation in neonatal hippocampus. β -gal-IR RN33B cell transplants in coronal sections of hippocampus at 2 (*a, b*), 5 (*c, d*), and 16 (*e, f*) weeks posttransplantation. *b, d*, and *f* are higher magnification photomicrographs of the fields shown in *a, c*, and *e*, respectively. At 2 weeks posttransplantation (*a, b*), many β -gal-IR RN33B cells are seen, the majority of which are undifferentiated. Some β -gal-IR RN33B cells in the pyramidal layer of CA1 (arrowheads in *a*) and CA3 (arrows in *a* and *b*) differentiated and extended apical and basal processes. At 5 weeks posttransplantation (*c, d*), fewer β -gal-IR RN33B cells are detected but a higher percentage are morphologically differentiated (e.g., CA3 region in *d*). At 16 weeks posttransplantation (*e, f*), most of the β -gal-IR RN33B cells have morphologically differentiated to assume phenotypes similar to neurons at the integration site. Some cells located in the granular cell layer (*gcl*) have morphologies characteristic of endogenous granular neurons (small arrows). Many β -gal-IR RN33B cells are located in the hilar (*H*) region (large arrows) and some in the CA3 pyramidal cell layer (arrowheads). Scale bars: *a, c*, and *e*, 200 μ m; *b, d*, and *f*, 100 μ m.

ronal phenotype of the transplanted RN33B cells. These data demonstrate that RN33B cells morphologically differentiate in response to regional microenvironmental cues, rather than follow a predetermined developmental fate.

Previous studies have demonstrated that immortalized, pluripotent, neuroepithelial precursor cell lines transplanted into the

neonatal CNS can differentiate into both neuronal and glial cell types characteristic of the specific host regions. Renfranz et al. (1991) and Snyder et al. (1992) saw neuronal differentiation only into neuronal phenotypes that were undergoing neurogenesis at the time of transplantation. In contrast, Gao and Hatten (1994) described differentiation into multiple neuronal pheno-

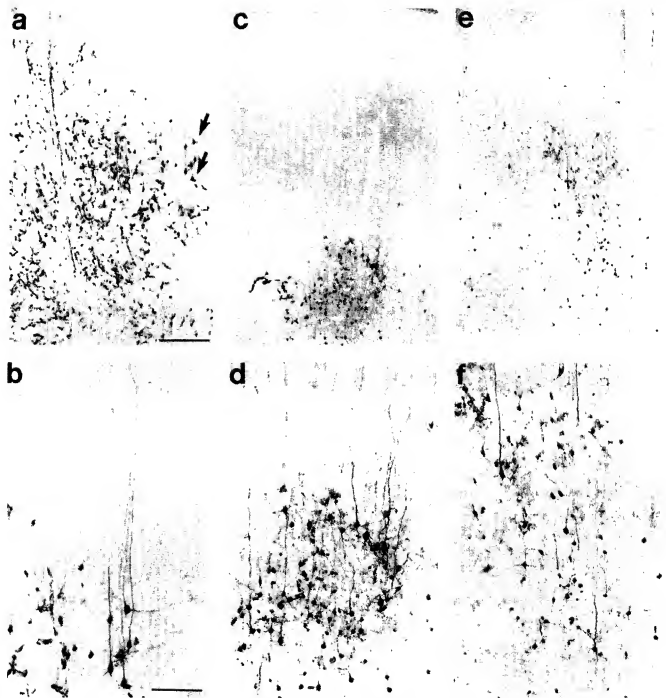


Figure 8. Temporal progression of RN33B cell survival and morphological differentiation in neonatal cerebral cortex. β -gal-IR RN33B cell transplants in coronal section of cerebral cortex at 2 (*a, b*), 5 (*c, d*), and 16 (*e, f*) weeks posttransplantation. *b, d*, and *f* are higher magnification photomicrographs of the fields illustrated in *a, c*, and *e*, respectively. At 2 weeks posttransplantation (*a, b*), a large number of β -gal-IR RN33B cells are dispersed throughout the thickness of the neocortex. The majority of these cells are undifferentiated, but a few have morphologically differentiated to resemble cortical pyramidal neurons (arrows), as shown in *b*. Note the long apical processes extending towards the pial surface. At 5 weeks posttransplantation (*c, d*), fewer cells are detected, but many more are morphologically differentiated. In *d*, a cluster of β -gal-IR RN33B cells located in deeper layers of the neocortex with morphologies similar to those of endogenous pyramidal cortical neurons is shown. At 16 weeks posttransplantation (*e, f*), most β -gal-IR RN33B cells have differentiated phenotypes. Scale bars: *a, c*, and *e*, 200 μ m; *b, d*, and *f*, 100 μ m.

types, both mitotically active and postmitotic, following transplantation of pluripotent granule cell precursors back into the cerebellum. All three groups defined multiple glial phenotypes. Similarly, we observed neuronal differentiation of RN33B cells

in both adult and neonatal hippocampus and cerebral cortex into cell types that are born prenatally or postnatally (Altman and Bayer, 1990a,b; Bayer et al., 1991). We interpret these differences between the data to reflect intrinsic differences between

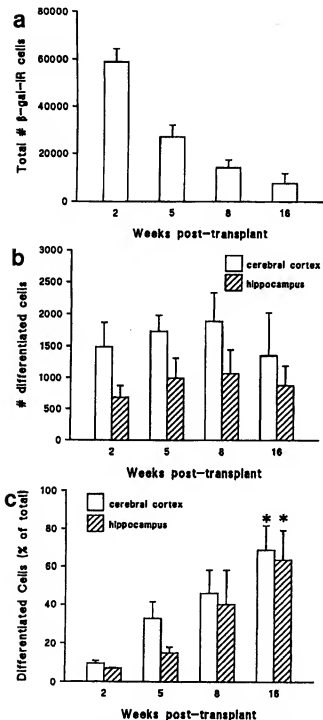


Figure 9. Temporal changes in β -gal-IR RN33B cell survival and differentiation following transplantation into the neonatal CNS. The total numbers of β -gal-IR RN33B cells were counted after variable posttransplantation survival intervals. Data represent the mean \pm SEM for four animals at each time point. *a*, The total number of RN33B cells significantly decreased with longer survival times in all regions (ANOVA, $df = 3, 12$, $F = 24.873$, $p < 0.0001$). Posthoc analysis (unequal N LSD, $p < 0.05$) showed that all time points differed significantly with the exception of 8 and 16 weeks. *b*, Counts of the total number of differentiated RN33B cells at variable survival times demonstrate that the total number of differentiated RN33B cells did not change in the cerebral cortex (ANOVA, $df = 3, 12$, $F = 0.267$, $p = 0.847$) or in the hippocampus (ANOVA, $df = 3, 12$, $F = 0.374$, $p = 0.773$) with longer

the respective neuroepithelial precursor cell lines. Variables such as the lineage stage of the infected precursor, the transforming gene used, and the site of retroviral integration all influence the terminal differentiated phenotype of the transplanted precursor cell line (Whittemore et al., 1995). The fact that RN33B cells differentiate only into neurons likely reflects their initial immortalization at a developmental stage where they had already committed to a neuronal lineage. Consistent with this interpretation, peak neurogenesis in the raphe nucleus occurs between E13–14 (Lauder and Bloom, 1974) and RN33B cells were derived from E13 raphe nuclei. The ability of RN33B cells to differentiate with multiple morphologies in the hippocampus and cerebral cortex indicates that while these cells are neuronally restricted they have not yet become committed to one single neuronal phenotype. This conclusion is supported by *in vivo* data of cortical transplants of fetal tissue that suggest an early, transient, period during which the ultimate phenotype assumed by uncommitted, neuronally restricted precursor cells remains sensitive to environmental factors in the host (Barbe and Levitt, 1991).

Both genetic and extrinsic factors may regulate the lineage choices of multipotential progenitors (Anderson, 1989; McKay, 1989) and the area-specific distinctions of cerebral cortical neurons (Rakic, 1988; O'Leary, 1989). Transplantation experiments have shown that the host tissue environment may alter the differentiation and neural connections of transplanted, developing donor cells (Frank and Wenner, 1993; O'Leary and Koester, 1993). Multiple growth factors are responsible for neuronal survival and differentiation (Cattaneo and McKay, 1990; Chao, 1992; Collazo et al., 1992; Segal et al., 1992). The high levels of $p75^{\text{NTR}}$, the presence of trkB mRNA, the expression of full-length trkB receptor (Whittemore and White, 1993), the induction of *c-fos* mRNA in response to BDNF treatment (data not shown), and the precise spatial differentiation of RN33B cells in CNS areas which produce high levels of BDNF and/or NT-3 and NGF (Enfors et al., 1990; Maisonnier et al., 1990), suggest that neurotrophin(s) may be also involved in RN33B differentiation *in vivo*.

Embryonic cerebellum transplants into the cerebellum of adult Purkinje cell degeneration mutant mice properly differentiate and integrate into the host circuitry (Sotelo and Alvarado-Malart, 1986). Transplanted NTera2 cells, a human tetracarboxinoma cell line capable of neuronal differentiation, establish molecular and structural polarity following transplantation into the adult rat brain (Trojanowski et al., 1993). Furthermore, long interfacular growth of axons from ectopic embryonic neurons is observed along fiber tracts of adult brain and spinal cord (Fuji, 1991; Davies et al., 1993, 1994), indicating that the microenvironment of the adult host tracts provides sufficient cues to induce axon elongation in neurons that do not normally project through those specific tracts. Collectively, these data suggest that the adult CNS has the potential to direct the specific integration and differentiation of immature embryonic neuronal precursor cells.

←

survival times. *c*, Counts of differentiated RN33B cells in cerebral cortex and hippocampus demonstrated a significant increase in the percentage of differentiated RN33B cells in the cerebral cortex (ANOVA, $df = 3, 12$, $F = 6.225$, $p = 0.008$) and in the hippocampus (ANOVA, $df = 3, 12$, $F = 4.454$, $p = 0.025$) at longer survival times. The asterisk (*) identifies time points that differed significantly from the 2 weeks time point using post hoc analysis, unequal N LSD, $p < 0.05$.

RN33B cells survive in both neonatal and adult hosts for ≥ 6 months without forming tumors or otherwise distorting the organization of the host brain. While the phenotypes assumed by RN33B cells were similar in adult and neonatal hosts, there was a difference in the temporal pattern of survival and differentiation. There was an initial period of cell loss shortly after transplantation in adult hosts, but the total number of RN33B cells stabilized by 2 weeks posttransplantation. In contrast, more RN33B cells were seen at early posttransplantation times in neonatal hosts, but the total number of RN33B cells decreased with longer survival times. The increased initial survival of transplants within young hosts, is consistent with results with primary CNS grafts (Gage et al., 1983; Crutcher, 1990). By 16 weeks, the total number of RN33B cells was same in both adult and neonatal hosts, constituting about 6% of the total number of cells transplanted. The low number of surviving RN33B cells in adult and neonatal rat hosts at 16 weeks posttransplantation is also consistent with results from primary neuronal transplants where $<10\%$ of the neurons routinely survive (Brundin and Björklund, 1987), but may also be due to the facts that RN33B cells were transplanted into an intact CNS. A recent study demonstrates that prior hippocampal lesion significantly improved fetal hippocampal graft survival (Shetty and Turner, 1995), presumably through induction of additional trophic support (Cotman et al., 1985).

The quantitative data represent the minimum estimate of surviving cells since exogenous gene expression driven from the murine Maloney leukemia virus (MMLV) LTR, such as the vector used here, has the potential to downregulate *in vivo* (Palmer et al., 1991; St. Louis and Verma, 1988; Onifer et al., 1993). However, these data do reflect the relative cell numbers and the extent of differentiation of transplanted, RN33B cells: after variable survival times within and between different age groups. The percentage of morphologically differentiated RN33B cells in adults increased with longer survival times, but did not exceed 27% of remaining cells, whereas, the percentage of differentiated RN33B cells in neonates increased with longer survival times, reaching a maximum of 68% at 16 weeks posttransplant. As the total number of differentiated cells did not apparently change over time, the increase in the percent of differentiated cells was due to the loss of undifferentiated cells, suggesting that differentiated RN33B cells survive for long times *in vivo*. Moreover, 2 weeks was sufficient for the initial morphological differentiation of transplanted, RN33B cells in the neonatal CNS. One explanation for these data would be that endogenous levels of specific neurotrophic factors (Maisonnier et al., 1990; Korsching, 1993), extracellular matrix (Sanes, 1989; Letourneau et al., 1994) and/or cell surface molecules (Stichel and Müller, 1992; Goodman and Shatz, 1993) have distinct patterns of spatial and temporal expression in the adult and neonatal CNS, and may differentially support the survival and differentiation of RN33B cells. The observed differences between adult and neonatal transplants further suggests that a distinct set(s) of effector molecule(s) was responsible for RN33B cell survival and differentiation.

Our results indicate that transplanted, immortalized, neuronal precursor cell lines are capable of extensive interactions with the host cells. Importantly, these cells survive chronically in both the adult and neonate CNS and maintain their differentiated neuronal phenotype. Such cell lines can be used in a variety of experimental paradigms to investigate discrete issues of developmental plasticity. Ultimately, appropriately derived immortal-

ized cell lines may prove therapeutically useful as a means to replace endogenous CNS neurons lost as a result of trauma or neurodegenerative disease. This could result both because of the inherent plasticity of these neuronal cell lines, and more importantly, because of the capacity of the adult CNS to precisely direct specific differentiation and integration of the transplanted cells.

References

- Altman J, Bayer SA (1990a) Migration and distribution of two populations of hippocampal granule cell precursors during the perinatal and postnatal periods. *J Comp Neurol* 301:365–381.
- Altman J, Bayer SA (1990b) Prolonged sojourn of developing pyramidal cells in the intermediate zone of the hippocampus and their settling in the stratum pyramidale. *J Comp Neurol* 301:343–364.
- Anderson DJ (1989) The neural crest cell lineage problem: neuropoiesis. *Neuron* 3:1–12.
- Barbe MJ, Levitt P (1991) The early commitment of fetal neurons to the limbic cortex. *J Neurosci* 11:519–533.
- Bayer S (1980) Development of the hippocampal region in the rat. II. Morphogenesis during embryonic and early postnatal life. *J Comp Neurol* 190:115–134.
- Bayer SA, Altman J, Russo RJ, Dai X, Simmons JA (1991) Cell migration in the rat embryonic neocortex. *J Comp Neurol* 307:499–516.
- Björklund A (1991) Neural transplantation—an experimental tool with clinical possibilities. *Trends Neurosci* 14:319–322.
- Björklund A, Stenevi U (1984) Intracerebral neural implants: neural replacement and reconstruction of damaged circuitries. *Annu Rev Neurosci* 7:299–308.
- Brundin P, Björklund A (1987) Survival, growth and function of dopamine-secreting neurons grafted to the brain. *Prog Brain Res* 71:293–308.
- Cattaneo E, McKay R (1990) Proliferation and differentiation of neuronal stem cells regulated by nerve growth factor. *Nature* 347:762–765.
- Cepko CL (1989) Immortalization of neural cells via retrovirus-mediated oncogene transduction. *Annu Rev Neurosci* 12:47–65.
- Chao MV (1992) Neurotrophin receptors: a window into neuronal differentiation. *Neuron* 9:583–593.
- Collazo D, Takahashi H, McKay RDG (1992) Cellular targets and trophic functions of neurotrophin-3 in the developing rat hippocampus. *Neuron* 9:643–656.
- Cotman CW, Nello-Sampedro M, Whitemore SR (1985) Relationships between neurotrophic factors and transplant-host integration. In: *Neural grafting in the mammalian CNS* (Björklund A, Stenevi U, eds), pp 169–178. Amsterdam: Elsevier.
- Crutcher KA (1990) Age-related decrease in sympathetic sprouting is primarily due to decreased target receptivity: implications for understanding brain aging. *Neurobiol Aging* 11:175–183.
- Davies SJA, Field PM, Raisman G (1993) Long fibre growth by axons of embryonic mouse hippocampus neurons micro-transplanted into the adult rat fimbria. *Eur J Neurosci* 5:95–106.
- Davies SJA, Field PM, Raisman G (1994) Intrafascicular axon growth from embryonic neurons transplanted into adult myelinated tracts. *J Neurosci* 14:1596–1612.
- Emmerich DE, Ragazzoine M, Lehman MN, Sanberg PR (1992) Behavioral effects of neural transplantation. *Cell Transplant* 1:401–427.
- Enfors P, Wetmore C, Olson L, Persson H (1990) Identification of cells in rat brain and peripheral tissues expressing mRNA for members of the nerve growth factor family. *Neuron* 5:511–526.
- Fisher LJ, Jinnah HA, Kale LC, Higgins GA, Gage FH (1991) Survival and function of intrastrially grafted primary fibroblasts genetically modified to produce L-dopa. *Neuron* 6:371–380.
- Frank E, Wenner P (1993) Environmental specification of neuronal connectivity. *Neuron* 10:779–785.
- Freed WJ, Morihisa JM, Spoor E, Hoffer BJ, Olson L, Seiger A, Wyatt RJ (1981) Transplanted adrenal chromaffin cells in rat brain reduce lesion-induced rotational behavior. *Nature* 292:351–352.
- Frotscher M, Kraft J, Zorn U (1988) Fine structure of identified neurons in the primate hippocampus: a combined Golgi/EM study in the baboon. *J Comp Neurol* 275:254–270.
- Fujii M (1991) Non-specific characteristics of intracerebral neuronal from the olfactory bulb transplanted into the young adult host neo-

- cortex or hippocampal formation. Demonstrated immunohistochemically by the mouse Thy-1 allelic system. *Neurosci Res* 9:285–291.
- Gage FH, Dunnett SB, Stenevi U, Björklund A (1983) Intracerebral grafting of neuronal cell suspensions. VIII. Survival and growth of implants of nigral and septal cell suspensions in intact brain of aged rats. *Acta Physiol Scand* 522:67–75.
- Gage FH, Wolff JA, Rosenberg MD, Xu L, Yee JK, Shults C, Friedman T (1987) Grafting genetically modified cells to the brain: possibilities for the future. *Neuroscience* 23:795–807.
- Gage FH, Kajawa MD, Fisher LJ (1991) Genetically modified cells: applications for intracerebral grafting. *Trends Neurosci* 14:328–334.
- Gage FH, Ray J, Fisher LJ (1995) Isolation, characterization, and use of stem cells from the CNS. *Annu Rev Neurosci* 18:159–192.
- Gahwiler BH (1984) Development of the hippocampus *in vitro*: cell types, synapses and receptors. *Neurosci* 11:751–760.
- Gao W-Q, Hatten ME (1994) Immortalizing oncogenes subvert the establishment of granule cell identity in developing cerebellum. *Development* 120:1059–1070.
- Gash DM, Collier TJ, Sladek JR (1985) Neural transplantation: a review of recent developments and potential applications to the aged brain. *Neurobiol Aging* 6:131–150.
- Gash DM, Nottet MFD, Okawa SH, Krause AL, Joynt RJ (1986) Amiotic neuroblastoma cells used for neural implants in monkeys. *Science* 233:1420–1422.
- Gill TJ III, Kunz HW, Misra DN, Hassett ALC (1987) The major histocompatibility complex of the rat. *Transplant* 43:773–785.
- Goodman SC, Shatz CJ (1993) Developmental mechanisms that generate precise patterns of neuronal connectivity. *Neuron* 10(Suppl):77–98.
- Hoffer BJ, Olson L (1991) Ethical issues in brain-cell transplantation. *Trends Neurosci* 14:384–388.
- Horellou P, Brundin P, Kalen P, Mallet J, Björklund A (1990) *In vivo* release of DOPA and dopamine from genetically engineered cells grafted to the denervated rat striatum. *Neuron* 5:393–402.
- Jäger CB (1985) Immunocytochemical study of PC12 cells grafted to the brain of immature rat. *Exp Brain Res* 59:615–624.
- Kordover JH, Nottet MFD, Gash DM (1987) Neuroblastoma cells in neural transplants: a neuroanatomical and behavioral analysis. *Brain Res* 417:85–98.
- Korsching S (1993) The neurotrophic factor concept: a reexamination. *J Neurosci* 13:2739–2748.
- Lauder JM, Bloom FE (1974) Ontogeny of monoamine neurons in the locus coeruleus, raphe nuclei and substantia nigra of the rat. *Cell Diff* 155:469–482.
- Letourneau PC, Condie ML, Snow DM (1994) Interactions of developing neurons with the extracellular matrix. *J Neurosci* 14:915–928.
- Lindvall O, Brundin P, Widner H, Rehncrona S, Gustavi B, Prackowiak R, Leenders KL, Svante G, Rothwell JC, Marden CD, Björklund A (1990) Grafts of fetal dopamine neurons survive and improve motor function in Parkinson's disease. *Science* 247:574–577.
- Maisonnier PC, Belluscio L, Friedman B, Alderson RF, Wiegand SJ, Furch ME, Lindsay RM, Yancopoulos GD (1990) NT-3, BDNF, and NGF in developing rat nervous system: parallel as well as reciprocal patterns of expression. *Neuron* 5:501–509.
- McKay RDG (1989) The origins of cellular diversity in the mammalian central nervous system. *Cell* 58:815–821.
- Nolan GR, Fiering S, Nicholas JH, Herzenberg LA (1988) Fluorescence-activated cell analysis and sorting of viable mammalian cells based on a β -D-galactosidase activity after transduction of *Escherichia coli* lacZ. *Proc Natl Acad Sci USA* 85:2603–2607.
- O'Leary DDM (1989) Do cortical area emerge from a protocortex? *Trends Neurosci* 12:400–406.
- O'Leary DDM, Koester SE (1993) Development of projection neuron types, axon pathways, and patterned connections of the mammalian cortex. *Neuron* 10:991–1006.
- Onifer SM, White LA, Whittemore SR, Holets VR (1993) *In vitro* strategies for identifying transplanted primary CNS tissue and neuronal cell lines. *Cell Transplant* 2:131–149.
- Onifer SM, Whittemore SR, Holets VR (1993) Variable morphological differentiation of a raphe-derived neuronal cell line following transplantation into the adult rat CNS. *Exp Neurol* 122:130–142.
- Palmer TD, Rosman GY, Osborne WRA, Miller AD (1991) Genetically modified skin fibroblasts persist long after transplantation but gradually inactivate introduced genes. *Proc Natl Acad Sci USA* 88:1330–1334.
- Paxinos G, Watson C (1986) The rat brain in stereotaxic coordinates. San Diego: Academic.
- Perlow MJ, Freed WJ, Seiger A, Olson L, Wyatt RJ (1979) Brain grafts reduce motor abnormalities produced by destruction of nigrostriatal dopamine system. *Science* 204:643–647.
- Rakic P (1988) Specification of cerebral cortical areas. *Science* 241:170–176.
- Ramon y Cajal S (1988) Cajal on the cerebral cortex, pp 23–54. New York: Oxford UP.
- Renfanz PJ, Cunningham MG, McKay RDG (1991) Region-specific differentiation of the hippocampal stem cell line HiB5 upon implantation into the developing mammalian brain. *Cell* 66:173–179.
- Sanes JR (1989) Extracellular matrix molecules that influence neural development. *Annu Rev Neurosci* 12:491–516.
- Segal M, Greenberg B, Milgram NW (1986) A functional analysis of connections between grafted septal neurons and a host hippocampus. *Prog Brain Res* 71:349–358.
- Segal RA, Takahashi H, McKay RDG (1992) Cellular targets and trophic functions of neurotrophin-3 in the developing rat hippocampus. *Neuron* 9:643–656.
- Seiger A (1985) Preparation of immature central nervous system regions for transplantation. In: *Neural grafting in the mammalian CNS* (Björklund A, Stenevi U, eds), pp 71–77. Amsterdam: Elsevier.
- Shetty AK, Turner DA (1995) Enhanced cell survival in fetal hippocampal suspension transplants grafted to adult rat hippocampus following kainate lesions: a 3-dimensional graft reconstruction study. *Neuroscience*, in press.
- Shimohama S, Rosenberg MB, Fagan AM, Wolff JA, Short MP, Breakfield XO, Friedmann T, Gage FH (1989) Grafting genetically modified cells into the rat brain: characteristics of *E. coli* β -galactosidase as a reporter gene. *Mol Brain Res* 5:271–278.
- Snyder EY, Deitcher DL, Walsh C, Arnold-Aldea S, Hartwig EA, Cepko CL (1993) Multipotent neural cell lines can engraft and participate in development of mouse cerebellum. *Cell* 66:33–51.
- Snyder EY, Taylor RM, Wolfe JH (1995) Neural progenitor cell engraftment corrects lysosomal storage throughout the MPS VII mouse brain. *Nature* 374:367–370.
- Sotelo C, Alvarado-Mallart RM (1986) Growth and differentiation of cerebellar suspensions transplanted into the adult cerebellum of mice with hereditodegenerative ataxia. *Proc Natl Acad Sci USA* 83:1135–1139.
- St Louis D, Verma IM (1988) An alternative approach to somatic cell gene therapy. *Proc Natl Acad Sci USA* 85:3150–3154.
- Stübel CC, Müller HW (1992) Expression of inherent neuronal shape characteristics after transient sensitivity to epigenetic factors. *Dev Brain Res* 68:149–162.
- Trojanowski JQ, Mantione JR, Lee JH, Seld DP, You T, Inge LJ, Lee VM-Y (1993) Neurons derived from a human tetraoctanoma cell line establish molecular and structural polarity following transplantation into the rodent brain. *Exp Neurol* 122:283–294.
- White LA, Keane RW, Whittemore SR (1994) Differentiation of an immortalized CNS neuronal cell line decreases their susceptibility to cytotoxic T lymphocyte cell lysis *in vitro*. *J Neuroimmunol* 49:135–143.
- Whittemore SR, White LA (1993) Target regulation of neuronal differentiation in a temperature-sensitive cell line derived from medullary raphe. *Brain Res* 615:27–40.
- Whittemore SR, White LA, Shihabuddin LS, Eaton MJ (1995) Phenotypic diversity in neuronal cell lines derived from raphe nucleus by retroviral transduction. In: *Methods, a companion to Methods in enzymology*, Vol 7 (Russo A, Green S, eds), pp 285–296. San Diego: Academic.
- Widner H, Brudin P (1988) Immunological aspects of grafting in the mammalian central nervous system. A review and speculative synthesis. *Brain Res Rev* 13:287–324.

Exhibit E

A service of the U.S. National Library of Medicine
and the National Institutes of Health

MyNCBI
(Sign In) (Register)

All Databases Journals Books PubMed Nucleotide Protein Genome Structure OMIM PMC

Search PubMed for

Go

Clear

Limits Preview/Index History Clipboard Details

Display AbstractPlus

Show

20

Sort By

Send to

All: 1 Review: 0

Links

☐ 1: Glia. 1993 Sep;9(1):25-40.

Lines of glial precursor cells immortalised with a temperature-sensitive oncogene give rise to astrocytes and oligodendrocytes following transplantation into demyelinated lesions in the central nervous system.

Trotter J, Crang AJ, Schachner M, Blakemore WF.

Department of Neurobiology, University of Heidelberg, Germany.

Immortalised lines of murine glial precursor cells expressing the neomycin resistance gene and a temperature-sensitive mutation of the SV 40 T oncogene were established from cultures of oligodendrocytes and precursor cells infected with a replication-incompetent, helper-free retrovirus. At the permissive temperature (33 degrees C), they could be continually propagated in vitro and cells were present expressing the O4 antigen specific for glial precursor cells and oligodendrocytes. At 38 degrees C, where the expression of the T antigen is down regulated, cell division largely ceased. During early passage in vitro, limited differentiation to a more mature phenotype, as evidenced by expression of GFAP and the oligodendrocyte marker O1 was observed at both 33 degrees C and 38 degrees C. When transplanted into demyelinating lesions in the spinal cords of adult rats early passages of the lines yielded myelin-forming oligodendrocytes and astrocytes. Cells from later passages of the lines although failing to synthesise myelin still associated specifically with the demyelinated axons. These experiments demonstrate the retention of physiological properties of these oncogene-carrying glial cells when transplanted in vivo and suggest that such immortalised populations can be used for the isolation of molecules regulating glial cell function.

PMID: 8244529 [PubMed - indexed for MEDLINE]

Related Links

In vitro and in vivo characterisation of glial cells immortalised with a temperature sensitive SV40 T antigen-containing retrovirus. [Neurosci Res. 1994]

Embryonic-derived glial-restricted precursor cells (GRP cells) can differentiate into astrocytes and oligodendrocytes in vivo. [Exp Neurol. 2001]

Differentiation of the O-2A progenitor cell line CG-4 into oligodendrocytes and astrocytes following transplantation into glia-deficient areas of CNS white matter. [Neurosci Res. 1995]

In vitro and in vivo analysis of a rat bipotential O-2A progenitor cell line containing the temperature-sensitive mutant gene of the SV40 large T antigen. [Eur J Neurosci. 1993]

Differentiation of glial precursor cells from developing cerebellar slices. [Neurosci Res. 1993]

> See all Related Articles...

Display AbstractPlus

Show

20

Sort By

Send to

[Write to the Help Desk](#)

[NCBI | NLM | NIH](#)

[Department of Health & Human Services](#)

[Privacy Statement](#) | [Freedom of Information Act](#) | [Disclaimer](#)



Gene therapy in the adult primate brain: intraparenchymal grafts of cells genetically modified to produce nerve growth factor prevent cholinergic neuronal degeneration

MH Tuszynski^{1,2}, J Roberts³, M-C Senut⁴, H-S U⁵ and FH Gage⁶

Departments of ¹Neurosciences and ²Neurosurgery, University of California, San Diego, CA; ³Department of Neurology, Veterans' Administration Medical Center, San Diego, CA; ⁴Department of Veterinary Sciences, University of California, Davis, CA, USA; ⁵Inserm U161, Paris, France; and ⁶The Salk Institute, La Jolla, CA 92037, USA

Gene therapy may be a useful means of delivering substances to the brain that are capable of preventing neuronal degeneration. In the present experiment, we determined whether intraparenchymal transplants of primary autologous cells genetically modified to produce nerve growth factor (NGF) would prevent injury-induced degeneration of cholinergic neurons. Cultured primary monkey fibroblasts were genetically modified to produce human NGF, and secreted 13.2 ng NGF/10⁶ cells/h *in vitro*. Adult monkeys then underwent fornix transections to induce degeneration of basal forebrain cholinergic neurons, and received autologous grafts of either NGF-producing or control, β -galactosidase-producing fibroblasts directly into the basal forebrain region. One month later, 61.7 \pm 8.9% of cholinergic neurons remained identifiable in NGF-graft recipients compared to 26.2 \pm 5.0% in control graft recipients ($P < 0.02$). Neuronal protection correlated with the accu-

racy of graft placement: up to 92% protection from neuronal degeneration occurred when NGF-secreting grafts were accurately placed immediately adjacent to injured neurons. Thus, intraparenchymal NGF delivery to the adult primate brain by gene transfer can prevent the degeneration of basal forebrain cholinergic neurons. Gene therapy can target intraparenchymal brain sites for regionally specific neurotrophin delivery, thereby avoiding limitations imposed by diffusion of substances across the blood-brain barrier and through CNS parenchyma, while avoiding adverse effects of neurotrophic factors delivered in a non-directed manner to the central nervous system. The delivery of NGF by gene transfer to the brain merits further study as a means of preventing cholinergic neuronal degeneration in human disorders such as Alzheimer's disease.

Keywords: Nerve growth factor; cholinergic neurons; medial septum; gene therapy; hippocampus; Alzheimer's disease

Introduction

Neuronal degeneration and loss occur during development, injury, aging or as a component of chronic neurodegenerative disorders.¹⁻³ Several neurotrophic factors have been identified that prevent neuronal degeneration at various periods during life in selected neuronal populations.⁴⁻¹⁰ The best characterized neurotrophic factor, nerve growth factor (NGF), prevents sympathetic and sensory neuronal death during development,⁶ prevents lesion-induced basal forebrain cholinergic neuronal degeneration in adult rats and primates,¹¹⁻¹⁵ and reverses age-related basal forebrain cholinergic neuronal degeneration and promotes partial cognitive recovery in rats.³ Basal forebrain cholinergic neuronal loss also occurs in Alzheimer's disease (AD). NGF may prevent this loss and improve cognitive function in AD.¹⁶⁻¹⁸

Gene therapy may be a useful tool for the delivery of

substances such as neurotrophic factors to the central nervous system (CNS),¹⁹ achieving intraparenchymal, regionally restricted and sustained neurotrophic factor delivery without risk of immunologically mediated graft rejection.²⁰ In rat models, somatic gene transfer has prevented the degeneration of basal forebrain cholinergic neurons^{21,22} and improved functional outcomes after brain injury.²³⁻²⁵ In primates, we recently reported that primary primate autologous fibroblasts could be transduced *in vitro* to produce NGF; when grafted to intraparenchymal sites in adult monkey brains these genetically modified cells elicited growth of neurites from adult cholinergic neurons for periods of at least 6 months.²⁶

In the present experiment, we sought to determine whether intraparenchymal NGF delivery by gene transfer could prevent neuronal degeneration in the brains of adult monkeys. Unilateral fornix transections were performed to interrupt projecting septohippocampal cholinergic axons, and primary adult primate fibroblasts, transduced to secrete NGF, were grafted into the medial septal region. One month later, brains were examined to determine whether NGF-secreting grafts prevented neuronal degeneration. Control subjects underwent fornix

transections followed by grafts of autologous fibroblasts genetically modified to produce the bacterial β -galactosidase (β -gal) molecule.

Results

(1) *In vitro*: Northern blot analysis showed expression of NGF mRNA from fibroblasts transduced with the NGF gene. Two-site ELISA showed that fibroblasts from Cynomolgus monkeys transduced with the NGF gene secreted an average of 18.1 ± 7 ng NGF/ 10^6 cells/h, while fibroblasts from Rhesus monkeys secreted an average of 12.6 ± 0.8 ng NGF/ 10^6 cells/h, an amount that did not differ significantly ($P = 0.6$). Previous results have also indicated that NGF secretion rates from NGF-transduced fibroblasts of these two species do not differ significantly.²⁰ Conditioned medium from NGF-transduced fibroblast cultures elicited neurite outgrowth from PC-12 cells, demonstrating the secretion of biologically active NGF as previously reported.^{20,26}

Following selection in G418, monkey fibroblast cultures transduced with the β -gal transgene showed intracytoplasmic immunolabeling for β -galactosidase up to the latest time-point tested, passage 14 (4 months in culture).

(2) *In vivo*: Genetically modified fibroblasts were harvested for grafting at passage numbers 10–14. All animals survived the experimental period and showed no behavioral abnormalities arising from unilateral fornix transection or cell grafting.

Graft morphology and location

Surviving fibroblast grafts were found in all subjects at the 1 month time-point with Nissl staining (Figure 1). Accuracy of graft placement relative to the medial septal

target region varied from 150 μ m to 2880 μ m (Table 1). In one animal the NGF-secreting graft was inadvertently placed in the corpus callosum and lateral ventricle, and it was excluded from further analysis. Animals that underwent pre-operative MRI localization showed substantially improved graft placement.²⁷ NGF grafts in Rhesus and macaque monkeys showed equivalent degrees of penetration of AChE- and p75 NGF receptor-labeled fibers (see below). Fibroblast cell density within grafts did not vary substantially between subjects.

Cholinergic neuronal degeneration

Animals that received grafts of NGF-secreting cells showed substantial prevention of retrograde cholinergic neuronal degeneration as assessed with p75 neurotrophin receptor and ChAT immunolabeling. Among NGF-secreting graft recipients, p75 receptor labeling showed persistence of $61.7 \pm 8.9\%$ (s.e.m.) of the original cholinergic neuronal population on the side of the fornix transection compared to only $26.2 \pm 5.0\%$ among animals with β -gal grafts ($P < 0.02$; Figures 2 and 3). Similarly, ChAT immunocytochemical labeling showed a persistence of $51.8 \pm 5.3\%$ of neurons among animals with septal NGF-secreting grafts but only $28.9 \pm 1.2\%$ of neurons in subjects with β -gal grafts ($P < 0.01$; Figure 3). Graft size and accuracy of graft placement generally correlated with host neuronal savings in NGF graft recipients, with up to 92% prevention of cholinergic degeneration occurring in a subject with the largest and most accurately placed graft. In contrast, an NGF graft that was small and distantly located (2.8 cm) from the mid-portion of the septum prevented the degeneration of only 37.6% of cholinergic neurons, an amount that differed little from β -gal graft recipients. Graft size and distance did not appear to correlate with the degree of cell loss in subjects with β -gal-producing grafts, and the degree of cell loss in subjects with β -gal grafts did not differ significantly from previous studies of fornix transections in primates.¹⁵ The

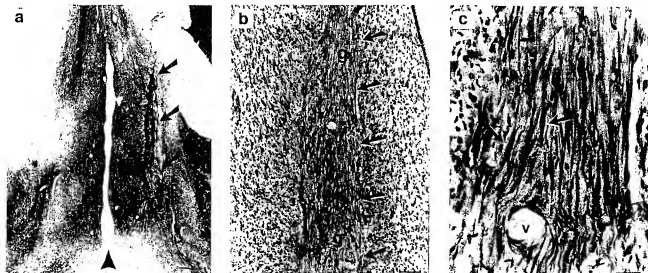


Figure 1 Fibroblast grafts in medial septum. (a) Acetyl cholinesterase (AChE)-stained NGF-secreting fibroblast graft in the septum 1 month after grafting. Graft is located adjacent to cholinergic neuron-containing region. Arrows indicate graft; arrowhead indicates midline. Calibration bar = 200 μ m. (b) Grafts integrate well with host tissue. Arrows indicate right lateral border of graft, g, Nissl stain; calibration bar = 25 μ m. (c) Nissl stain of NGF-secreting graft shows cells with typical fibroblast morphology (examples indicated by arrows). Left lateral border of graft indicated by asterisks. Calibration bar = 10 μ m.

Table 1 Characteristics of each experimental subject

Animal	Type of graft	Species	NGF production ng/10 ⁶ cells/h	Distance (μ m)*	Graft volume (mm ³ \times 10 ³)	% Labelled neurons*	Pre-operative MRI†
1	NGF	Cyno	8.6	250	2200	92.1	+
2	NGF	Cyno	13.1	700	224	65.7	+
3	NGF	Rhesus	11.7	500	247	56.3	+
4	NGF	Rhesus	13.4	700	221	56.9	+
5	NGF	Cyno	19.1	2880	14	37.6	-
6	β -gal	Cyno	0	500	95	34.4	+
7	β -gal	Cyno	0	150	10	17.3	+
8	β -gal	Cyno	0	2500	269	27.0	-

*Graft distance from central medial spectrum.

†Percentage of neurons labelled by immunocytochemical antibody directed against the low-affinity (p75) neurotrophin receptor, lesioned side/intact side.

NGF, NGF-secreting graft; β -gal, β -galactosidase-producing graft; Cyno, Cynomolgus monkey (*Macaca fascicularis*); Rhesus (*Macaca mulatta*); +, MRI performed; -, MRI not performed.

degree of septal cholinergic neuronal degeneration among NGF recipients did not correlate significantly with NGF secretion rates from grafted cells measured *in vitro* prior to grafting ($r^2 = 0.7$).

Cholinergic neurite sprouting

Grafts of NGF-secreting cells were penetrated by AChE-labeled fibers, as previously observed (Figure 4).²⁰ Control grafts were not penetrated by these fibers. Cholinergic sprouting in the dorsolateral quadrant of the septum was not detectable.

In vivo transgene expression

Immunolabeling for NGF and bacterial β -galactosidase was present in NGF-transfected and control grafts, respectively, indicating continued expression of transgenes for at least 1 month *in vivo* (Figure 5). Approximately 10–20% of cells within grafts appeared to demonstrate immunoreactivity for their respective gene products.

After 6 months *in vivo*, fresh dissection of an NGF-secreting graft from one animal yielded 24.4 ng NGF/g tissue (total sample weight 5.1 mg). Less than 2 ng NGF/g tissue was detected from a second sample of cortex located adjacent to the first NGF-graft-containing sample (a distance of approximately 1 cm from the region of the graft). Less than 2 ng NGF/g tissue were detected from two samples of normal cortex from the contralateral cerebral hemisphere in the same animal.

Discussion

Somatic gene transfer of NGF can prevent basal forebrain cholinergic neuronal degeneration in the adult primate brain. Following cholinergic neuronal injury, intraseptal grafts of autologous monkey fibroblasts genetically modified to produce NGF prevented the degeneration of 62% of medial septal cholinergic neurons labeled for the p75 neurotrophin receptor. Lesioned animals with control grafts showed a persistence of only 26% of the original population of cholinergic neurons.

Therapeutic trials of neurotrophic factors have been suggested for preventing neuronal loss in several CNS neurodegenerative disorders including AD,^{16,17} but the optimal method for delivering these substances to the brain is

uncertain.¹⁸ Neurotrophic factor effects on target neurons are mediated by specific binding to high- and low-affinity neurotrophin receptors that are distributed along the length of the axon and cell body.²⁸ To date, most experiments in rats and primates have utilized intracerebroventricular (ICV) NGF delivery to stimulate neurotrophin receptors,^{11,14,15,29–31} thereby releasing large amounts of NGF into the cerebrospinal fluid (CSF). The resulting broad distribution of NGF throughout the CSF space has caused weight loss³² and sprouting of sympathetic neurites around the cerebral vasculature³³ in rats. NGF delivery to the spinal cord also induces sprouting of sensory neurites from the dorsal root ganglia into the CNS.³⁴ Further, chronic ICV NGF infusions into the CNS induce extensive migration of Schwann cells and sprouting of sensory and sympathetic neurites into the subpial space surrounding the spinal cord and brainstem.³⁵ A case study of one human AD patient treated with ICV NGF reported activation of a herpes zoster infection during the infusion period,³⁶ a virus that exists in a latent state in the sensory dorsal root ganglion. Thus, ICV infusions are a useful means of circumventing diffusion restrictions imposed by the blood-brain barrier on large protein molecules such as NGF (MW 13 250 daltons), but adverse effects result from neurotrophic factor influences on non-targeted neuronal populations. It is also unclear whether NGF that is infused ICV will diffuse for sufficient distances through solid brain parenchyma to reach basal forebrain neurons in humans. NGF diffusion through brain parenchyma may be limited to distances as low as 1 mm,³⁷ and basal forebrain neurons in humans are located more than 1 cm from the ependymal and cortical surfaces. Extensive NGF diffusion through brain parenchyma may not have been required in previous studies that examined prevention of cholinergic neuronal loss in the primate brain after ICV NGF delivery,^{11,14,15,29–31} since axotomized cholinergic neurons in the latter studies were located in the lateral ventricle and had direct access to NGF.

Gene therapy may offer an alternative means of providing neurotrophic factors to the CNS in an intraparenchymal, regionally specific, chronic and well-tolerated manner. Intraparenchymal grafts of autologous fibroblasts, genetically modified to produce NGF, prevented the degeneration of 62% of basal forebrain cholinergic neurons after fornix transections in this study. The largest

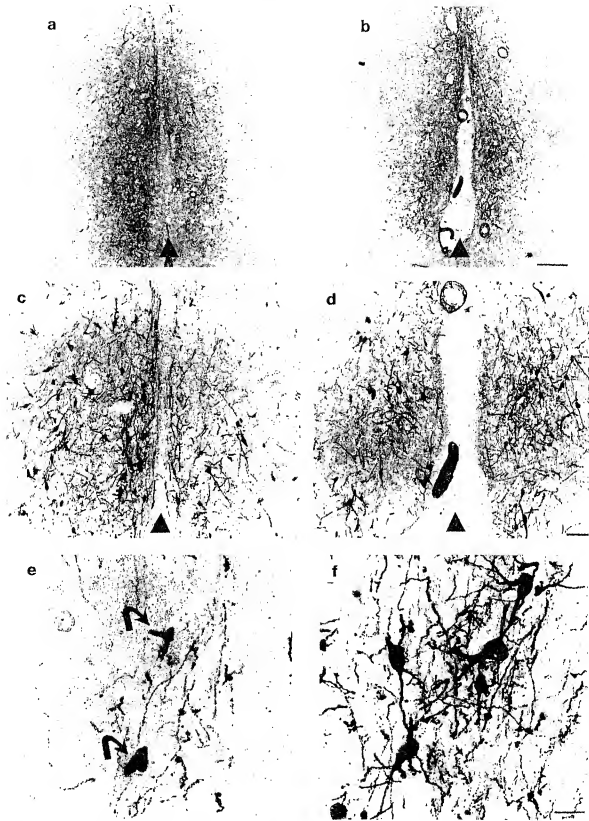
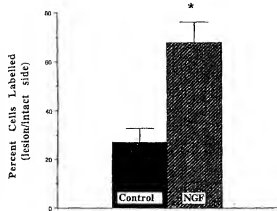


Figure 2. NGF receptor immunolabeled cells in the medial septum. Low-power view of medial septum in control, β -galactosidase producing graft (a) and NGF-secreting graft (b). Calibration bar = 120 μ m. (c) Retrograde degeneration of cholinergic cell bodies on the right (lesioned) side of the medial septum occurs in animals with control grafts following transection of the fornix. Arrow indicates midline. (d) Among subjects that receive NGF-secreting genetically modified cell grafts there is prevention of retrograde degeneration after fornix lesions. Calibration bar (c,d) = 50 μ m. (e) Higher magnification in animal with control graft shows cells undergoing retrograde degeneration (arrows). Remaining neurons are atrophic. (f) There are fewer degenerating neuronal profiles after placement of NGF-secreting grafts. Calibration bar (e,f) = 15 μ m.

a Percentage Cell Savings: NGF Receptor



b Percentage Cell Savings: ChAT

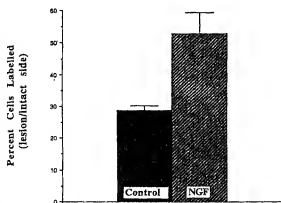


Figure 3 Cell savings: (a) $61.7 \pm 8.9\%$ (s.e.m.) of basal forebrain cholinergic neurons remain immunocytochemically labeled for the p75 low-affinity NGF receptor in animals with NGF-secreting grafts, compared to $26.2 \pm 5.0\%$ in animals with β -gal producing grafts. Asterisk denotes significant differences between groups, $P = 0.02$. (b) ChAT immunocytochemical labeling showed a persistence of $51.8 \pm 5.3\%$ of neurons among animals with septal NGF-secreting grafts but only $28.9 \pm 1.2\%$ in control subjects. Asterisk denotes significant differences between groups, $P = 0.01$.

and most accurately targeted intraparenchymal NGF-secreting graft prevented the degeneration of 92% of cholinergic neurons, exceeding the 80% degree of cholinergic protection attained in previous studies using ICV administration of NGF.¹⁵ Since none of the most accurately targeted β -gal grafts were as large as the accurately targeted NGF-secreting grafts in this experiment, it cannot be stated unequivocally that cholinergic neuronal protection was attributable solely to the NGF gene. However, previous studies in rats have shown no cholinergic neuronal protection from β -gal grafts that were of identical size to NGF grafts.²¹ Furthermore, control grafts in the present experiment did not elicit ingrowth of cholinergic neurites labeled for acetylcholine esterase, indicating a lack of control graft influence on the cholinergic

neuronal phenotype. The cholinergic cell rescue observed in this experiment was achieved with an intraparenchymal NGF delivery rate at least 40 times lower than that used in our prior ICV infusion studies (fibroblasts secreted an average of $0.32 \mu\text{g}$ NGF/day *in vitro* prior to grafting, compared to $12.9 \mu\text{g}$ NGF/day delivered with ICV infusions¹⁹). When NGF-secreting grafts were placed at distances greater than 3 mm from host target neurons or were inadvertently placed in the lateral ventricle adjacent to the medial septum (data not shown), they did not prevent neuronal degeneration, supporting the possibility that NGF diffusion through brain parenchyma is limited. No damage to the host brain was evident from the grafting procedure.

Previous experiments have reported sprouting of cholinergic neurites into the dorsolateral quadrant of the medial septum after ICV NGF delivery.^{14,30,31} This sprouting could have adverse functional consequences, since cholinergic innervation of the brain is regionally specific and neurites do not normally innervate the dorsolateral septal region. In the present study, sprouting was not observed into the dorsolateral septum, presumably since NGF delivery was restricted to intraparenchymal brain sites and did not establish a ventricular gradient of NGF to which injured neurites were attracted. On the other hand, cholinergic neurites did sprout into the NGF-secreting grafts themselves; this sprouting too could have adverse functional consequences. Behavioral studies are in progress to address this possibility. Ultimately, the usefulness of NGF therapy for disorders such as AD may reflect a balance between beneficial effects resulting from prevention of neuronal degeneration, and adverse effects resulting from neurite sprouting in different brain regions.

Significant issues should be addressed before gene therapy is utilized to treat human CNS disorders. First, extended *in vivo* gene expression must be documented. After 1 month *in vivo*, approximately 10–20% of grafted cells in this experiment were immunocytochemically labeled for their respective gene products; this was a substantial decline from virtual 100% labeling of cells *in vitro* prior to grafting. Yet 6 months after grafting, NGF protein was elevated 10- to 20-fold above physiological levels³⁸ within a cortical sample containing an NGF-secreting graft in the single animal in which it was measured. In rats, NGF-secreting grafts in the spinal cord have also shown NGF protein production by ELISA and NGF mRNA (by reverse transcriptase PCR) 1 year after *in vivo* grafting.³⁹ Additional data from primates is needed to confirm these preliminary results. Second, biological effects of genetically modified cells in the host brain should be demonstrated at extended time-points in primate models. We have reported persistent sprouting of cholinergic neurites into NGF-secreting grafts 6 months after *in vivo* grafting in adult monkeys;²⁰ additional studies are in progress. Third, regulation of transgene expression *in vivo* would be a desirable property of a delivery system such as this. Although a technically challenging task, regulation of *in vivo* expression may be necessary if transduced cells produced too much or too little NGF. A means of eliminating grafted cells after *in vivo* placement would also be a desirable property if the cells exhibited uncontrolled growth or other undesirable effects; insertion of an inducible death gene into grafted cells such as thymidine kinase^{40,41} may achieve this

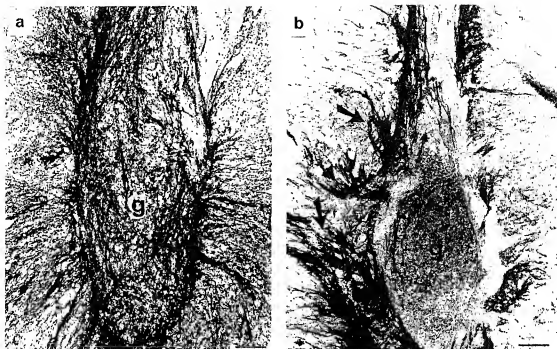


Figure 4 Cholinergic fiber penetration into grafts: (a) NGF-secreting grafts show dense penetration by cholinergic neurites (AChE stain). g, core of graft. Calibration bar = 45 μ m. (b) β -gal grafts show neurite sprouting along graft periphery (arrows) but not into the graft core (g); sprouting in the periphery probably results from NGF secretion from host astrocytes.^{40,44} Calibration bar = 45 μ m.

capability. Alternatively, accurately placed electrolytic lesions could eliminate grafted cells while minimally affecting the host brain. To date, we have not observed uncontrolled cell growth or graft cell migration distant from the injection site in more than 200 fibroblast grafts to the adult primate brain. Finally, it remains to be determined how many graft sites of genetically modified cells will be required to provide adequate neurotrophin delivery to the relatively large brains of primates, and particularly humans. In a human affliction such as Parkinson's disease, a single graft per affected side of the brain may be sufficient to deliver neurotrophins to the relatively small region of the substantia nigra. On the other hand, in AD, basal forebrain cell loss occurs over an intraparenchymal distance extending over approximately 5 cm. In the present experiment, no NGF was detected from a brain biopsy located 1 cm from an NGF-secreting graft, thus the delivery of cells to treat the basal forebrain region in humans will probably require multiple grafts.

The present study confirms that adult primate basal forebrain neurons maintain NGF-responsiveness following axotomy, that this responsiveness can be promoted by neurotrophin delivery to the region of the neuronal soma, and that neuronal savings may be elicited by much lower NGF doses than utilized previously if NGF is delivered intraparenchymally. An increasing number of CNS neurons have been found to maintain neurotrophic factor responsiveness in adulthood, including cholinergic basal forebrain neurons,^{3,11-13,42} entorhinal cortical neurons,⁴³ thalamic neurons,⁴⁴ locus ceruleus neurons,⁴⁵ spinal sensory neurites³⁴ and spinal motor neurons.⁴⁶⁻⁵⁵ The broad responsiveness of diverse brain regions to neurotrophic factors may lead to the development of effective therapies for a variety of neurodegenerative and trau-

matic disorders; gene therapy may be an efficient means of providing these neurotrophins to the CNS in circumstances requiring regionally restricted and accurately targeted drug delivery.

Materials and methods

Experimental subjects

Seven adult *Macaca fascicularis* (Cynomolgus) monkeys and two adult *Macaca mulatta* (Rhesus) monkeys were experimental subjects (Table 1). Two species of monkey were used because of restricted primate availability; previous work has shown no difference in neurotrophic factor responsiveness between these primate species.²⁰ All procedures and animal care adhered strictly to NIH, AAALAC, USDA, Society for Neuroscience, and institutional guidelines for experimental animal health, safety and comfort.

Primary cultures of dermal fibroblasts

Experimental subjects were anesthetized with 25 mg/kg ketamine intramuscularly, and the fur over the dorsal L4 region of the back was clipped and shaved. The skin was cleansed with Betadine Scrub, and a skin biopsy 25 \times 25 mm in size was obtained. The biopsies were de-cleansed in alcohol, then cut into very small pieces (1 \times 1 mm) and placed in culture wells containing Dulbecco's minimal essential medium (DMEM) with 10% fetal calf serum (FCS). When cells reached 90% confluence, they were passaged by trypsinization then resuspended and replated. Fibroblasts were propagated by replating at a density of 1:4. Passage numbers were noted.

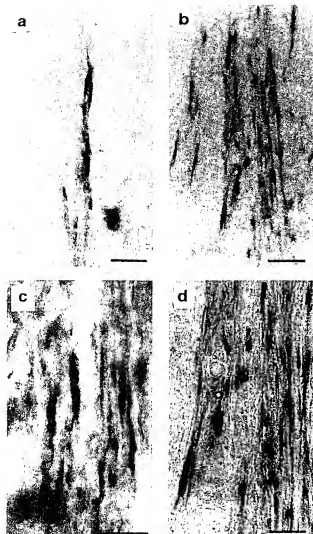


Figure 5 *In vivo* transgene expression at 1 month: NGF (a,b) and β -galactosidase (c,d) immunocytochemical labels show persistent production of transgene products 1 month after *in vivo* grafting. Calibration bars = 50 μ m (a), 60 μ m (b), 10 μ m (c), and 20 μ m (d).

Retroviral vector construction

Structural genes of the Moloney murine leukemia virus (MLV) were replaced with either (a) the entire coding sequence for the biologically active, β -fragment of human NGF (cDNA a gift of the Syntex/Synergen Collaboration, Palo Alto, CA, USA), or (b) *E. coli* β -gal under control of the viral 5' long terminal repeat (LTR) promoter, as previously described.²¹ Bacterial β -gal was chosen as a control gene for use in these experiments because it is readily detectable as a transgene product but has no known biological activity in the rat or primate brain. A dominant selectable marker imparting neomycin resistance (*neo*^r) comprised a second inserted gene in the plasmid, under control of an internal Rous sarcoma virus (RSV)-LTR promoter.²¹

Transfection of producer cells and infection of primary fibroblasts

The NGF or β -gal plasmids were introduced into the ectotropic producer cell line psi-2 by the calcium phosphate precipitation procedure. Psi-2 cells packaged the desired

vectors into viral particles that were subsequently used to infect the amphotropic producer cell line PA317. This resulted in secretion of high titers of amphotropic virus that were used to infect primary primate fibroblasts. Target fibroblasts that successfully incorporated the transgene of interest were then selected *in vitro* with the neomycin analog G418 at a concentration of 400 μ g/ml.

Assays of NGF expression

NGF production by the transfected fibroblasts was assayed in four ways:

(1) **Northern blot analysis:** Total RNA from confluent cultures of monkey fibroblasts transduced to express NGF were prepared by guanidine isothiocyanate methods and analyzed by Northern blot using a ³²P-labeled random-primed human NGF cDNA probe.⁵⁶ Non-transduced primary fibroblasts were used as negative controls and mouse submaxillary gland as a positive control. Approximately 20 μ g total RNA were loaded into each lane.

(2) **NGF immunoassay:** Culture-medium NGF levels were measured with a two-site enzyme-linked immunoassay sensitive to 5 pg/ml,⁵⁸ using antibodies directed against human NGF (gift of Syntex). Culture medium was collected after 24 h of incubation.

(3) **NGF biological assay:** The ability of NGF from *in vitro* cell extracts and conditioned media to elicit neurite outgrowth was quantified in rat PC12 cell cultures, an assay sensitive to 100 pg/ml.

(4) **NGF immunocytochemistry:** *In vivo* production of NGF from fibroblasts was assessed with a specific polyclonal NGF antibody (gift of Dr James Connor, University of California-San Diego). Sections 40 μ m-thick were rinsed three times in phosphate buffer-physiological saline solution, then subjected to a membrane permeabilization procedure that enhances presentation of NGF antigenic epitopes for immunolabeling. Several controls assessed specificity of the immunolabel: (a) labeling in β -gal producing fibroblasts; (b) labeling in NGF fibroblast sections with primary antibody excluded; and (c) ability of the same antibody to elicit NGF signal from immunoassay reported in step (2) above.

Assay of β -galactosidase production

An immunocytochemical label for bacterial β -gal (Promega, Madison, WI, USA) was utilized to study *in vitro* and *in vivo* production of this control gene. Primate β -gal does not cross-react with *E. coli* β -gal immunocytochemical label (unpublished observation).

In vitro harvesting of cells for grafting

Fibroblasts that successfully incorporated the NGF or β -gal transgenes were assayed for transgene production, and cells secreting the highest amounts of the transgenes were chosen for amplification of cell numbers and grafting. Cultures were maintained as bulk transfectants, and final cell concentrations for grafting were adjusted to 1.0×10^6 cells/ μ l.

Animal surgery

For all surgical procedures primates were preanesthetized with 25 mg/kg ketamine i.m. then anesthetized with

either isoflurane administered by endotracheal intubation or intravenous nembutal (30 mg/kg). Post-operatively animals were closely monitored and received supportive care and analgesics as needed.

Magnetic resonance imaging (MRI) for transplant site localization: Five subjects (Table 1) underwent skull implantation of magnetodense beads and subsequent MRI to generate a stereotaxic atlas for each monkey to improve accuracy of graft placement, after initial results in animals without using MRI showed suboptimal graft placement (see Results). Animals were anesthetized and placed in a primate stereotaxic apparatus. A midline scalp incision exposed the skull. A 5-mm spherical glass bead filled with a 0.04 M solution of CuSO_4 was attached to the skull midline with cyanoacrylate at stereotaxic AP coordinate +4.0 cm.²⁷ The scalp was closed in layers. After animals recovered, serial coronal 3 mm thick MR images of the brain were obtained using a 1.5 tesla magnet to provide accurate localization of medial septal sites for grafting. Antero-postero (AP) coordinates for cell grafting into the medial septal nucleus were determined utilizing the previously implanted magnetodense glass bead as an AP zero reference point.²⁷

Cell transplantation: Animals were placed in a primate stereotaxic apparatus. A midline scalp incision exposed the skull. The previously implanted magnetodense glass bead was removed, and the base of its stereotaxic location measured in the AP plane. A 2.5 × 5 cm sagittally oriented craniotomy was then performed on each side of the hemispheric. A medio-lateral (ML) zero reference point was obtained by measuring the midpoint of the superior sagittal sinus. The dura was incised and reflected to expose sites for cell injections into the medial septum. A third reference point in the ventro-dorsal (VD) plane was measured at the cortical surface over each injection site. Utilizing zero reference points measured in the AP, ML and VD planes on the animal and comparing these to intended grafting sites visualized on the same animal's MRI, cell injection sites targeting the medial septum were calculated. Ten microliters of cells were injected into each of three medial septal sites spaced 1 mm apart, using a 25-gauge Hamilton syringe. Cells were injected at a rate of 5 $\mu\text{l}/\text{min}$.

Fornix transection: Moving caudally 1 cm in the AP plane, a second craniotomy for transection of the fornix was performed 4 mm anterior to the intra-aural line. The ipsilateral hemisphere was retracted from the falx cerebri to expose the corpus callosum. A core of tissue was removed from the underlying white matter with microscissors and electrocauterization to create an opening into the ventricular system to visualize the trigonal region. The bundle of the fornix was identified and transected. Visualization of midline draining veins indicated complete medial transection of the fornix.

Perfusion

After a 1-month survival period, animals were killed for histological analysis. Animals were very deeply anesthetized with ketamine and nembutal and perfused transcardially for 1 h with a 4% solution of paraformaldehyde in 0.1 M phosphate buffer followed by 5% sucrose solution

in the same buffer for 20 min. The brains were stereotaxically blocked in the coronal plane.

Histology

Sections were cut at 40 μm intervals on a freezing microtome. Every sixth section was processed for thionine (Nissl) or hematoxylin and eosin staining; acetylcholinesterase (AChE) histochemistry; low-affinity neurotrophin receptor (p75 kindly provided by Dr Mark Bothwell, University of Washington, Seattle, WA, USA); and choline acetyltransferase (CHAT; kindly provided by Dr Bruce Wainer, Albert Einstein College of Medicine, Bronx, NY, USA) immunocytochemical labeling. p75 Receptor labeling has previously been shown to label 95% of basal forebrain cholinergic neurons.^{37,38}

Basal forebrain cholinergic neuronal numbers were quantified by counting the number of NGF-receptor and ChAT labeled neurons over the entire rostral-caudal extent of the medial septum. Seven to eight sections per animal containing medial septal neurons were quantified, amounting to no fewer than 400 neurons per animal. Cell numbers were quantified with a 10× objective using a 0.5 × 0.5 mm counting grid. Cells were counted that labeled positively with peroxidase reaction product and possessed either a cell body with emerging neurite or a pyramidal shaped cell body with well defined nucleus. Neuron numbers on the lesioned side of the septum were added and expressed as a percentage of remaining neurons labeled on the unlesioned side of the septum in the same animal. Thus, each animal served as its own histological control.

Stereological quantification and measurement of graft distance from target region

Graft volumes were assessed utilizing stereological techniques.⁵⁹ Briefly, a regular 18 × 30 grid matrix was superimposed on a television monitor containing a 10× projected image of Nissl-stained graft sections. Graft area per microscopic section was determined by counting the number of grid points contained within a graft, multiplied by the true intergrid-point distance. The total volume of each graft was obtained by summing the sectional area measurements in each graft section, and multiplying this sum by the distance between successive sections (240 μm). Graft distance from medial septal target cells was measured utilizing a 100 μm scale inserted into the optical path of an Olympus Vanox microscope, and directly measuring the nearest distance from each graft to the brain midline in the septal section containing the graft.

Determination of in vivo NGF protein production

One additional Rhesus monkey received an NGF-secreting autologous fibroblast graft into the neocortex for the purpose of assessing long-term *in vivo* NGF gene expression. 2 × 10⁶ Fibroblasts in a 20 μl volume were placed into the superficial parietal cortex. Six months later, the graft was dissected from the brain. An area of cortex adjacent to the graft was also separately dissected, together with two samples of control (ungrafted) brain from the contralateral hemisphere. The presence of NGF protein in the four fresh frozen tissue samples was assessed by ELISA as described above.

Statistics

Group differences were determined by Students' *t* test, with results presented as mean \pm s.e.m. Multiple group comparisons were made by analysis of variance with post-hoc analysis using Fisher's least square difference.

Acknowledgements

We thank Dr James Connor for performing NGF ELISA, and Bobbie Miller for expert technical assistance. This research was supported by grants from the NIH (AGO0353A, AGO5512, AG10435, TW04813), the Veterans Administration, NATO (58C91FR) and the California Regional Primate Research Center (Base Grant RR00169).

References

- 1 Cowan WM, Fawcett JW, O'Leary DD, Stanfield BB. Regressive events in neurogenesis. *Science* 1984; 225: 1258-1265.
- 2 Armstrong DM et al. Response of septal cholinergic neurons to axotomy. *J Comp Neurol* 1987; 264: 421-436.
- 3 Fischer W et al. Amelioration of cholinergic neuron atrophy and spatial memory impairment in aged rats by nerve growth factor. *Nature* 1987; 329: 65-68.
- 4 Yahr MD. The Parkinsonian syndrome. In: Merritt H (ed). *A Textbook of Neurology*. Lee & Febiger: Philadelphia, 1984, pp 526-537.
- 5 Katzman R. Alzheimer's disease. *New Engl J Med* 1986; 314: 964-973.
- 6 Levi-Montalcini R. The nerve growth factor 35 years later. *Science* 1987; 237: 1154-1162.
- 7 Barde Y-A et al. Brain-derived neurotrophic factor. *Prog Brain Res* 1987; 71: 185-189.
- 8 Oppenheim RW et al. Reduction of naturally occurring motoneuron death *in vivo* by a target-derived neurotrophic factor. *Science* 1988; 240: 919-922.
- 9 Maisonnier PC et al. Neurotrophin-3: a neurotrophic factor related to NGF and BDNF. *Science* 1990; 247: 1446-1451.
- 10 Gotz R et al. Neurotrophin-6 is a new member of the nerve growth factor family. *Nature* 1994; 372: 266-269.
- 11 Hefti F. Nerve growth factor (NGF) promotes survival of septal cholinergic neurons after fimbria transection. *J Neurosci* 1986; 6: 2155-2162.
- 12 Kromer LF. Nerve growth factor treatment after brain injury prevents neuronal death. *Science* 1987; 235: 214-216.
- 13 Williams LR et al. Continuous infusion of nerve growth factor prevents basal forebrain neuronal death after fimbria-fornix transection. *Proc Natl Acad Sci USA* 1986; 83: 9231-9235.
- 14 Tuszyński MH, U HS, Amaral DG, Gage FH. Nerve growth factor infusion in primate brain reduces lesion-induced cholinergic neuronal degeneration. *J Neurosci* 1990; 10: 3604-3614.
- 15 Tuszyński MH, U HS, Gage FH. Recombinant human nerve growth factor infusions prevent cholinergic neuronal degeneration in the adult primate brain. *Ann Neurol* 1991; 30: 625-636.
- 16 Hefti F, Weiner WJ. Nerve growth factor and Alzheimer's disease. *Ann Neurol* 1986; 20: 275-281.
- 17 Appel SH. A unifying hypothesis for the cause of amyotrophic lateral sclerosis, Parkinsonism, and Alzheimer disease. *Ann Neurol* 1981; 10: 499-505.
- 18 Tuszyński MH and Gage FH. Neurotrophic factors and Alzheimer's disease. In: Terry R, Katzman R and Bick KL (eds). *Alzheimer's Disease*. Raven Press: New York, 1994, pp 405-418.
- 19 Gage FH et al. Gene therapy in the CNS: intracerebral grafting of genetically modified cells. *Prog Brain Res* 1990; 86: 205-217.
- 20 Tuszyński MH et al. Fibroblasts genetically modified to produce NGF promote sprouting in the adult primate brain. *Neurobiol Dis* 1994; 1: 67-78.
- 21 Rosenberg MB et al. Grafting genetically modified cells to the

- damaged brain: restorative effects of NGF expression. *Science* 1988; 242: 1575-1578.
- 22 Strömberg J et al. Rescue of basal forebrain cholinergic neurons after implantation of genetically modified cells producing recombinant NGF. *J Neurosci Res* 1990; 25: 405-411.
- 23 Wolff JA et al. Grafting fibroblasts genetically modified to produce L-dopa in a rat model of Parkinson disease. *Proc Natl Acad Sci USA* 1989; 86: 9011-9014.
- 24 Horellou P et al. Behavioural effects of genetically engineered cells releasing dopa and dopamine after intracerebral grafts in a rat model of Parkinson's disease. *J Physiol (Paris)* 1991; 85: 158-170.
- 25 Chen K, Gage FH. Somatic gene transfer of NGF to the aged brain: behavioral and morphological amelioration. *J Neurosci* 1995; 15: 2819-2825.
- 26 Barnett J et al. Human beta nerve growth factor obtained from a baculovirus expression system has potent *in vitro* and *in vivo* neurotrophic activity. *Exp Neurol* 1990; 110: 11-24.
- 27 Alvarez-Royo P, Clower RP, Zola-Morgan S, Squire LR. Stereotaxic lesions of the hippocampus in monkeys: determination of surgical coordinates and analysis of lesions using magnetic resonance imaging. *J Neurosci Meth* 1991; 38: 223-232.
- 28 Parada LF et al. The Trk family of tyrosine kinases: receptors for NGF-related neurotrophins. *Cold Spring Harb Symp Quant Biol* 1992; 57: 43-51.
- 29 Koliatsos VE et al. Mouse nerve growth factor prevents degeneration of axotomized basal forebrain cholinergic neurons in the monkey. *J Neurosci* 1990; 10: 3801-3813.
- 30 Emeric DW et al. Implants of polymer-encapsulated human NGF-secreting cells in the nonhuman primate: rescue and sprouting of degenerating cholinergic basal forebrain neurons. *J Comp Neurol* 1994; 349: 148-164.
- 31 Kordower JH et al. The aged monkey basal forebrain: rescue and sprouting of axotomized basal forebrain neurons after grafts of encapsulated cells secreting human nerve growth factor. *Proc Natl Acad Sci USA* 1994; 91: 10898-10902.
- 32 Williams LR. Hypophagia is induced by intracerebroventricular administration of nerve growth factor. *Exp Neurol* 1991; 113: 31-37.
- 33 Crutcher KA, Davis JN. Sympathetic noradrenergic sprouting in response to central cholinergic denervation. *Trends Neurosci* 1981; 4: 70-72.
- 34 Tuszyński MH et al. Fibroblasts genetically modified to produce nerve growth factor induce robust neuritic growth after grafting to the spinal cord. *Exp Neurol* 1994; 126: 1-14.
- 35 Winkler J et al. Induction of Schwann cell hyperplasia *in vivo* after intracerebroventricular administration of nerve growth factor. *Soc Neurosci Abstr* 1995; 21: 278.
- 36 Olson L et al. Nerve growth factor affects 11C-nicotine binding, blood flow, EEG, and verbal episodic memory in an Alzheimer's patient. *J Neural Transm* 1992; 4: 79-95.
- 37 Lapchak PA, Araujo DM, Carswell S, Hefti F. Distribution of 125I nerve growth factor in the rat brain following a single intracerebral injection: correlation with topographical distribution of trkA messenger RNA-expressing cells. *Neuroscience* 1993; 54: 445-460.
- 38 Weskamp G, Otten U. An enzyme-linked immunoassay for nerve growth factor (NGF): a tool for studying regulatory mechanisms involved in NGF production in brain and in peripheral tissues. *J Neurochem* 1987; 48: 1779-1786.
- 39 Tuszyński MH et al. Fibroblasts and Schwann cells genetically modified to produce neurotrophic factors induce robust neuritic growth after transplantation to the spinal cord. *Soc Neurosci Abstr* 1994; 20: 10.
- 40 Ezzeddine ZD et al. Selective killing of glioma cells in culture and *in vivo* by retrovirus transfer of the herpes simplex virus thymidine kinase. *New Biologist* 1991; 3: 608-614.
- 41 Barba D, Hardin J, Ray J, Gage FH. Thymidine kinase-mediated killing of rat brain tumors. *J Neurosurg* 1993; 79: 729-735.
- 42 Hefti F, Knusel B, Lapchak PA. Protective effects of nerve growth factor and brain-derived neurotrophic factor on basal

- forebrain cholinergic neurons in aged rats with parietal fornix transections. *Prog Brain Res* 1993; 98: 257-263.
- 43 Cotman C, Cummings BJ, Pike C. Molecular cascades in adaptive versus pathological plasticity. In: Gorio A (ed). *Neuroregeneration*. Raven Press: New York, 1993, pp 217-240.
- 44 Clatterbuck RE, Price DL, Koliatos VE. Ciliary neurotrophic factor prevents retrograde neuronal death in the adult central nervous system. *Proc Natl Acad Sci USA* 1993; 90: 2222-2226.
- 45 Arenas E, Persson H. Neurotrophin-3 prevents the death of adult central noradrenergic neurons *in vivo*. *Nature* 1994; 367: 368-371.
- 46 Oppenheim RW, Qin-Wei Y, Prevette D, Yan Q. Brain-derived neurotrophic factor rescues developing avian motoneurons from cell death. *Nature* 1992; 360: 755-757.
- 47 Yan Q et al. Retrograde transport of BDNF and NT-3 by spinal motoneurons. *Soc Neurosci Abstr* 1991; 17: 1119.
- 48 Sendtner M et al. Brain-derived neurotrophic factor prevents the death of motoneurons in newborn rats after nerve section. *Nature* 1992; 360: 757-759.
- 49 Mitsuhashi H et al. Arrest of motor neuron disease in wobbler mice cotreated with CNTF and BDNF. *Science* 1994; 265: 1107-1110.
- 50 Arakawa Y, Sendtner M, Thoenen H. Survival effect of ciliary neurotrophic factor (CNTF) on chick embryonic motoneurons in culture: comparison with other neurotrophic factors and cytokines. *J Neurosci* 1990; 10: 3507-3515.
- 51 Magal E, Burnham P, Varon S. Effects of ciliary neurotrophic factor on rat spinal cord neurons *in vitro*: survival and expression of choline acetyltransferase and low-affinity nerve growth factor receptors. *Brain Res* 1991; 63: 141-150.
- 52 Oppenheim RW et al. Control of embryonic motoneuron survival *in vivo* by ciliary neurotrophic factor. *Science* 1991; 251: 1616-1618.
- 53 Wewetzer K, MacDonald JR, Collins F, Unsicker K. CNTF rescues motoneurons from ontogenetic cell death *in vivo*, but not *in vitro*. *NeuroReport* 1990; 1: 203-206.
- 54 Sendtner M, Kreutzberg GW, Thoenen H. Ciliary neurotrophic factor prevents the degeneration of motor neurons after axotomy. *Nature* 1990; 345: 440-444.
- 55 Sendtner M et al. Ciliary neurotrophic factor prevents degeneration of motor neurons in mouse mutant neuronopathy. *Nature* 1992; 358: 502-504.
- 56 Chirgman JM, Poznybyla BA, MacDonald RJ, Rutter WJ. Isolation of biologically active ribonucleic acid from sources enriched in ribonuclease. *Biochemistry* 1979; 18: 5294-5299.
- 57 Kordower JH et al. Nerve growth factor receptor immunoreactivity in the nonhuman primate (*Cebus apella*): distribution, morphology, and colocalization with cholinergic enzymes. *J Comp Neurol* 1988; 277: 465-486.
- 58 Batchelor PE, Armstrong DM, Blaker SM, Gage FH. Nerve growth factor receptor and choline acetyltransferase colocalization in neurons within the rat forebrain: response to fimbria-fornix transection. *J Comp Neurol* 1989; 284: 187-204.
- 59 Coggeshall RE. A consideration of neural counting methods. *Trends Neurosci* 1992; 15: 9-13.
- 60 Furukawa S, Furukawa Y, Satoyoshi E, Hayashi K. Synthesis and secretion of nerve growth factor by mouse astroglial cells in culture. *Biochem Biophys Res Comm* 1986; 136: 57-63.
- 61 Yoshida K, Gage FH. Fibroblast growth factors stimulate nerve growth factor synthesis and secretion by astrocytes. *Brain Res* 1991; 538: 118-126.